8-2011

Cyber physical complex networks, modeling, analysis, and control

Neveen Shlayan
University of Nevada, Las Vegas

CYBER PHYSICAL COMPLEX NETWORKS, MODELING, ANALYSIS, AND CONTROL

By

Neveen Shlayan

Masters of Science in Electrical Engineering
University of Nevada, Las Vegas
2008

A dissertation submitted in partial fulfillment
of the requirements for the

Doctor of Philosophy in Electrical Engineering
Department of Electrical and Computer Engineering
College of Engineering

Graduate College
University of Nevada, Las Vegas
August 2011

THE GRADUATE COLLEGE

We recommend the dissertation prepared under our supervision by

Neveen Shlayan

entitled

Cyber Physical Complex Networks, Modeling, Analysis, and Control

be accepted in partial fulfillment of the requirements for the degree of

Doctorate of Philosophy in Electrical Engineering
Department of Electrical and Computer Engineering

Pushkin Kachroo, Committee Chair

Alexander Paz, Committee Co-Chair

Rama Venkat, Committee Member

Ebrahim Saberinia, Committee Member

YiTung Chen, Graduate College Representative

Ronald Smith, Ph. D., Vice President for Research and Graduate Studies
and Dean of the Graduate College

August 2011

ABSTRACT

Stochastic Radon Transform Inversion Models for Estimation

by

Neveen Shlayan

Dr. Pushkin Kachroo, Examination Committee Chair
Professor of Electrical and Computer Engineering
University of Nevada, Las Vegas

This research scrutinize various attributes of complex networks; mainly, modeling, sensing, estimation, safety analysis, and control. In this study, formal languages and finite automata are used for modeling incident management processes. Safety properties are checked in order to verify the system. This method introduces a systematic approach to incident management protocols that are governed by mostly unsystematic algorithms. A portion of the used data in this study is collected by means of radar and loop detectors. A weighted t-statistics methodology is developed in order to validate these detectors. The detector data is then used to extract travel time information where travel time reliability is investigated. Classical reliability measures are examined and compared with the new entropy based reliability measure proposed in this study. The novel entropy based reliability measure introduces a more consistent measure with the classical definition of travel time reliability than traditional measures. Furthermore, it measures uncertainty directly using the full distribution of the examined random variable where previously developed reliability measures only use first and second moments. Various approaches of measuring network reliability are also investigated in this study. Finally, feedback linearization control scheme

is developed for a ramp meter that is modeled using Godunov's conditions at the boundaries representing a switched system. This study demonstrates the advantages of implementing a feedback liberalized control scheme with recursive real time parameter estimation over the commonly practiced velocity based thresholds.

ACKNOWLEDGMENTS

I would like to acknowledge my advisor Dr. Pushkin Kachroo for his tremendous assistance, support, training, as well as for his enlightening innovative scientific approach and dedication to knowledge. I also acknowledge my co-advisor Dr. Alexander Paz for his valuable advice in Transportation related problems. In addition, I acknowledge my committee members, Dr. Rama Venkat, Dr. Ebrahim Saberinia, Dr. Yitung Chen, and Dr. Mohamed Trabia for dedicating some of their time to serve on my committee. I gratefully acknowledge the contribution of Freeway and Arterial System of Transportation (FAST) for their support and in providing the data. I also acknowledge the support of the Nevada Department of Transportation.

TABLE OF CONTENTS

LIST OF FIGURES

CHAPTER 1

Introduction

1.1 Motivation and Research Goal

Most modern systems are becoming increasingly networked such as transportation, communication, sensor, and power networks. These systems can be described as cyber physical complex networks since they feature a tight combination and coordination among physical elements, such as, human factors as well as computational science.

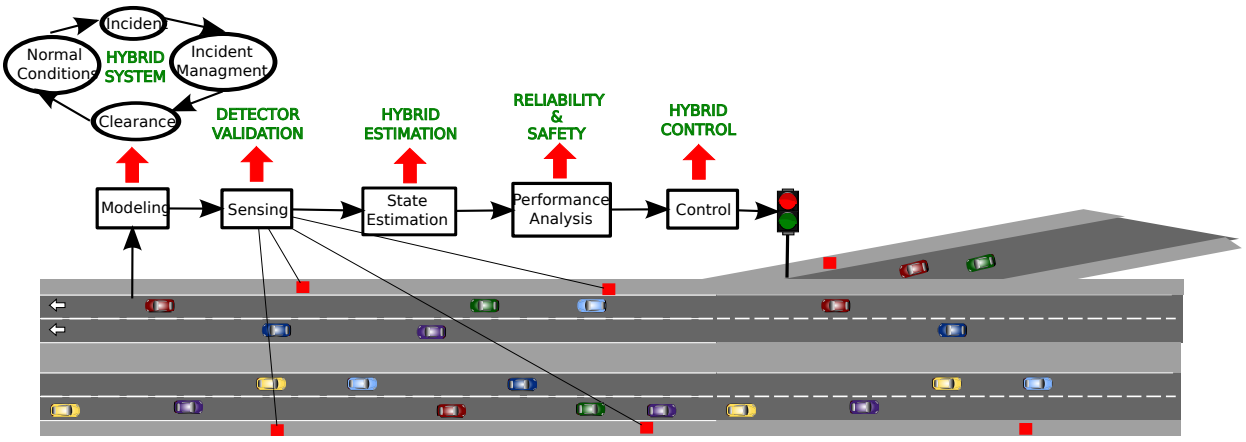

Figure 1.1: Overall research work

Traditionally, modeling of complex systems has been based either on continuous dynamics or on discrete modeling paradigms. However, most real systems have a combination of continuous and discrete dynamics, i.e. they can be viewed as hybrid dynamical systems. Hybrid dynamics provide us with solutions to extremely challenging control problems such as systems with major uncertainty. Therefore, a rigorous study

of deterministic and stochastic hybrid dynamical systems and networks is necessary for understanding the dynamics of such systems as well as for proper analysis and design in order to generate appropriate optimal solutions. Hybrid control provides us with solutions to extremely challenging control problems such as systems with major uncertainty, or nonlinear systems where continuous control laws are not applicable. This research will make original contributions to the very important emerging area of developing mathematical tools for complex systems and networks. The specific technique studied will be in the area of deterministic and stochastic dynamic systems that provides a powerful framework for studying such systems. Applications will be in sustainable transportation networks. However, many of the developed models can also be used in other cyber physical systems such as in communication networks where packet delivery is parallel to traffic in transportation systems as well as power systems where demand and service must be addressed. It is evident that concepts such as reliability, controls, safety, as well as data analysis compose a common ground to such cyber complex highly networked systems.

Interstate 15 (I-15) is one of the most important commute system in the Las Vegas valley. This cyber physical system is composed of networked physical as well as cyber elements. The physical elements are composed of traffic flow, human response, and roadway network; whereas the cyber element is composed of sensor networks, computational engines, data bases, and actuation. It is highly desired, by various agencies such as Nevada Department of Transportation (NDOT) as well as the commuter, to enhance the performance of this freeway stretch. Performance evaluation can be

embodied by different notions. One may consider safety as an indication of performance, other might consider travel time reliability as a good measure performance, and similarly, reduced congestion. These are all valid measures of performance, and there is no one measure that is the correct one. However, one can have a favorite measure based on the functionality of interest. For instance, travel time reliability is usually desired in manufacturing. In order to properly evaluate performance, the system must be "observable" or at least "detectable" in some sense. The I-15 is featured with detectors, radars as well as loop detectors, which collect traffic counts as well as speeds. Additional data is obtained from agencies that collect it such as incident data. In this research all possible data is obtained in order to have the best evaluation possible of the transportation system at stake. Hybrid modeling is recognized to be a suitable modeling strategy of the transportation system, as depicted in Figure 1.1. In this research, the hybrid dynamics modeling of traffic involves four discrete states corresponding to normal operations, an occurrence of an incident, incident management stage, and incident clearance stage. Formal modeling is used for implementation and verification of the discrete modeling. In each state the continuous dynamics of traffic flow is running. The continuous traffic flow is modeled macroscopically based on partial differential equations that normally are used to describe compressible fluids. The continuous models in each state are very similar in their construction; however, the parameters used are different in each model and highly depend on the physical change that is taking place due to nonrecurring events such as incidents. In addition to addressing certain performance measures, sensing, and modeling, this research also provides control schemes for the system based on the estimated data from mea-

surements. Ramp metering is a common actuation methodology that is used in the I-15. Therefore, this research develops hybrid control strategy for ramp metering and compares it to currently implemented ramp metering algorithms.

1.2 Contributions

This research scrutinize various attributes of complex networks; mainly, modeling, sensing, estimation, safety analysis, and control. In this study, formal languages and finite automata are used for modeling incident management processes. Safety properties are checked in order to verify the system. This method introduces a systematic approach to incident management protocols that are governed by mostly unsystematic algorithms. A portion of the used data in this study is collected by means of radar and loop detectors. A weighted t-statistics methodology is developed in order to validate these detectors. The detector data is then used to extract travel time information where travel time reliability is investigated. Classical reliability measures are examined and compared with the new entropy based reliability measure proposed in this study. The novel entropy based reliability measure introduces a more consistent measure with the classical definition of travel time reliability than traditional measures. Furthermore, it measures uncertainty directly using the full distribution of the examined random variable where previously developed reliability measures only use first and second moments. Various approaches of measuring network reliability are also investigated in this study. Finally, feedback linearization control scheme

is developed for a ramp meter that is modeled using Godunov's conditions at the boundaries representing a switched system. This study demonstrates the advantages of implementing a feedback liberalized control scheme with recursive real time parameter estimation over the commonly practiced velocity based thresholds. The specific contributions of this dissertation work are listed below.

1.2.1 Modeling

- **Formal Language Modeling of Incident Management:** Formal language and automata theory is used for modeling, analyzing, and implementing traffic incident management process.
- **Hybrid Modeling of a freeway on-ramp:** Godunov based conditions are used in determining boundary conditions of the hyperbolic PDE used in modeling traffic flow on a freeway section.

1.2.2 Sensing

- **Detector Validation:** A weighted t- statistics developed in order to compare a set of uncertain data with another set of uncertain data with various levels of uncertainty.

1.2.3 State Estimation

- **Hybrid Estimation:** Estimation techniques are developed in order to estimate from the data the time of occurrence of various events such as the time of incident and the time of incident clearance.

1.2.4 Performance Analysis

- **Reliability Theory:** Average travel time is a good indicator of the performance of a highway segment or a transportation network in general. However, by itself, it lacks information about the overall performance of the transportation system. Hence, for proper assessment of the transportation system's performance, this research develops and uses five different reliability measures for freeway and arterials in Las Vegas: variability based on normalized standard deviation, analysis of variance (ANOVA), average time mean estimation, reliability as a measure of non-failures, and information theory.

- **Entropy Based Reliability:** A novel travel time reliability is developed that is based on measuring the uncertainty of travel time from data.

- **Network Reliability:** Max-plus algebra is proposed in order to extend the reliability measure of a component to network reliability.

- **Bayesian Networks:** A Bayesian network is a probabilistic model which represents relationships between uncertain variables and can be used as a framework

for various applications. This research develops a Bayesian traffic safety analyzer using crash data and other surrogate information to estimate risks at various locations.

1.2.5 Control

- **Hybrid Ramp Control:**A hybrid control scheme is developed in order to maintain a given freeway segment at certain desired conditions.

1.3 Outline of the Dissertation

This dissertation is divided into the following chapters.

Formal Language Modeling of Incident Management is presented in Chapter 2. Flow Detectors Validation is in Chapter 3. Classical Reliability is in Chapter4, then Entropy-based Reliability is presented in Chapter 5. Chapter 6 presents the Min-Plus Semi-ring Algebraic Structure of Network Reliability. Bayesian Safety Analyzer is demonstrated in Chapter 7. Chapter 8 presents Hybrid Modeling and Control of Ramps. Finally the Conclusions are in Chapter 9.

Part I

Modeling

CHAPTER 2

Formal Language Modeling of Incident Management

2.1 Overview

This chapter discusses the modeling aspect of nonrecurring events as shown in Figure 2.1. Understanding nonrecurring events is crucial when investigating characteristics of complex networked systems. The reliability of network is a particular trait of interest that is directly influenced by such events which will be studied in later chapters. Furthermore, proper modeling of nonrecurring events is necessary for the system's state estimation which leads to implementing the appropriate control methodology.

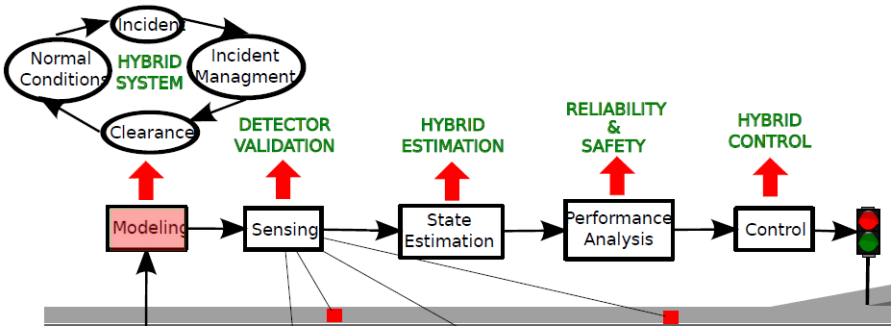

Figure 2.1: Overall research work

Traffic Incident Management is a multi-jurisdictional process. Complications with communications, compatibility, coordination, institutional responsibilities, and legal issues are inherent in the traffic incident management system. Increased delay in incident clearance due to various conflicts has vital economical, safety, environmental,

and social impacts. Therefore, a thorough and rigorous modeling of the system is necessary to better understand its properties and systematically discern issues that might arise. This study proposes the use of formal language and automata theory for modeling and analyzing the traffic incident management process. Incident management is a very practical discipline; however, theoretical modeling and analysis can help in finding inefficiencies in the system and improving it. Formal language and automata theory provides the foundation that has been used successfully in numerous hardware and software developments with applications in digital design, compilers, programming languages, etc. Every agency involved in the incident management process can be modeled as an individual processing unit that interacts with other units. Formal language and automata theory provide us with powerful tools for developing, analyzing, and debugging such models. Creating an incident management model with a systematic structure permits a methodical identification of the system's "bugs". This study demonstrates the development of models of some first response incident management agencies through a case study in the Las Vegas area using formal languages and automata theory. Sequence properties are checked for the developed models.

Glossary for Actions Used in Finite State Process (FSP) Models is presented in Table 2.1.

Table 2.1: Glossary

Action	Translation
alt_route	Alternative route
anthrtow	Another tow
arriveloc	Arrive to location
call_rc	call received
callf	Call fire department
congt_clrd	Congestion cleared (Program 2)
congtn_clrd	Congestion cleared (Figure 2.3)
congtnotclr	Congestion not cleared
driveloc	Drive to location
ernotarrv	Emergency responders have not arrived
ernotreq	Emergency responders are not required
ertaskincmplt	Emergency responders task is not complete
eqptavl	Equipment available
fbusy	Fire department is busy
fmbusy	Fire and Medical are busy
freq	Fire department is required
mbusy	Medical department is busy
mreq	Medical required
noeqpt	No equipment
rdnt_call	Redundant call
tow_nformed	Towing company is informed
townotavl	Towing truck not available
trfcjam	Traffic jam (Figure 2.7(b))
trfjam	Traffic jam (Program 2)

2.2 Introduction

In traffic flow operations, traffic incidents are non-recurring events that often cause delay due to congestion and safety hazards. These incidents account for approximately one third of all delays caused by traffic congestion on U.S. highways and are responsible for nearly 60% of delays triggered by weather, construction, and special events [2]. The operating capacity of a typical three-lane freeway segment is reduced by 63% during a one-lane obstruction and by 77% during a two-lane obstruction [3]. Incidents, such as a disabled passenger car parked on the shoulder of the roadway, reduce the available capacity by up to 17% [3]. The impact of traffic incidents stretches beyond safety degradation and traffic congestion. In addition, Human productivity loss and fuel waste are definite economical outcomes [4] [5]. In 2005, congestion costs were estimated to be $78.2 billion in 437 U.S. urban areas where 52 to 58% of the total motorist delay was due to traffic incidents [3]. The benefits of crash reduction or crash avoidance can be significant, as illustrated by an evaluation conducted by the Minnesota Department of Transportation in 2004. This evaluation reported that 68% of the monetary benefits of a traffic incident management program were due to the reduction in crashes.

When an incident occurs, medical, law enforcement, fire, and other public emergency agencies are usually among the first to respond. In addition, private agencies, such as towing companies and hazardous materials contractors, are most likely to be involved [2]. On one hand, the existence of specialized entities delivers high quality work in

handling tasks at the incident scene. On the other hand, this also raises challenges since each of these agencies has different priorities and views [2].

Moreover, every agency has a separate communication system through which dispatchers communicate information about the incident to their agents. The independence in communication leads to additional delays in the incident clearance process. Carson, et. al. [6] conducted a comprehensive evaluation of an incident response team program for the Washington State Department of Transportation, designed to determine its effectiveness. The study claims a 20.6 minute reduction in average duration of incidents from 1994 to 1995 resulting in $20,600 to $61,800 savings per incident [6]. This study concluded that an organized traffic incident management process is necessary that promotes integration and bonding of multi agency operations as well as communications at the incident scene. A well planned incident management system, using both formal and informal processes, improves efficiency and communications between the multi-jurisdictional responses, thus reducing incident clearance times and vehicle delays [4] [5]. However, an attempt to create such coordination faces with many obstacles that are inherent in the system, such as uncertainty, sudden events, resource shortage, faulty information, and disruption of infrastructure support [7]. In addition to support systems, incident management is currently formulated and implemented conventionally, based on manual methods that rely on personal experiences of the personnel from within the incident management field; which has its shortcomings [8]. The current conventional approach does not allow for conflict detection or for alternative incident management scenario evaluation due to time constraints [8].

Furthermore, personal experiences are likely limited or else widely varied, they also vary among people's different experiences which may lead to clashes at the incident scene. This often results in further conflicts and difficulties, thus adversely impacting the traffic operations.

This study proposes the use of formal languages and automata theory for modeling and analyzing the traffic incident management process. Formal languages and automata theory modeling allows us to perform rigorous debugging on existing and future incident management systems, covering wide range of possibilities for inefficiencies and problems for which we can find solutions. The modeling approach introduced herein provides the flexibility to evaluate any Incident Management process, depending on the various variables involved for a certain urban region. Through formal methods modeling, customized software tools can be developed for a specific region, significantly enhancing the Incident Management process. In Section 2.3, a literature review on previous work for Incident Management modeling will be discussed. Section 2.4, describes the IM process in the Las Vegas area as well as the Incident Command System (ICS). An overview of the modeling method and approach used are presented in Section 2.5. Section 2.6 presents a demonstration on how formal methods are used to model the IM process by means of a case study. Conclusions are provided in Section 2.7.

2.3 Literature Review

Effective traffic incident management systems consist of three main aspects: multiagency communications and control, decision making, and sharing of limited resources. In order for a model to be successful, these three aspects have to be addressed; otherwise, complications in the incident management system may be overlooked. In this section, some proposed approaches to improve Incident Management processes are discussed.

Sullivan [9] argues key issues in the document, *"Assessing the National Incident Management System;"* in specific communications. In his study, Sullivan evaluates private and public stakeholders that have key roles in the incident management system on a national level and also discusses the administrative or technological challenges. However, Fries [10], examines the effectiveness of specific Incident Management strategies, such as quick clearance laws. He argues that investing in advertisements regarding quick clearance laws are beneficial to the Incident Management process [10]. Skabardonis [11] also examines the effectiveness of specific Incident Management programs. Skabardonis compiled before and after data relating to the implementation of Freeway Service Patrol (FSP) programs. It was found that FSP contributed to the reduction of the number of accidents; however, no significant effect was found on the incidents duration [11]. Karlaftis [12] uses regression models and a five- year incident database in order to identify primary incidents' characteristics that increase the likelihood of secondary incidents. Pal [13] analyzes Incident Management data in order to make

recommendations to improve the Incident Management.

Konduri, et. al. [14] proposes incident prediction models based on analysis of incident patterns, frequency, and duration and uses them for improving the freeway management system by assessing various IM strategies. Scherer [15] proposes a statistical approach in order to model congestion caused by freeway incidents. Linear regression has shown evident relationships between incident severity and congestion levels that can be used in congestion level prediction [15]. Such models would be very useful in incident management systems; however, methods based on static data are not sufficient to comply with the required short term actions necessary in the most effective incident management systems [16]. An agent-based approach for monitoring, analyzing, and supporting Incident Management processes by error detection and providing support for such errors is proposed in [17]. Temporal Trace Language (TTL) was used as a tool for formal representations of system's properties. The author's approach is adequate; however, the scope of this modeling involves error detection for improving techniques in current incident management support systems that detect contradictory and unreliable information. This approach does not address broader issues in incident management, such as the overall interaction and harmony between the involved agencies, limited and shared resources, or liveness properties of the incident management system as a whole.

Ozbay [18] introduces Rutgers Incident Management System (RIMS) software. RIMS is an evaluation software that is able to compare different incident management tech-

nologies and programs as well as strategies [18]. Moreover, RIMS introduces a modeling method that can be used to build software for incident management. Mingwei in [8] proposes a real-time Evaluation and Decision Support System (REDSS) for IM that detects traffic incidents, estimates impacts of incidents, formulates guidance scenarios, and monitors and evaluates scenario implementations. REDSS integrates a series of information analysis and processing technologies such as data fusion, expert systems, data warehousing and, data mining [8]. However, REDSS has not yet been validated. Chen, in [7], recognizes the constraints on responder's capabilities to analyze coordination problems due to the requirement of rapidness in decision making. Therefore, a life cycle approach is introduced providing a broad and systematic view of activities relating to emergency response management. Roccetti introduces an inter-vehicular communication system design is proposed in [19]. This system provides the ability to quickly discover and transmit real time multimedia information from an incident location to the approaching first responders [19]. Kim in [20] introduces a conceptual model that explains the efficiency of decision-making of the Critical Incident Management Systems (CIMS) [21].

Researchers have demonstrated numerous attempts in improving the incident management process [8]; however, in the history of IM, such attempts have been focused mainly on supporting systems. Such systems are used, in large part, to assist participating agency in assigning tasks and making decisions. These systems may or may not integrate all aspects necessary for a successful incident management modeling as well as implementation of strategies. A successful IM necessitates a broad and

integrated response to incidents [22]. The formal languages modeling proposed in this study forms a suitable environment for validation and debugging of supporting expert systems, thus increasing efficiency and accuracy of such systems.

After a great deal of calibration, simulation and modeling based tools are very suitable for evaluation and comparison purposes. For instance, a paper by Sinha develops methodology to predict incidents using such models as Poisson and Negative Binomial.etc. Methodology based on the formal language theory does not compete with these excellent methods. Instead, it provides additional tools to improve the overall system by concentrating on finding "process bugs". A regular, discrete, simulation-based modeling approach serves a different purpose in Incident Management Modeling than the proposed methods. Hence, since these methods work on different aspects of the incident management process, their results do not address comparable methodologies. In this study, an incident management representation is proposed that provides the ability to account for any desired aspect of the IM process and to integrate the aspects into one systematic model. Moreover, this proposed representation can specify as well as verify properties for the system before implementation. The proposed model provides the ability to validate and verify existing incident management processes, including supporting systems. Most importantly, it provides a method to verify the interaction between such systems as well as between multi-agency processes.

2.4 The Incident Command System (ICS) and Incident Management in the Las Vegas Area

According to the Federal Highway Administration's *Simplified Guide to the Incident Command System for Transportation Professionals* (FHW-HOP-06-004, 2006), "The ICS is a systematic tool used for the command, control, and coordination of an emergency response [23]". The purpose of the ICS is to improve interagency communications through common terminology and operating procedures. However, according to this simplified guide the incident command system (ICS) by the FHWA [23], only 64% of surveyed agencies indicate that an ICS is used on-scene to manage traffic incidents in their jurisdiction. Until recently, Las Vegas has been one of the fastest growing cities in the United States. Consequently, highway capacity investment has not been able to keep pace with the growth in traffic; therefore, major roadways have experienced substantial congestion during off-peak periods as well as peak periods. Users cost per hour for a closure on Highway I-15 was recently estimated at $240,000 and can go up to $750,000 during the afternoon peak period. Report produced by Iteris [24] identified the existing institutional relationships, which include operational agreements between various agencies for the Las Vegas area. Furthermore, this report showed the responsibilities of various organizations during an incident management process. Emergency responders in Las Vegas include, but are not limited to, the following agencies: Department of Safety - Nevada Highway Patrol (NHP), Las Vegas Metropolitan Police Department (LVMPD), Regional Transportation Commission of Southern Nevada (RTC), Freeway Arterial Transportation System (FAST), Clark

County Office of Emergency Management and Homeland Security, Clark County Fire Department (CCFD), and Coroner's Office.

In the hopes of resolving any conflicts resulting in an improved communications, enhanced coordination, and an efficient incident management process in the Las Vegas area, a local traffic incident management (TIM) Coalition has been formed where various emergency responder agencies meet and discuss regional issues involving traffic incidents. The Freeway and Arterial System of Transportation, or FAST, operates the freeway and arterial traffic signal systems. FAST also supports incident management through traffic control [24]. According to the Incident Management Strategies Draft Report, incident management is the key motivation for the existence of FAST in Las Vegas. Specifically, FAST provides data and tools to identify incidents and also assists with remote monitoring of the incidents.

Las Vegas has witnessed drastic improvements in the incident management process as a result of FAST efforts in detecting and monitoring incident occurrences and also a result of TIM's efforts to resolve any miscommunication issues among local agencies. However, from analyzing crashes obtained from LVMPD (arterial) and NHP (freeway), it was found that the average management and clearance times of incidents need improvement, as presented in Tables 2.2(a) and 2.2(b) and as depicted in Figures 2.2(a) and 2.2(b). Thus, a systematic approach through quantitative modeling is necessary for revealing inefficiencies of the system and understanding its nature.

Table 2.2: Average Arrival, Management, and Clearance times for incidents that occurred on the I15 and arterials in the Las Vegas area

(a) LVMPD data

Year	AVG Arrival Time	AVG Management	AVG Clearance Time
2003	0:18:04	1:05:16	1:23:29
2004	0:22:37	1:11:20	1:33:39
2005	0:25:08	1:10:29	1:35:37
2006	0:25:09	1:13:12	1:38:21
2007	0:21:51	1:13:28	1:34:38
2008	0:19:47	1:43:21	1:46:00

(b) NHP data

Month	AVG Arrival Time	AVG Management	AVG Clearance Time
Jul-08	0:11:30	1:12:04	1:30:01
Aug-08	0:11:10	1:13:22	1:30:27
Sep-08	0:11:06	1:13:18	1:31:35
Oct-08	0:10:53	1:16:39	1:33:47
Nov-08	0:10:43	1:08:20	1:25:59
Dec-08	0:13:21	1:10:58	1:31:33
Jan-09	0:11:22	1:13:12	1:28:49
Feb-09	0:12:12	1:08:40	1:27:29
Mar-09	0:11:42	1:07:50	1:24:54
Apr-09	0:12:38	1:08:42	1:27:07
May-09	0:11:22	1:07:06	1:23:33
Jun-09	0:11:52	1:07:18	1:26:40

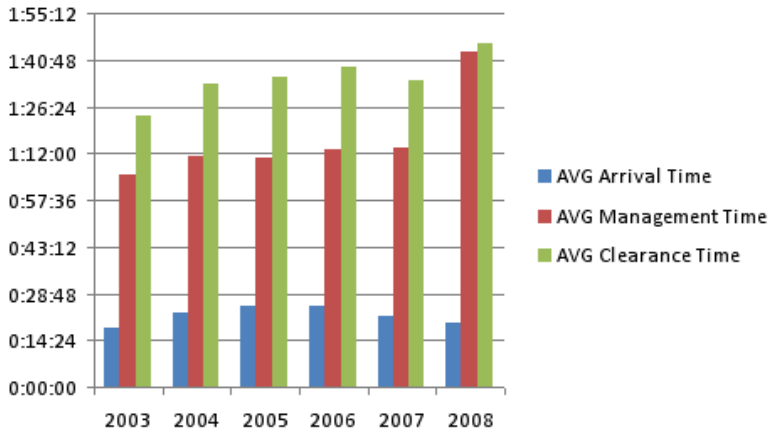

(a) LVMPD data, incidents occurred on arterials

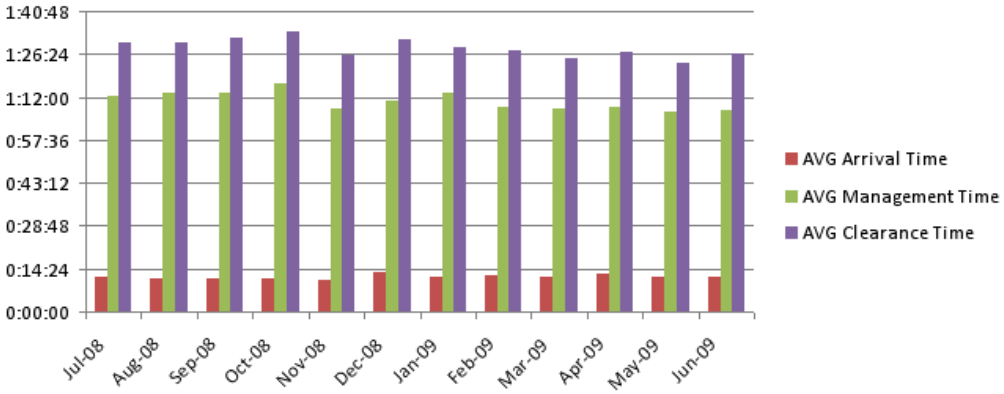

(b) NHP data, Incidents occurred on the I15

Figure 2.2: Average arrival, management, and clearance times for incidents that occurred in the Las Vegas area

2.5 THEORETICAL BACKGROUND AND MODEL APPROACH

2.5.1 Basic Definitions

Alphabet, $\sum$ is a finite nonempty set of symbols.

Letter is an element of the alphabet. Letters are not restricted to single characters.

Word a sequence of symbols $a_1a_2a_3 \ldots a_n$ of length n where $a_i \in \sum \forall \in N$.

Empty Word, λ is the word consisting of zero letters or it is the empty string.

Deterministic Finite Automaton is a mathematical model of a machine that accepts a specific set of words generated using a certain given alphabet $\sum$. It can be considered as finite state control.

Formally, a deterministic finite automaton is defined as follows:

$\{\sum, S, s_0, \delta, F\}$

1. $\sum$: the input alphabet
2. S : a finite nonempty set of states
3. s_0 : the initial state
4. δ : the state transition function, $\delta : S \times \sum \rightarrow S$
5. F : the set of finite or accepting states.

2.5.2 Formal Languages and Automata Theory Overview

The purpose of formal languages theory is to bring order to complex system anarchy [25]. Formal languages are characterized by predefined rules, such as formal notations in mathematics, logic, and computer science [26, 25]. A finite automaton is a string processor that assists in defining certain formal languages by accepting or rejecting a sequence of symbols [25]. Applications that require pattern recognition techniques have fundamental interest in finite automata [26]. A deterministic finite automaton consists of a finite number of states or conditions in which a system can exist. Only one of these states can be an "initial" state. Additionally, such an automaton must contain at least one or more "terminal" or "accepting" states. Transitioning may be performed through two different actions, either switching to another state or remaining in the current state [26]. Execution of state transition depends on the current state and the action identified by the symbol.

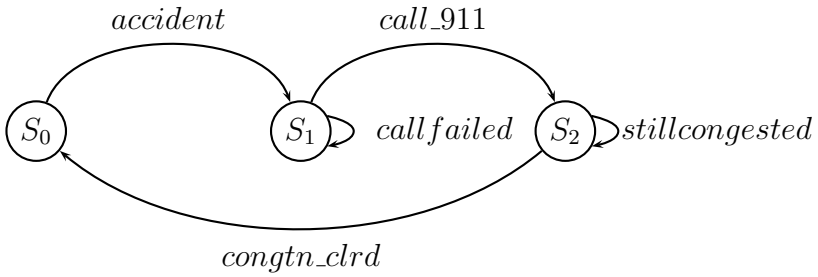

Figure 2.3: A simple state diagram based model for an incident occurrence

Using finite automata, a simple example of an incident may be modeled in a pictorial form called a state diagram, as depicted in 2.3. A glossary for Finite State Process (FSP) actions is introduced before the "Introduction" section in this study. State

"S_0" represents a pre-accident situation which might imply traffic is in a free-flow state. The symbol "*accident*" represents an occurrence of an incident that causes the system to switch to state "S_1" implying an incident scene. Once the system is in state "S_1" only two transitions are possible represented by the symbols "$call\_911$" and "$callfailed$"; the first symbol which causes the system to switch to state "S_2" implying that the incident is in the management process. The second symbol causes the system to remain in the same state, implying that no advancements can be made unless an emergency responder is informed. Once the system reaches the management state, it can switch states when congestion is cleared ("*congtn_clrd*") and go back to free traffic flow in pre accident conditions (state "S_0"). Otherwise, it remains in the management state "S_2" " if congestion is not cleared ("*stillcongested*").

The following is the deterministic finite automaton of an incident model:
$\{\sum, S, s_0, \delta, F\}$

1. $\sum$: *accident*, $call\_911$, $callfailed$, *stillcongested*, *congtn_clrd*.
2. $S : S_0, S_1, S_2$.
3. $s_0 : S_0$.
4. δ :
   (a) $(S_0, accident) \rightarrow S_1$
   (b) $(S_1, callfailed) \rightarrow S_1$

(c) $(S_1, call\_911) \rightarrow S_2$

(d) $(S_2, stillcongested) \rightarrow S_2$

(e) $(S_2, congtn\_clrd) \rightarrow S_0$

5. $F : S_0$.

2.5.3 Modeling and Simulation Software

Labeled Transition System Analyzer (LTSA) v3.0 and Modeling Software is used to construct Finite State Processes (FSP) and to perform property checking on developed models. This is a Java-based open source software. The exact algorithms as well as executions are given in this study under Programs.

Modeling the evolution of an incident scene by using finite automata is methodically appropriate in terms of a sequence of events. Furthermore, many transitioning possibilities can be considered, depending on various conditions, which add flexibility in modeling any Incident Management system. Every Incident Management process, however, is an interaction between multiple processes occurring concurrently. Thus, concurrency is an aspect that must be addressed in the Incident Management model.

Shared actions in Labeled Transition Systems (LTS) Analyzer provide the ability to model concurrent finite state machine processes. They are described textually as finite

state processes, and are displayed and analyzed by the LTS analysis tool [27]. The LTS analysis tool provides the ability to structure complex systems as sets of simple activities represented as sequential processes using Finite State Processes (FSP) [27]. Processes can overlap or run concurrently, reflecting real-world situations as in the Incident Management process.

Program 1 An FSP model for an incident occurrence process

```
PRE_ACCIDENT   = (accident->ACCIDENT),
ACCIDENT       = (call_911->CLRNSinPROCESS|callfailed->ACCIDENT),
CLRNSinPROCESS = (congtn_clrd->PRE_ACCIDENT|stillcongested->CLRNSinPROCESS).
```

Finite state processes (FSP) have a predefined language for their description. Actions can be de- scribed using the action operator " $\rightarrow$ ". For instance, $(x \rightarrow P)$ describes a process that initially engages in the action "x" and then behaves as described by process P [27]. In order to model choice, the choice operator "|" is used, for instance $(x \rightarrow P|y \rightarrow Q)$ describes a process that may engage in either action "x", which leads the system to behave as described by process P, or action "y" leading the system to behave as described by process Q [27]. Program 1 demonstrates an FSP process illustrating the incident model described in Figure 2.3.

Concurrency can be modeled by using the parallel operator "||". For example, $(P||Q)$ represents the concurrent execution of the processes P and Q [27]. Parallel processes have the capability to interact via shared actions which are executed at the same time by all participant processes [27].

Program 2 LVMPD model integrating three conccurent processes, Calltaker, Dispatch, and Officer

```
//CALL TAKER PROCESS
CALLTAKER_LVMPD = (call_911->MFP_QUESTION|nocall_911->CALLTAKER_LVMPD),
MFP_QUESTION    = (medical->MED_TRNSFR|fire->FIRE_TRNSFR|police->POLICE_TRNSFR),
MED_TRNSFR      = (med_busy->MED_TRNSFR|trnsfr_med->CALLTAKER_LVMPD),
FIRE_TRNSFR     = (fire_busy->FIRE_TRNSFR|trnsfr_fire->CALLTAKER_LVMPD),
POLICE_TRNSFR   = (police_busy->POLICE_TRNSFR|trnsfr_police->CALLTAKER_LVMPD).

//DISPATCH PROCESS
DISPATCH_LVMPD  = (trnsfr_police->INFO_LVMPD|nocall_lvmpd->DISPATCH_LVMPD),
INFO_LVMPD      = (getinfo_lvmpd->RDNCHECK_LVMPD),
RDNCHECK_LVMPD  = (rdnlvmpd_call->DISPATCH_LVMPD|newlvmpd_call->ASSN_OFFICER),
ASSN_OFFICER    = (officer_order->OTHER_ER|officer_unavl->ASSN_OFFICER),
OTHER_ER        = (nother_er->DISPATCH_LVMPD|fm_req->CALL_FM|m_req->CALL_M|f_req->CALL_F),
CALL_FM         = (fm_busy->CALL_FM|called_fm->DISPATCH_LVMPD),
CALL_M          = (m_busy->CALL_M|called_m->DISPATCH_LVMPD),
CALL_F          = (f_busy->CALL_F|called_f->DISPATCH_LVMPD).
POLICE_BLOCKEDOPT = (another_route->GOtoSCENE|no_other_route->STUCK_LVMPD),

//LVMPD OFFICER MISSION PROCESS

OFFICER_LVMPD   = (nofficer_order->OFFICER_LVMPD|officer_order->GOtoSCENE),
GOtoSCENE       = (officer_drive->STREET_CON),
STREET_CON      = (trfjam_lvmpd->STREET_CON|blocked_police->POLICE_BLOCKEDOPT|arrive_police->
                                    SCENE_LVMPD),
SCENE_LVMPD     = (notneeded_er->TOWorNOT|fm_needed->GET_FM|m_needed->GET_M|f_needed->GET_F),
GET_FM          = (fm_busy->GET_FM|called_fm->TOWorNOT),
GET_M           = (m_busy->GET_M|called_m->TOWorNOT),
GET_F           = (f_busy->GET_F|called_f->TOWorNOT),

TOWorNOT          = (tow_needed->CONTACT_TOW|tow_notneeded->ER_ARRIVAL),
CONTACT_TOW       = (tow_notavl->CONTACT_TOW|tow_informed->ER_ARRIVAL),
ER_ARRIVAL        = (notaller_arrived->ER_ARRIVAL|towarrive_loc->ERTASK_COMPLETION),
                                        //aller_arrived=towarrive_loc
ERTASK_COMPLETION = (towdone_goback->TRAFFIC_MGT|ertasks_notcmplt->ERTASK_COMPLETION),
                                        //ertasks_cmplt=towdone_goback
TRAFFIC_MGT       = (congtn_notclrd->TRAFFIC_MGT|congtn_clrd->OFFICER_LVMPD).



//CONCURRENT PROCESS
||LVMPD     = (CALLTAKER_LVMPD || DISPATCH_LVMPD || OFFICER_LVMPD).
```

Since FSP provides the ability to model parallel processes as well as their interactions, the incident model can be expanded to include an emergency response agency where the occurrence of an incident and the agency's operation are running in parallel and have a shared action "*call*_911". Program 2 illustrates the model of LVMPD based on the corresponding agency in Las Vegas.

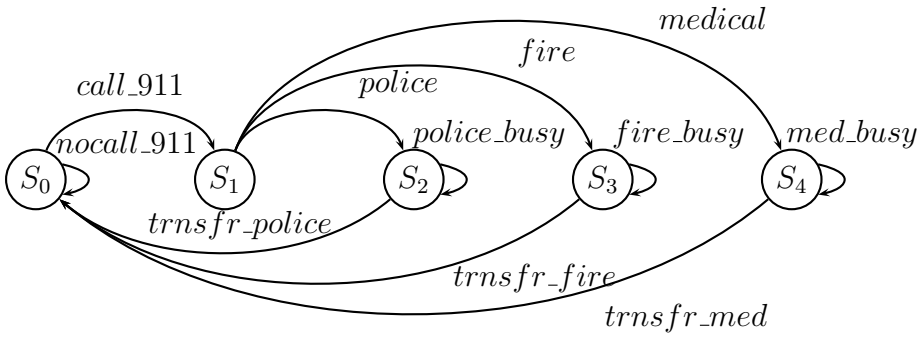

Figure 2.4: A state diagram for the call taker process in the LVMPD model

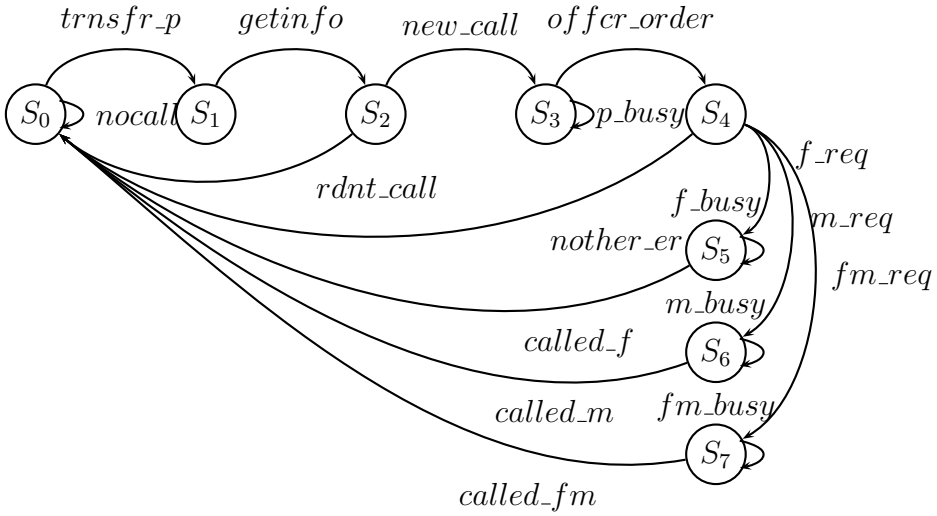

Figure 2.5: A state diagram for the dispatch process in the LVMPD model

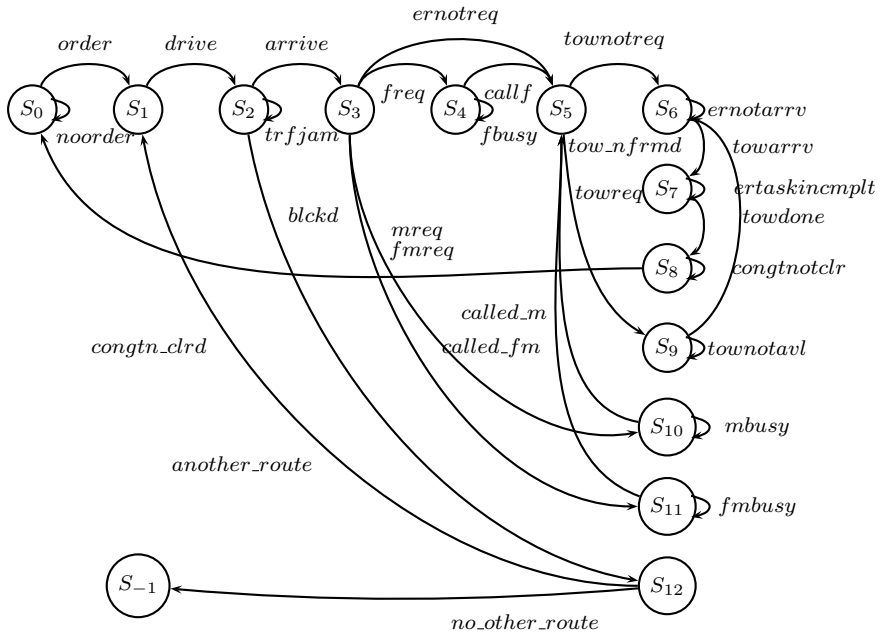

Figure 2.6: A state diagram for the officer process in the LVMPD model

As demonstrated in Program 2, there exist within LVMPD several processes that are executed in parallel and interact through shared actions. LVMPD has three main separate entities that function concurrently: call takers, dispatchers, and officers. When an accident occurs and 911 is dialed ("call911"), a 911-operator (CALLTAKER) from LVMPD will answer the call. The operator has three options for transferring the call: Police, Fire, or Medical. The call will be transferred to the requested agency. Freeway incidents are under NHP's jurisdiction. Therefore, the call will be transferred to NHP if incident location is freeway. If police is requested, LVMPD dispatch will receive the call, accomplished by the shared action "trnsfr police", then, LVMPD will acquire information about the incident; verify redundancy of the call; send an officer to the scene (which immediately starts the process of the officer through the shared action "officer order"); contact fire, medical, or both depending on the severity of the

incident; and then go back to the initial state, indicating that dispatch is available to accept new calls. As 911-operators and dispatchers are available to receive new calls, an officer is driving to the incident scene and could be faced with various conditions, such as traffic congestion, blocked streets, and faulty information about the actual incident severity. These are all examples of possible scenarios that can be considered in the model. The officer's task is not accomplished until the system returns to normal conditions. This acknowledgment is achieved by means of the shared action "congt-nclrd" between the LVMPD model and the incident model, as described in Figure 2.3. Figures 2.4, 2.5, and 2.6 demonstrate the state diagram for the LVMPD model in Program 2.

Executing the three processes concurrently produces 520 different states, and the illustration of that becomes challenging to express pictorially. Using FSP and LTSA, properties of states and transitions for the system can be specified and then analyzed. If a system satisfies a given property, then that property is true for every possible execution [27].

There are mainly two types of properties that are of fundamental interest: safety and liveness. Informally, a safety property guarantees that "nothing bad happens", whereas a liveness property guarantees that "something good eventually happens". Using temporal logic, a canonical safety property can be expressed as $\Box p$, whereas a

liveness property is of the form $\Diamond p$ [28]. Formally, p is a safety formula if and only if (iff) any sequence p' violating p, contains a prefix $p'[0..k]$ all of whose infinite extensions violate p [28]. p is a liveness formula iff any arbitrary finite sequence $s_0,\ldots,s_k$ can be extended to an infinite sequence satisfying p [28].

In the LTS analyzer software, liveness property is checked by using the progress property, of which liveness is a subclass. A progress property is violated if a terminal set of states are found that do not contain any of the progress set actions. In other words, if the officer depicted in Figure 2.6 reaches a state that does not provide a transition back to the desired state for instance, the action "no other route" is chosen - then the system is in state " - 1," which does not provide an action for recovery or for reaching "cngstn clrd" action; at that point, the system is not alive or progress property is not satisfied for "cngstn clrd". The safety property is verified by specifying a set of actions that the system must satisfy at all times. This specification is executed concurrently with the system's model for analysis. A case study is presented in Section 2.6, using an existing IM model and analyzed using LTS tools.

2.6 Case Study

In a meeting held by the local traffic incident management (TIM) team, where representatives from various emergency responder agencies had gathered in order to discuss regional issues involving traffic incidents, a certain incident (a rollover) that occurred in Las Vegas was the center of discussion. In the rollover, towing services were needed. Therefore, a private towing company was contacted with some information about what kind of equipment was needed and the location of the rollover. However, the tow truck arrived 30 minutes late. Upon arriving, the wrong vehicle was towed. At that point, it was discovered that different equipment was required to tow the vehicle of interest. After that, the officer and the tow company discussed whose responsibility it was to clean-up the scene. This process delayed the scene clearance by two hours. Clearly, such complications are a result of decisions that are made in real time. A systematic way to discover and solve possible disruptions does not exist, leading to inefficiencies inherent in the present system.

In order to model the Incident Management process in the rollover case, the incident and LVMPD models presented in Programs 1 and 2 are used. A model describing the tow company operation is presented in Program 3 takes into consideration the issues discussed relevant to this specific case.

Program 3 Tow company model integrating two concurrent processes Dispatch and Driver

```
//DISPATCH PROCESS
DISPATCH_TOW      = (tow_informed->INFO|nocall->DISPATCH_TOW),
INFO              = (get_info->RDN_CHECK),
RDN_CHECK         = (rdn_call->DISPATCH_TOW|new_call->GIVE_ORDER),
GIVE_ORDER        = (driver_order->DISPATCH_TOW|driver_unavl->GIVE_ORDER).

//TOW MISSION PROCESS
DRIVER_TOW        = (no_order->DRIVER_TOW|driver_order->GET_EQPT),
GET_EQPT          = (eqpt_unavl->GET_EQPT|eqpt_avl->READYtoDRIVE),
READYtoDRIVE      = (drive_loc->TRAFFIC_SITUATION),
TRAFFIC_SITUATION = (traffic_jam->TRAFFIC_SITUATION|blocked->BLOCKED_OPT|towarrive_loc->EVAL_LOC),
BLOCKED_OPT       = (alt_route-> READYtoDRIVE|no_alt_route->STUCK),
EVAL_LOC          = (wrong_eqpt->GET_EQPT|truck_notneeded->RESOURCE_WASTE|right_eqpt->WAITtoTOW),
RESOURCE_WASTE    = (drive_back->DRIVER_TOW),
WAITtoTOW         = (waittotow->WAITtoTOW|cantow->CANTOW),
CANTOW            = (another_tow->CANTOW|towdone_goback->DRIVER_TOW).

//CONCURRENT PROCESS
||TOW_COMPANY     = (DISPATCH_TOW || DRIVER_TOW).
```

The towing company has two concurrent processes: 1) dispatching which receives calls and information from customers; and 2) delivering ('driver') the proper equipment to the scene. State diagrams for the towing company model are depicted in Figures 2.7(a) and 2.7(b).

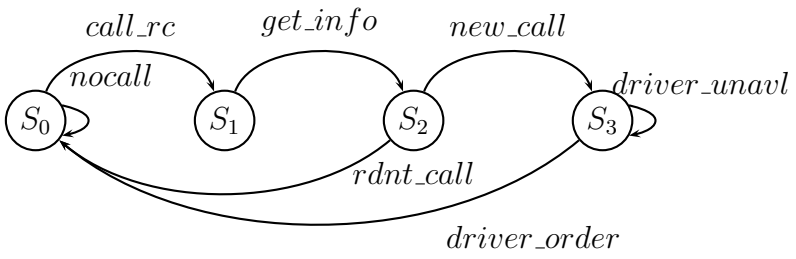

(a) Dispatch process

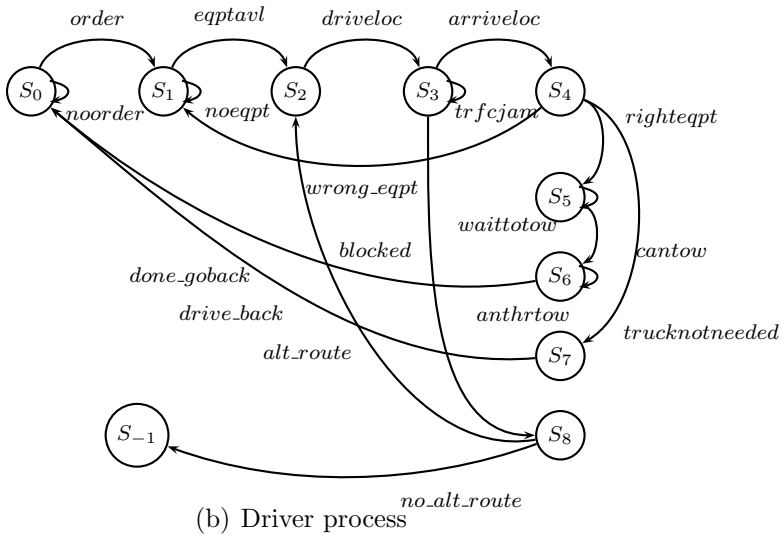

(b) Driver process

Figure 2.7: State diagrams for the tow company model

The state diagram representation of the towing company, which includes the two processes "Dispatching" and "Delivering," becomes too complicated to represent pictorially. After the models of the incident scene, LVMPD, and Towing Company are obtained, they are executed in parallel by the process described by the FSP in Program 4.

Program 4 IM process as a concurent execution of three processes tow company, LVMPD, and Incident scene

```
||ER_MNGMNT = (TOW_COMPANY || LVMPD ||PRE_ACCIDENT)
```

Safety and liveness properties for the system are verified. Safety property is verified by the process illustrated in Program 5, which indicates that at every state, the system is not going into a situation where the process is blocked. The results of the safety analysis execution for the complete Incident Management model and the towing company model are depicted in the simulation results in Program 6.

Program 5 Safety property specification

```
property ACCIDENT_RESOLVED =(accident->call_911->congtn_clrd->ACCIDENT_RESOLVED).

||ER_MNGMNT  = (TOW_COMPANY || LVMPD ||PRE_ACCIDENT|| ACCIDENT_RESOLVED).
```

Program 6 implies that there exists a trace where the system does not comply with the safety requirement. Thus, the system is not safe and requires improvement in the specified trace. In this case study, the system is not safe since the officer can reach a blocked state that prevents the arrival to the incident scene. Other safety checks may be specified for the Incident Management system or the individual agencies.

Program 6 System verification for safety property

```
Trace to property violation in LVMPD.OFFICER_LVMPD:
accident
call_911
police
trnsfr_police
getinfo_lvmpd
newlvmpd_call
officer_order
officer_drive
blocked_police
no_other_route
Trace to property violation in DRIVER_TOW:
call_rc
get_info
new_call
driver_order
eqpt_avl
drive_loc
blocked

no_alt_route
```

Liveness property is specified by the process illustrated in Program 7 which provides that the system will eventually reach a certain "acceptable" state; the desired action in this case would be congestion clearance "cngstn clrd." The analysis results of the liveness check program execution is demonstrated in Program 8.

Program 7 Liveness property specification

```
progress LVMPD_MISSION_ACCOMPLISHED = congtn_clrd
```

Formal Methods modeling allows for two types of property checking safety and liveness. After the models were created, the LTSA software was used in order to perform properties checking. Programs 5 and 7 show the exact command lines for checking safety and liveness, respectively. Program 6 and 8 show the results after the execution of the safety and liveness commands. The execution of the safety checking is

Program 8 System verification for liveness property

```
Progress Check...
-- States: 14 Transitions: 107 Memory used: 4022K
Finding trace to cycle...
Finding trace in cycle...
Progress violation: LVMPD_MISSION_ACCOMPLISHED
TOW_MISSION_ACCOMPLISHED
Trace to terminal set of states:
accident
call_911
police
trnsfr_police
getinfo_lvmpd
newlvmpd_call
officer_order
officer_drive
blocked_police
no_other_route
Cycle in terminal set:
nocall
Actions in terminal set:
no_order, nocall, nocall_911, nocall_lvmpd,
 notaller_arrived, stillcongested

Progress Check in: 62ms
```

demonstrated in Program 6, where it lists the accepted strings by the given automata model. However, it reaches the state "no_alt_route."This clearly indicates that, at some point in time, the process could enter an undesired state. Similarly, when liveness checking was executed, the software entered the "stillcongested" state, indicating that complete clearance is not accomplished. Obtaining these results depends greatly on the user-defined model.

The liveness check indicates that the system will not reach the desired state if it reaches one of the listed terminal states. The analysis in Program 8 recognizes the set of terminal states where progress property is violated. It also provides the trace to terminal states. Therefore, the system is not "alive" and requires improvement in the indicated actions. Even though the issues in the rollover incident were taken

into consideration in modeling the IM system, analysis of the model has identified a trace that leads to the action "no other route." This action is also recognized to be a member of the terminal set whose members avert the system's progression.

Ultimately, every Incident Management process should be live, implying it will always eventually reach a desired terminal state where the incident is cleared. Ideally, every Incident Management process should be perfectly safe, signifying that the system is always safe. Safety can take various forms, according to which specifications are executed. For instance, a certain Incident Management system may be considered safe if delay does not exceed a certain amount or if only certain routes are allowed.

2.7 Conclusions

This study demonstrated incident management modeling using formal languages and automata theory. Formal languages methodology provides the ability to perform rigorous debugging and analysis through which robustness of the Incident Management system can be achieved upon implementation. This approach allows analysis to be conducted of processes concurrently executed processes that have specifications for

liveness and safety properties specifications. The purpose of this approach is to model the traffic management processes in various coordinating agencies and then to find out if undesirable situations, such as "semaphores locking" exist. This method offers flexibility in modeling various Incident Management systems that account for many possible existing scenarios. Formal modeling can lead to the development of customized systems resulting in a more successful Incident Management process. The approach studied in this study can be expanded to include a wider range of resources for every process within the agencies as well as to model additional agencies that might be involved in the Incident Management process. In addition, this model can be enhanced to include real-time information within the states representing traffic conditions or other continuous, random activities. Finally, real-time data and statistics can be incorporated to support predictions and estimations.

Using formal methods, modeling provides practical and accessible techniques that aid evaluating designs for concurrent software. The incident management process is composed of a combination of sequential and concurrent events that are performed by multiple agencies. Therefore, it is inevitable that incident management software must feature high level of concurrency in its design. Formal methods are found to be very suitable and natural for incident management modeling, from which incident management software can be developed. Using formal methods modeling and its associated features, such as concurrency and property checking, can provide flexible and appropriate tools for software design, leading to enhancement in communica-

tions, response, and management. From a practical point of view, formal methods modeling as well as associated software are used in order to ensure that the incident management process is well defined. The user - and in this case, the user can be any of the responder agencies, the Department of Transportation, or any party that has an active role in managing incidents - takes an active role in determining the structure of the model and defining the desired safety and liveness properties.

Formal methods based approach is particularly useful for complex systems where high levels of hierarchy and concurrency are required. Complex models can be built based on modular structure. The software allows modular interaction through event sharing. This method is also useful when quantification of qualitative procedures is needed. For instance, the various Incident Management systems across the nation are evaluated based on the Incident Command. However, the Incident Command system stands as a document that is described qualitatively. This introduces challenges in achieving a common means of evaluation as well as a common structure among the different IM systems.

This modeling scheme will help us understanding nonrecurring events for investigating characteristics of complex networked systems. The reliability of network is a particular trait of interest that is directly influenced by such events which will be studied in later chapters. Furthermore, proper modeling of nonrecurring events is necessary for the system's state estimation which leads to implementing the appropriate control

methodology.

Part II

Validation and Estimation

CHAPTER 3

Flow Detectors Validation

3.1 Overview

This chapter discusses the detector validation aspect of complex networks as shown in Figure 3.1. In this chapter, we examine the detectors that were used in order to collect most of the data on the roadway network treated in this research. The detectors' counts are compared with manual video counts. T-statistics was used since both sets of data are experimental and the actual mean is not available. A weighted statistical approach is developed in order to give more weight to data obtained from clear videos. Additional statistical processing is performed in order to remove the bias of the video ratings since they are assigned by different people.

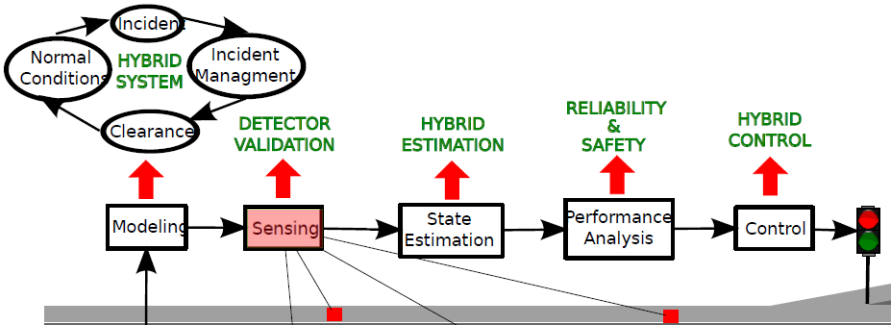

Figure 3.1: Overall research work

3.2 Introduction

According to the FAST/NDOT inter-local agreement for the freeway management system (FMS) scope of service, traffic volumes from Freeway Flow Detectors (FDD) need to be compared and verified. The total lane-by-lane traffic counts need to be verified to assure that the FDD is properly aligned and calibrated. This Scope of work outlines tasks for the implementation of traffic count verification for the freeway flow detectors on segments of I-15, US-95 and CC 215. FAST provided traffic counts and corresponding videos of traffic flow extracted from the FMS database and freeway surveillance videos of the same time periods and locations to be verified. UNLV TRC verified the traffic counts (lane-by-lane) from the videos. Data analysis was applied to the traffic counts and verification, and this study was generated to document the verification results.

This study provides methods for analysis and hypothesis testing for paired data where one source of data has to be tested against another source for validation, which has varied levels of reliability. In this work, traffic counts for some highway locations obtained from flow detectors had to be validated against the data obtained by manual counting of video data obtained from those sites. However, the video data had various levels of clarity that was recorded by the human observers, and hence a technique that performed validation with such recorded data with variable accuracy was needed. This method was developed in the project.

3.2.1 Tasks Performed

1. **Data acquisition:**

   (a) Data from 146 detectors was provided.

   (b) Videos that correspond to the same time frame of the given detector data were provided

   (c) The GIS information on FAST detectors was provided in a kml file in the Google earth format.

2. **Manual video counting for the validation process:**

   (a) Adobe Premier Pro was used to edit the videos to fifteen minute time frames that correspond to the provided data.

   (b) Adobe Photoshop was used to draw a line on a still frame from the video which was used as a reference point for counting each lane.

   (c) Multiple lane data were extracted simultaneously by assigning one student to each.

   (d) A difficulty rating for each lane with 0 being the easiest and 10 being the hardest was recorded.

   (e) One highly rated video was chosen and recounted by students multiple times in order to determine the accuracy of the manual counting method used.

3. **Data Analysis:**

(a) Analysis was performed on the percent differences between the detector and manually counted video data.

(b) A method for identifying possibly faulty detectors was developed and executed.

(c) A method for using video quality ratings was developed for analysis.

(d) This new method was used to perform data analysis.

4. **Recommendations based on the work performed were developed**

3.2.2 Software Tools

- Adobe Premier Pro
- Adobe Photoshop
- Microsoft Excel
- R - statistical software

3.3 Background

According to the FAST/NDOT inter-local agreement for the freeway management system (FMS) Scope of Service, traffic volumes from freeway flow detectors (FDD) need to be compared and verified. The total lane-by-lane traffic counts need to be verified to assure that the FFD is properly aligned and calibrated.

3.3.1 Project Description

The scope of work performed at the Transportation Research Center (TRC) at UNLV for the implementation of traffic count verification for the freeway flow detectors on segments of I-15, US-95 and CC 215 involved the following main steps:

1. Obtaining the list of detectors and their location
2. Obtaining the data from the detectors and the corresponding video data for comparison of volume data obtained at 15 minutes interval for the various lanes
3. Performing manual count of volume data
4. Performing statistical analysis of the flow detector data and the manual counts

3.3.2 Methodology

FAST/NDOT provided videos of traffic flow recorded at the sensors verified. Adobe Premier Pro was used to edit the videos to fifteen minute time frames that correspond to the provided data. Adobe Photoshop was used to draw a line on a still frame from the video. The line would depict the cross section of the freeway where the sensor would be counting cars. During the manual counts, one student was assigned to one lane, so that multiple lane data could be extracted simultaneously. Due to vehicles switching lanes and other factors that made counting difficult, the overlayed line was used as a reference point for counting each lane.

After each viewing, the counts were recorded in a table next to the sensor counts. A difficulty rating for each lane with 0 being the easiest and 10 being the hardest, was also recorded. Factors including but not limited to large numbers of vehicles changing lanes, camera angles that were difficult to view, and clarity of picture in the video were the basis for the difficulty ratings. If there were any particular problems with a certain video, a note of it was included with the data.

Moreover, in order to determine the level of accuracy of student counts, a video with a high rating indicating that it was hard to view for counting was chosen. Students were asked to count the same video multiple times so that different students would take turns counting the data on different lanes. The data was recorded in an Excel spreadsheet, and then compiled in another spreadsheet for further analysis.

3.3.3 Description of the Data

The GIS information on FAST detectors was provided in a kml file in the google earth format. The graphical display of the detectors on google earth is shown in Figure 3.2.

3.3.3.1 Freeway Flow Detector (FFD) Raw Data

The data values that we used for analysis are defined as follows:

- DateTimeStamp - This is the date and time when each new segment of data

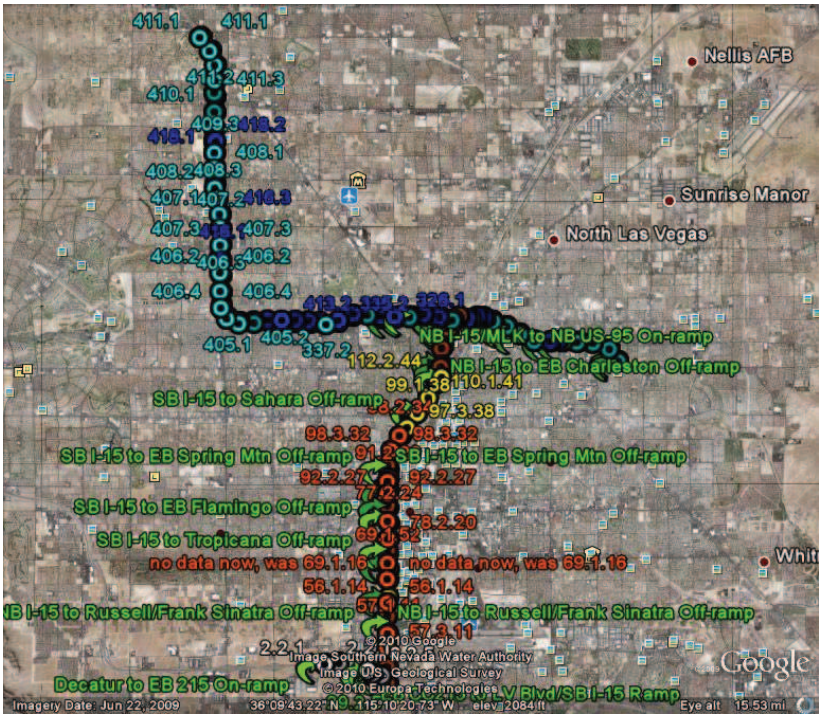

Figure 3.2: Detector Locations in KML

was recorded. Detectors record their data at 15 minute intervals, and this value specifies the interval in question.

- RoadwayID, SegmentID, and DeviceID - These are all specifications indicating which detector was used.

- Lane - This indicates which lane is counted by the detector. Lane 1 is farthest from the detector, and higher number lanes are closer.

- Volume - This is the total number of vehicles that the detector counted during the time interval.

- Volume1, Volume2, Volume3, Volume4, Volume5, and Volume6 are vehicle counts based on different lengths of vehicles and all add up to the total number

of vehicles shown in the Volume field.

- Occupancy, Speed, Poll_Count, Failure, RoadType, Location, and Polling_Period were not used for analysis and can be disregarded for this study.

NOTE: Because they are not necessary for the analysis and to save space, the Volume1, Volume2, Volume3, Volume4, Volume5, Volume6, Occupancy, Speed, Poll_Count, Failure, RoadType, Location, and Polling_Period values are not included in this study.

3.3.3.2 Verification Data

The following values were used in verification:

- DateTimeStamp - This is the same as the DateTimeStamp above and specifies the interval in question.
- RoadwayID, SegmentID, and DeviceID - These are the same as above and specify which detector was used.
- Lane - This is the same as above and indicates which lane the data corresponds to.
- Detector Volume - This is the same value as the Volume value above and represents the total number of vehicles counted by the detector.

- Counted Volume - This is the total number of vehicles counted in the manual count for the specified lane.

- Lane Rating - This is a difficulty rating recorded for statistical purposes. It indicates how hard it was to do a manual count of the specified lane. The rating is from 0 to 10 with 0 being the easiest and 10 being the most difficult. Factors that affect the rating include camera angle, distance of the camera to the detector, vehicles changing lanes, shaky cameras, unclear images, etc.

3.4 Problem Statement for Data Analysis

Data from 146 detectors was provided. Each device detects a range of 1 to 5 lanes. Videos that correspond to the same time frame of the given detector data were also provided. The time interval was 15 minutes for every detector. Manual counting was performed for every lane where results were compared to given detector counts. It was noted that video quality was not consistent for each detector or even for every lane; therefore, the level of difficulty ranging from 0 to 10 was given to every lane.

An screenshot of a video from which the vehicle count was manually obtained is shown in Figure 3.3(a). The location of the corresponding flow detector on Google Map is shown in Figure 3.3(b).

We use the variable d_{ij_i} as the detector counts for the detector D_i. Here, we have

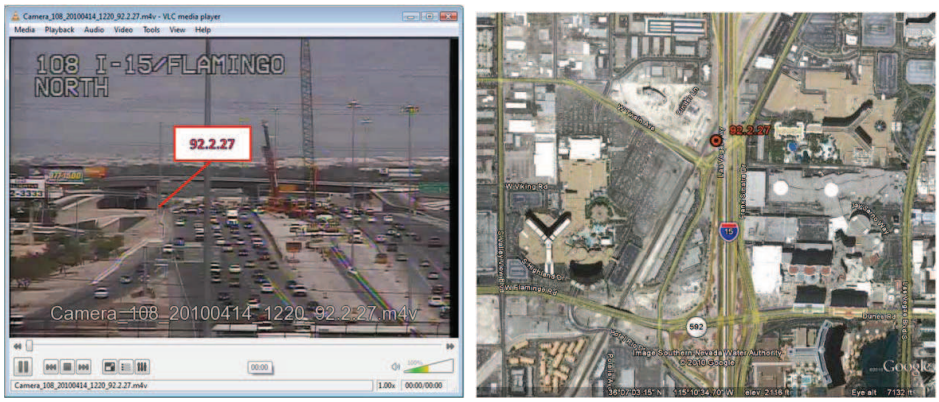

(a) Video for Traffic (b) Location of the Flow Detector

Figure 3.3: Traffic Video and Flow Detector Location

$i \in \{1, 2, \cdots, N_d\}$, where $N_d = 146$ which is the total number of detectors; $j_i \in \{1, 2, \cdots, N_i\}$, where N_i is the number of lanes for detector D_i. For our data, we have, $N_i \in \{1, 2, \cdots, 5\}$. Corresponding to each d_{ij_i}, we have v_{ij_i}, which is the manual vehicle counts from the video camera C_i corresponding to the detector D_i for lane L_{j_i}. We, similarly also have scores w_{ij_i} given by the human observer for the difficulty level associated with obtaining the vehicle counts v_{ij_i}.

Now, let us denote the total number of comparisons by N. We have for the N the formula given by Equation 3.1.

$$N = \sum_{i=1}^{N_d} N_i \tag{3.1}$$

We list each detector data in a single vector whose elements are given by $x_i, i \in \{1, 2, \cdots, N\}$; similarly the manual video data is given by $y_i, i \in \{1, 2, \cdots, N\}$, and

the corresponding rating of difficulty of video measurements by $r_i, i \in \{1, 2, \cdots, N\}$.

3.5 Literature Review

In this work, traffic volume readings were manually verified from videos where a rating is associated with each video based on difficulty in viewing and human errors. Since the problem statement in this study is very specific to validation with data that has varying reliability, relevant literature that was found was very limited and did not directly target the specific methods used in this research. However, various papers on general detector verification projects were studied. In general, when two sets of data are compared where the population's standard deviation is unknown, paired student t-test is used. However, in this work every data point has a unique distribution that is different than the other data points due to the variable error involved in each. Previous studies have not typically targeted the described statistical problem. However, a number of papers were collected in order to assist in developing the theory for the specific goal of this project.

In Kang's paper [29] an anisotropic magneto-resistive (AMR) sensor was tested by measuring traffic volumes on the highway with the detector and comparing with the exact traffic volumes in a highly congested traffic. It was found that performance of this sensor highly depends on the rate at which vehicles are flowing. Verification done in this study did not well define "exact traffic volumes". Even though defining it is

not the main scope of Kang's paper, statistical analysis must take error possibilities under consideration for accuracy and reliability of results.

Interestingly, Chen's paper [30] presented an L_∞ norm Path flow estimator (PFE) model in order to handle inconsistencies of traffic counts and the systematic bias of the total demand estimate encountered in the PFE model. This technique was shown to be capable of determining the maximal absolute error needed to define the set of inequality constraints, traffic counts and capacities, while estimating the path flows. This research work even though not directly related to the scope of this paper, however it provides a very interesting approach for handling errors in counts.

In Fathy's research work [31], traffic movements at junctions were measures using image processing techniques. The results of the operations of the proposed algorithms show an error rate of 9.5%. For the purpose of this study, 9.5% error rate is not acceptable. Error rates in that same range are always associated with any available commercial or open source software specially that quality of video differs based on view angle and position of the camera in relation with the detector. Therefore, manual vehicle counts had to be done for this research project.

In Zhuang's work on statistical methods to estimate vehicle count using traffic cameras [32], two methods were developed for constructing traffic models, one using statistical machine learning based on Gaussian models and the other using analytical derivation from the origin-destination (OD) matrix. It was found that Gaussian-based statis-

tical learning method outperforms correlation coefficient based method. Simulations showed that it reduces the average estimation error by up to 72%. Variance estimation can also be provided. This method is particularly useful for roads with more dynamic and uncertain traffic. When training data is missing, Given that traffic is somewhat stable, then the developed OD matrix based method is superior to the statistical learning methods.

Zimmerman [33] has focused in his study on type 1 error probability of the Student t test which arises by unequal variances combined with unequal sample sizes. The Welch student t test is known to eliminate these effects. Zimmerman found conditional probabilities of rejecting the null hypothesis, for both significance tests, given various conditions on the sample variances implying that inspection of sample data alone cannot protect the significance level and power of the t test.

3.6 Data Analysis

In this section, we present the descriptive and inferential statistics based on the detector data, the manual video data, and the corresponding ratings. We also analyze the data obtained from the repeated manual video counting of a single site, to extract a model for the relationship between the ratings and the distribution of the errors. We use the open-source statistical package R for the descriptive and inferential data analysis.

3.6.1 Descriptive Statistics

First the data was put in a table, a sample of which is shown in Figure 3.4. The three variables, x, y, and r, in this table in Figure 3.4 are given below. Additionally, three more derived variables, PDx, PDy, and PD, are also presented, that created in the subsequent R-code.

x	y	r
122	144	3
116	118	2
71	81	2

Figure 3.4: Basic Data for Analysis

x**:** Detector data

y**:** Counted data

r**:** Rating of the video quality

PDx**:** $100(x-y)/x$

PDy**:** $100(x-y)/y$

PD**:** if $r \geq 5$ then PDx else PDy

Listing 1 shows the code that allows to transfer data to the R software and presents the basic summary.

This listing indicates that the summary statistics for X and Y are close to each other. This is indicated by the fact, e.g. that the mean for X is 275 and for Y is 270.7. Similarly,

Listing 1 Summary Statistics

```
> inputdata<-read.table(file = "clipboard")
> x <- inputdata$V1
> y <- inputdata$V2
> r <- inputdata$V3
> PDx <- 100*(x-y)/x
> PDy <- 100*(x-y)/y
> for (i in 1:length(r))
+ if (r[i] < 5) PD[i] <= PDy[i] else PD[i] <= PDx[i]
> summary(inputdata)
       V1              V2              V3
 Min.   : 22.0   Min.   : 21.0   Min.   : 0.000
 1st Qu.:196.0   1st Qu.:200.0   1st Qu.: 1.000
 Median :286.0   Median :280.0   Median : 2.000
 Mean   :277.6   Mean   :274.0   Mean   : 2.411
 3rd Qu.:355.0   3rd Qu.:345.0   3rd Qu.: 3.000
 Max.   :946.0   Max.   :973.0   Max.   :10.000
```

the values of the order statistics are close, such as for the first, second(median), and third quartiles. However, as the summary of the statistics for the difference of x and y indicates that although their distributions have similar statistics, the percent difference shows more variation. We define the percent difference to be $PDx = 100(x - y)/x$. The statistics for the percent difference are shown in Listing 2

Listing 2 Summary Statistics for the Difference

```
Min.   1st Qu.    Median      Mean   3rd Qu.      Max.
-1067.000    -4.822     0.495    -3.187     6.351    82.070
```

This analysis shows us clearly that there are some outliers in the data based on the extreme values of the minimum and the maximum. To identify these outliers, we present some more plots. First, we present the boxplots and violin plots for the raw x and y data. These are shown in Figure 3.5.

The box plots show many outliers for x and y data. The violin plots show the order

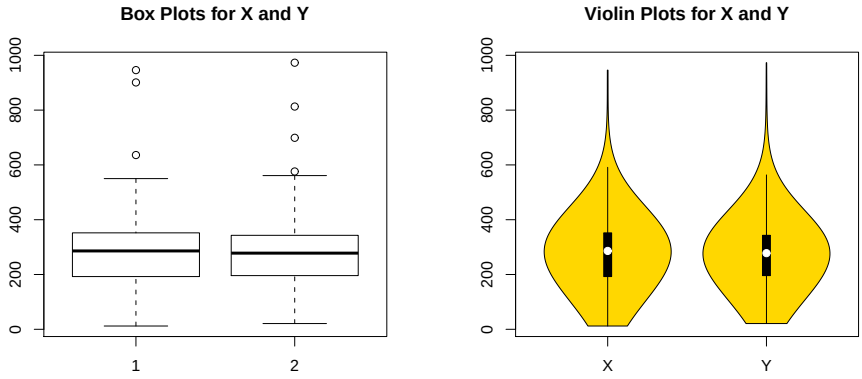

(a) Box Plots (b) Violin Plots

Figure 3.5: Box and Violin Plots for X and Y

statistical information and dispersion of these variables on the same plot. The same plots for the percent difference is shown in Figure 3.6.

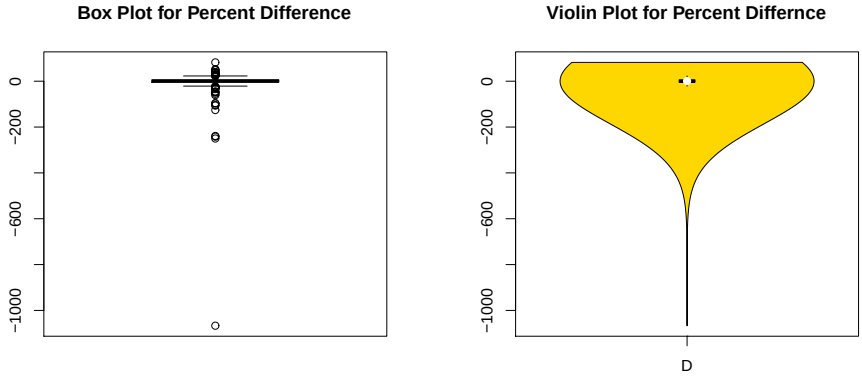

(a) Box Plot (b) Violin Plot

Figure 3.6: Box and Violin Plots for Percent Difference

Figure 3.6 shows that there are some outliers in the data. The analysis of the outliers can help in identifying faulty flow detectors.

Figure 3.7 shows the histogram plot for the percentage difference, $PDx = 100(x - y)/x$

between the volume data and the manual video count values, and its density plot.

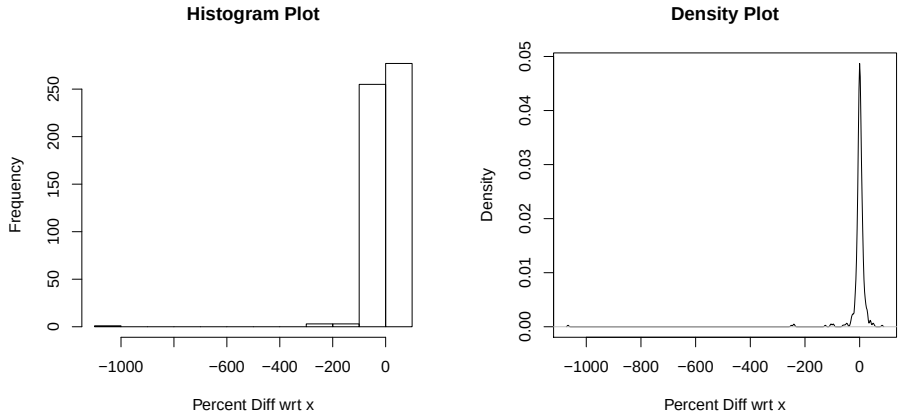

(a) Histogram (b) Density Plot

Figure 3.7: Histogram and Density Plots for Percent Difference

3.6.2 Analysis of the Conditionally Normalized Percent Difference Data

The code for plotting PD data is shown in Listing 3. The plot itself of the PD data is shown in Figure 3.8.

Listing 3 R-code for PD Plotting

```
hist(PD, freq = FALSE, ylim = c(0, 0.06))
lines(density(PD))
rug(PD, side=1)
```

The reason for the formula for the PD variables is as follows. We need to find the percent difference between the two data, where the percentage is taken over the better estimate out of the two counts (one from the video and one from the detector). Hence we choose to normalize PD with respect to x if the video is not clear, i.e. $r \geq 5$, and with respect to y if the video is clear, i.e. $r < 5$. The summary of the PD data is shown in Listing 4.

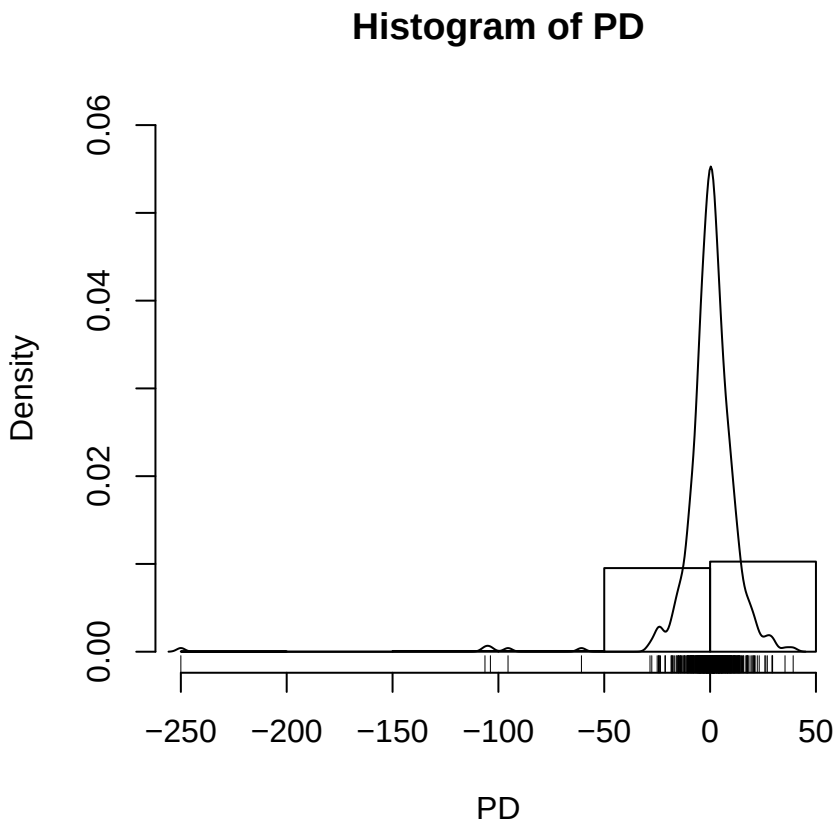

Figure 3.8: Basic Data for Analysis

Listing 4 Summary of PD Data

```
summary(PD)
     Min.   1st Qu.    Median      Mean   3rd Qu.      Max.
-250.0000   -4.4150    0.4717   -0.3376    5.5650   39.2400
```

Now, 95% of the sample data is between −23.11984% and 20.64176%. This is obtained using the R-code shown in Listing 5.

Listing 5 Summary of PD Data

```
> quantile(PD, probs=.025)
     2.5%
-23.11984
> quantile(PD, probs=.975)
   97.5%
20.64176
```

3.6.2.1 Hypothesis Testing and Confidence Intervals for the Mean

We hypothesize that the PD data is coming from a population of zero mean. This is our null hypothesis. This indicates that the percentage error in the detectors is unbiased, and that essentially the detectors and the video data are compatible.

Null Hypothesis:

Mean value of the percent difference between the FAST detector flow rates and the video counted rates is zero.

To perform the hypothesis testing, we will use the t-test. The assumptions and the basic implementation of paired t-test are available from any textbook on statistics, such as [34]. We present the very basics here.

Given two independent random variables X and Y, where X has a normal distribution with 0 mean 1 variance, and Y has a chi-square distribution with n degrees of freedom, then the random variable T given by 3.2 has a t-distribution.

$$T = \frac{X}{Y/\sqrt{n}} \tag{3.2}$$

For the data that we have, we use PD for the X variable here, and σ for the Y variable, and we get the t-statistic as given by

$$t = \frac{\overline{PD}}{\sigma/\sqrt{N}} \tag{3.3}$$

Here, we have for sample mean

$$\overline{PD} = \frac{\sum_{i=1}^{N} PD_i}{N} \tag{3.4}$$

and for sample variance

$$\sigma = \frac{\sum_{i=1}^{N} (PD_i - \overline{PD})^2}{N-1} \tag{3.5}$$

The application of the t-test to the PD data gives the result shown in Listing 6. The result shows a p-value of 0.6595 which clearly shows that the null hypothesis can not be rejected. Hence, we accept the null hypothesis, which means that we claim that the flow detector data has been validated by the video counted data.

Listing 6 T-test of PD Data

```
> t.test(PD)

        One Sample t-test

data:  PD
t = -0.4408, df = 486, p-value = 0.6595
alternative hypothesis: true mean is not equal to 0
95 percent confidence interval:
 -1.842502  1.167272
sample estimates:
 mean of x
-0.3376151
```

The confidence interval, at the confidence level, γ for the population mean, μ is given by Equation 3.6.

$$\overline{PD} - \frac{c\sigma}{\sqrt{n}} \leq \mu \leq \overline{PD} + \frac{c\sigma}{\sqrt{n}} \tag{3.6}$$

The value of c is obtained based on the level of confidence γ. For instance, for 95% confidence level, the value for c is 1.96. Listing 6 gives the 95% confidence interval for the population mean as $(-1.842502, 1.167272)$.

3.6.2.2 Confidence Interval for the Variance

In this subsection, we will estimate the confidence interval for the variance of the percent error that we expect from the population. This will indicate to us what performance can be expected from flow detectors of the type that were tested.

The steps to determine the confidence interval for the variance of the population are as follows (see [34], page 185 for details).

First Step

Choose a confidence level γ.

Second Step

Using the chi-squared distribution with $n-1$ degrees of freedom, solve for c_1 and c_2 from $F(c_1) = (1-\gamma)/2$, $F(c_2) = (1+\gamma)/2$.

Third Step

Compute $(n-1)s^2$ where s^2 is the sample variance.

Fourth Step

Compute $k_1 = (n-1)s^2/c_1$ and $k_2 = (n-1)s^2/c_2$.

Fifth Step

Compute confidence interval for the variance as $k_2 \leq \sigma^2 \leq k_2$.

These steps applied to the analysis of the PD data produce the following.

First Step

$\gamma = 0.95$.

Second Step

We get $F(c_1) = (1-0.95)/2 = 0.025$, and $F(c_2) = (1+0.95)/2 = 0.975$

For $F(c_1) = 0.025$, $c_1 = (h-1.96)^2/2$, where $h = \sqrt{2m-1}$, m being the number of

degrees of freedom, i.e. $m = n - 1$. For our data, $n = 487$, which gives $c_1 = 426.3455$. Similarly, for $F(c_2) = 0.975$, $c_2 = (h + 1.96)^2/2$, which gives $c_2 = 548.4961$.

Third Step

Variance of the PD data is 285.6768. Hence, $(n-1)s^2 = 138838.9$.

Fourth Step

Now, $k_1 = (n-1)s^2/c_1 = 325.6488$ and $k_2 = (n-1)s^2/c_2 = 253.1265$.

Fifth Step

Hence, the confidence interval for the variance is $253.1265 \leq \sigma^2 \leq 325.6488$. This implies that the confidence interval for the standard deviation is $(15.90995, 18.04574)$.

3.6.2.3 Normalized Plot of Percent Errors and Analysis

Based on the sample mean and the sample variance, we can create a normal curve to show the approximate performance in terms of the percent difference for the flow detectors. The code for this plot is shown in Listing 7, and the corresponding plot is shown in Figure 3.9.

Listing 7 Code for Normal Curve for PD Data

```
> mean <- mean(PD)
> sd <- sd(PD)
> x <- seq(-4,4,length=100)*sd + mean
> hx <- dnorm(x,mean,sd)
> plot(x, hx, type="l", xlab="PD", ylab="Density",main="Percent Error Plot")
```

We can use this plot for some basic approximate analysis. For instance, if we want to find out what percentage we get errors between the values of $(-5\%, +5\%)$, we use the pnorm function in R, and obtain the answer of 21.73%. Similarly, for errors between the values of

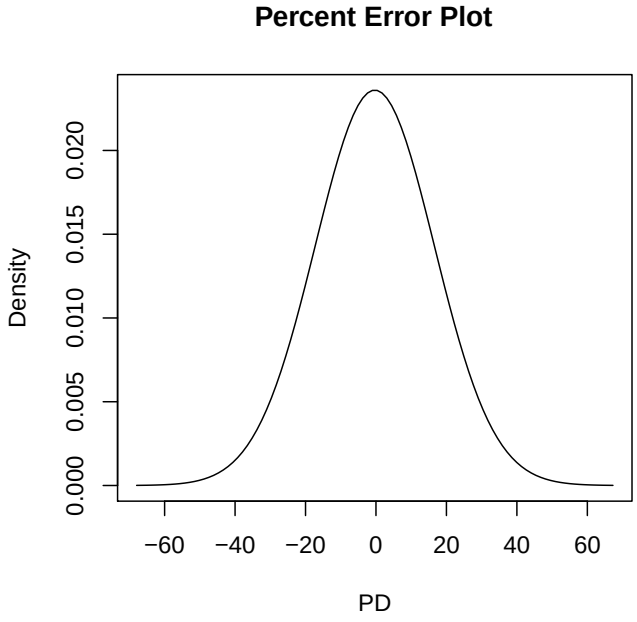

Figure 3.9: Normal Plot for Percent Errors

$(-10\%, +10\%)$, we get 43.25%, and for errors between the values of $(-15\%, +15\%)$, we get 61.43%. The R-code for this analysis and the corresponding results are shown in Listing 8.

Listing 8 Code for Analysis of PD Data

```
> 2*(0.5 - pnorm(-5,mean,sd))
[1] 0.2173356
> 2*(0.5 - pnorm(-10,mean,sd))
[1] 0.4324558
> 2*(0.5 - pnorm(-15,mean,sd))
[1] 0.6143293
```

3.6.3 Methodology for using Ratings for Statistical Analysis

In order to develop the methodology for using the ratings data for statistical analysis, we use the ratings given by people who were performing the manual counts to a fixed video, when the counting was performed multiple times on the same video. The ratings for the

five lanes of the video given by multiple raters is presented in Table 3.1.

Lane1	r	Lane2	r	Lane3	r	Lane4	r	Lane5	r
15.33	7	27.02	6	-4.57	3	-8.65	3	7.53	1
16.02	6	8.78	7	1.02	2	-5.48	3	2.08	4
12.36	7	9.70	4	7.61	6	-7.78	3	8.05	4
15.56	4	13.86	8	-1.52	6	-3.75	3	7.79	5
27.46	7	10.16	7	-1.52	2	-2.59	3	11.69	5
10.30	6	5.54	6	5.08	4	-7.78	4	6.75	4
15.10	6	10.16	7	-1.52	0	-0.58	1	4.42	1

Table 3.1: Ratings of the Video

The columns of the Table 3.1 show the percentage difference with respect to X compared with the ratings for each lane of the video. For each lane, we obtain the mean rating as well as the variance of the percentages for that lane. These values are presented in Table 3.2.

Mean Rating	6.14	6.42	3.29	2.86	3.43
Variance Percent Diffference	29.75	48.83	18.20	9.25	9.14

Table 3.2: Variance of the Percentage Difference in Counts vs Average Rating

The data in Table 3.2 is curve fitted using three curves, linear, power curve, and a log-linear curve. The plot of the data and the three curves is shown in Figure 3.10.

The analysis of this data for curve fitting is presented in the following code. The data for the mean ratings is stored in variable rm, and the variance of the percent differences in rxv, as seen in Listing 9.

Listing 9 Variables for Mean rating and Variance

```
> rm
[1] 6.14 6.42 3.29 2.86 3.43
> rxv
[1] 29.75 48.83 18.20  9.25  9.14
```

The data is stored in a data frame as shown in Listing 10.

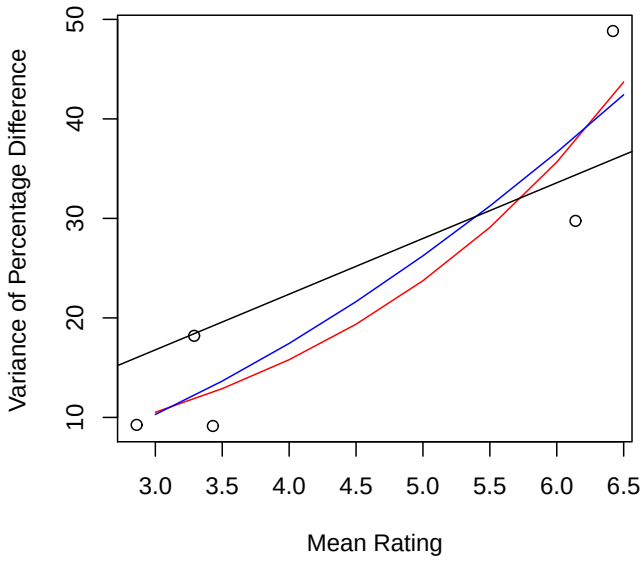

Figure 3.10: Plot of Variance in Percent Difference to Mean Rating

Listing 10 Data frame for the Variables

```
> ds <- data.frame(x = rm, y = rxv)
> str(ds)
'data.frame':   5 obs. of  2 variables:
 $ x: num  6.14 6.42 3.29 2.86 3.43
 $ y: num  29.75 48.83 18.2 9.25 9.14
```

The code and interaction for linear regression model with zero intercept (so as not to have non-positive variance) is given in Listing 11.

Listing 11 Linear Regression

```
> rfit <- lm(rxv ~ rm + 0)
> abline(rfit)
> summary(rfit)

Call:
lm(formula = rxv ~ rm + 0)

Residuals:
       1        2        3        4        5
 -4.6118  12.9012  -0.2121  -6.7556 -10.0556

Coefficients:
   Estimate Std. Error t value Pr(>|t|)
rm   5.5964     0.8732   6.409  0.00304 **
---
Signif. codes:  0 '***' 0.001 '**' 0.01 '*' 0.05 '.' 0.1 ' ' 1

Residual standard error: 9.145 on 4 degrees of freedom
Multiple R-squared: 0.9113,     Adjusted R-squared: 0.8891
F-statistic: 41.08 on 1 and 4 DF,  p-value: 0.003045
```

The code and interaction for the power regression model is given in Listing 12. The code and interaction for the log-linear regression model is given in Listing 13.

The log-linear fit gives the best performance. Hence, we will use it for statistical inference. The formula for variance in terms of the rating score therefore, is given by Equation 3.7.

$$s(r) = e^{1.13+0.41r} \tag{3.7}$$

Listing 12 Power Regression

```
> m.2 <- nls(y ~ rhs(x,intercept, power), data = ds, start = list(intercept = 1,
+ power = 2),trace = T)
183.6028 :  1 2
180.8829 :  1.159547 1.916102
178.7074 :  1.355049 1.833367
178.1608 :  1.376444 1.831493
178.1608 :  1.376735 1.831399
> summary(m.2)

Formula: y ~ rhs(x, intercept, power)

Parameters:
          Estimate Std. Error t value Pr(>|t|)
intercept   1.3767     1.4787   0.931   0.4205
power       1.8314     0.6047   3.029   0.0564 .
---
Signif. codes:  0 '***' 0.001 '**' 0.01 '*' 0.05 '.' 0.1 ' ' 1

Residual standard error: 7.706 on 3 degrees of freedom

Number of iterations to convergence: 4
Achieved convergence tolerance: 5.62e-06

> plot(rm,rxv)
> lines(s, predict(m.2, list(x = s)), lty = 1, col = "blue")
```

Listing 13 Loglinear Regression

```
> m.e <- nls(y ~ I(exp(1)^(a + b * x)), data = ds, start = list(a = 0,
+ b = 1), trace = T)
508654.9 :  0 1
61724.38 :  -0.5294191  0.9373290
6359.583 :  -0.4243993  0.7921467
542.5241 :  0.4408596 0.5634763
165.3981 :  1.0201739 0.4315203
159.0372 :  1.1207667 0.4090216
159.0220 :  1.1312375 0.4071317
159.0220 :  1.1320508 0.4069949
159.0220 :  1.1321105 0.4069849
> summary(m.e)

Formula: y ~ I(exp(1)^(a + b * x))

Parameters:
  Estimate Std. Error t value Pr(>|t|)
a   1.1321     0.7566   1.496   0.2315
b   0.4070     0.1253   3.248   0.0475 *
---
Signif. codes:  0 '***' 0.001 '**' 0.01 '*' 0.05 '.' 0.1 ' ' 1

Residual standard error: 7.281 on 3 degrees of freedom

Number of iterations to convergence: 8
Achieved convergence tolerance: 3.461e-06

> lines(s, predict(m.e, list(x = s)), lty = 1, col = "red")
> title(xlab="mean rating")
> plot(rm,rxv, xlab="Mean Rating",ylab="Variance of Percentage Difference")
> lines(s, predict(m.e, list(x = s)), lty = 1, col = "red")
> lines(s, predict(m.2, list(x = s)), lty = 1, col = "blue")
```

3.7 Identification of Potentially Faulty Detectors

The correlation between the flow detector values and the manually counted values is very high. The plot shown in Figure 3.11 shows the linear relationship between the data and also the regression line obtained from the data.

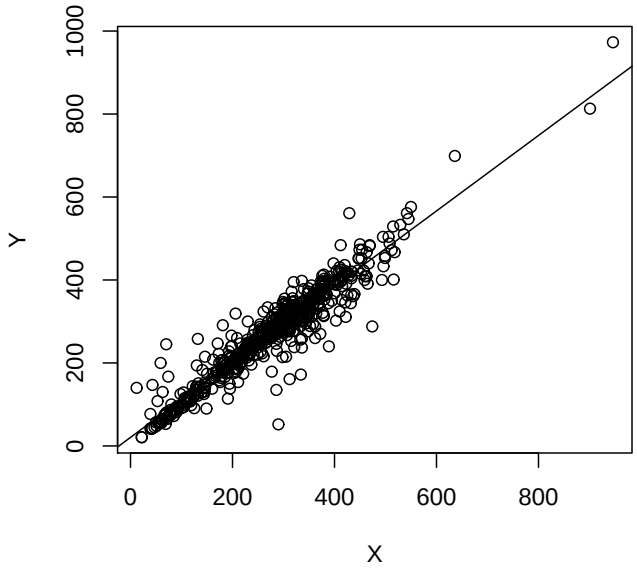

Figure 3.11: Plot showing Linear Relationship

A call to the linear regression function in R produces the result shown in Listing 14.

The regression result shows strong linear relationship with the intercept 0.90974. The values of Pearson, Spearman, and Kendall rank coefficients are given in Table 3.3.

Using the ecdf()() function in R on the percent difference data, we find that 90% of the values are within ±21% difference. We use this percentage as the threshold for designing a decision

Listing 14 Regression Analysis Result

```
> fit <- lm(Y ~ X)
> summary(fit)

Call:
lm(formula = Y ~ X)

Residuals:
      Min        1Q    Median        3Q       Max
-232.4050  -15.5883   -0.8347   17.0857  160.7384

Coefficients:
            Estimate Std. Error t value Pr(>|t|)
(Intercept) 20.57962    3.92018    5.25  2.2e-07 ***
X            0.90974    0.01302   69.87  < 2e-16 ***
---
Signif. codes:  0 '***' 0.001 '**' 0.01 '*' 0.05 '.' 0.1 ' ' 1

Residual standard error: 37.07 on 537 degrees of freedom
Multiple R-squared: 0.9009,     Adjusted R-squared: 0.9007
F-statistic:  4882 on 1 and 537 DF,  p-value: < 2.2e-16
```

Coefficient Name	**value**
Pearson Coefficient	0.95
Spearman Coefficient	0.94
Kendall Coefficient	0.81

Table 3.3: Correlation Coefficients

system to identify faulty detectors. We use percentage of X and also of Y and identify all the detectors whose errors from either percentage is greater than 21%. Table shown in Figure 3.12 shows some data that is analyzed to identify potentially faulty detectors.

x	y	r	PDx	RoadID	SegID	Lane	DevID	Sign Diff	Pdy
122	144	3	-18.03	23	1	1	8	-1	-15.28
116	118	2	-1.72	23	2	1	8	-1	-1.69
71	81	2	-14.08	39	2	1	8	-1	-12.35
277	179	7	35.38	39	2	2	8	1	54.75
132	258	8	-95.45	39	2	3	8	-1	-48.84
43	147	9	-241.86	56	2	1	13	-1	-70.75
146	215	9	-47.26	56	2	2	13	-1	-32.09
230	300	9	-30.43	56	2	3	13	-1	-23.33
319	328	9	-2.82	56	2	4	13	-1	-2.74
439	366	9	16.63	49	2	1	12	1	19.95
340	378	9	-11.18	49	2	2	12	-1	-10.05
340	303	9	10.88	49	2	3	12	1	12.21
286	135	9	52.80	49	2	1E	12	1	111.85
372	270	9	27.42	49	2	2E	12	1	37.78
328	343	3	-4.57	49	3	1	15	-1	-4.37
400	368	3	8.00	49	3	2	15	1	8.70
367	353	3	3.81	49	3	3	15	1	3.97

Figure 3.12: Sample Data Table

The columns of the data in Figure 3.12 are given in Table 3.4.

x	Flow detector data
y	Manually Counted Video data
r	Rating
PDx	Percent Difference $100(X-Y)/X$
$RoadID$	Road identification number
$SegID$	Road segment identification number
$Lane$	Lane number
$DevID$	Flow detector identification number
$SignDiff$	$(X-Y)/\|X-Y\|$
PDy	Percent Difference $100(X-Y)/Y$

Table 3.4: Variables in the Data

The algorithm to find out if a given detector is possibly faulty is as follows. For any detector which has any instance where condition 3.8 is true, we apply the the test given in Equation 3.10. We take the percentage threshold to be denoted by p_{Th} and we take it equal to 21%.

This threshold is the 90^{th} percentile value for the absolute value of the function h applied to every data entry.

$$\frac{d_{i_{j_i}} - v_{i_{j_i}}}{h(r_{i_{j_i}}, v_{i_{j_i}}, d_{i_{j_i}})} \geq p_{Th} \tag{3.8}$$

The formula for the function h is given in Equation 3.9.

$$\begin{array}{lll} \text{if} \quad r_{i_{j_i}} \geq 5 \quad \text{then} & h(r_{i_{j_i}}, v_{i_{j_i}}, d_{i_{j_i}}) = d_{i_{j_i}} \\ \text{otherwise} & h(r_{i_{j_i}}, v_{i_{j_i}}, d_{i_{j_i}}) = v_{i_{j_i}} \end{array} \tag{3.9}$$

Given detector D_i,

$$\begin{array}{lll} \text{if} \quad \dfrac{\sum_{j_i=1}^{N_i} \dfrac{d_{i_{j_i}} - v_{i_{j_i}}}{s(r_{i_{j_i}})h(r_{i_{j_i}}, v_{i_{j_i}}, d_{i_{j_i}})}}{\sum_{j_i=1}^{N_i}(1/s(r_{i_{j_i}}))} > p_{Th} & \text{then } D_i \text{ is defective} \\ \text{otherwise} & D_i \text{ is not defective} \end{array} \tag{3.10}$$

The formula for $s(r_{i_{j_i}})$ is given in Equation 3.7. This algorithm was applied on an excel sheet to identify detectors that should be tested to see if they are faulty. Figure 3.13 shows a

snapshot of the excel sheet analysis where the possible faulty detectors are identified by red cells. Unique detectors are identified by unique combinations of RoadID and SegID fields. The pink colored cells show the detectors that satisfy the condition given by Equation 3.8. The red colored cells show the detectors that satisfy the condition given by Equation 3.10.

x	y	r	PDx	RoadID	SegID	Pdy	1/s(r)	pd	apd	v_pd	sumK	sumN	Def
122	144	3	-18.03	23	1	-15.28	0.09	-15.28	15.28	1.44			
116	118	2	-1.72	23	2	-1.69	0.14	-1.69	1.69	0.24			
71	81	2	-14.08	39	2	-12.35	0.14	-12.35	12.35	1.76			
277	179	7	35.38	39	2	54.75	0.02	35.38	35.38	0.65			
132	258	8	-95.45	39	2	-48.84	0.01	-95.45	95.45	1.16	0.17	3.56	20.64
43	147	9	-241.86	56	2	-70.75	0.01	-241.86	241.86	1.95			
146	215	9	-47.26	56	2	-32.09	0.01	-47.26	47.26	0.38			
230	300	9	-30.43	56	2	-23.33	0.01	-30.43	30.43	0.25			
319	328	9	-2.82	56	2	-2.74	0.01	-2.82	2.82	0.02	0.03	2.60	80.59
439	366	9	16.63	49	2	19.95	0.01	16.63	16.63	0.13			
340	378	9	-11.18	49	2	-10.05	0.01	-11.18	11.18	0.09			
340	303	9	10.88	49	2	12.21	0.01	10.88	10.88	0.09			

Figure 3.13: faulty Detector Identification Worksheet Sample

3.8 Analysis using Ratings

We can use the ratings of the videos to design an algorithm that takes the accuracy of videos into account for analysis. The method uses the formula for variance in terms of the rating score from Equation 3.7.

3.8.1 Weighted Mean Method

In the weighted-mean method, we choose the weighted estimator for the mean as shown in Equation 3.11.

$$\overline{PD}^* = \frac{\sum w_i PD_i}{\sum w_i} \tag{3.11}$$

The weights in this equation will be taken as $w_i = 1/s(r_i)$. This equation can be equivalently be written as

$$\overline{PD}^* = \sum g_i PD_i \tag{3.12}$$

where

$$g_i = \frac{w_i}{\sum w_i} \tag{3.13}$$

To make coding easier, we can replace each PD_i by a weighted PD_i value as shown in Equation 3.14. Then, we can perform the standard analysis, such as a t-test using these values. The statistics for the weighted percent difference are shown in Listing 15.

$$wPD_i = \frac{w_i}{\frac{\sum w_i}{N}} PD_i \tag{3.14}$$

Listing 15 Summary Statistics for the Weighted Difference

```
> inputdata<-read.table(file = "clipboard")
> wPD <- inputdata$V1
> summary(wPD)
    Min.  1st Qu.   Median     Mean  3rd Qu.     Max.
-99.4400  -2.6450   0.2636   0.1922   3.7390  45.7000
```

The code for plotting wPD data is shown in Listing 16. The plot itself of the wPD data is shown in Figure 3.14.

Listing 16 R-code for wPD Plotting

```
hist(wPD, freq = FALSE, ylim = c(0, 0.1))
lines(density(wPD))
rug(wPD, side=1)
```

Now, 95% of the sample data is between -18.33740% and 22.49848%. This is obtained using the R-code shown in Listing 17.

Listing 17 Summary of wPD Data

```
> quantile(wPD, probs=.025)
     2.5%
-18.33740
> quantile(wPD, probs=.975)
   97.5%
22.49848
```

3.8.1.1 Hypothesis Testing and Confidence Intervals for the Weighted Mean

We hypothesize that the wPD data is coming from a population of zero mean. This is our null hypothesis. This indicates that the percentage error in the detectors is unbiased, and that essentially the detectors and the video data are compatible.

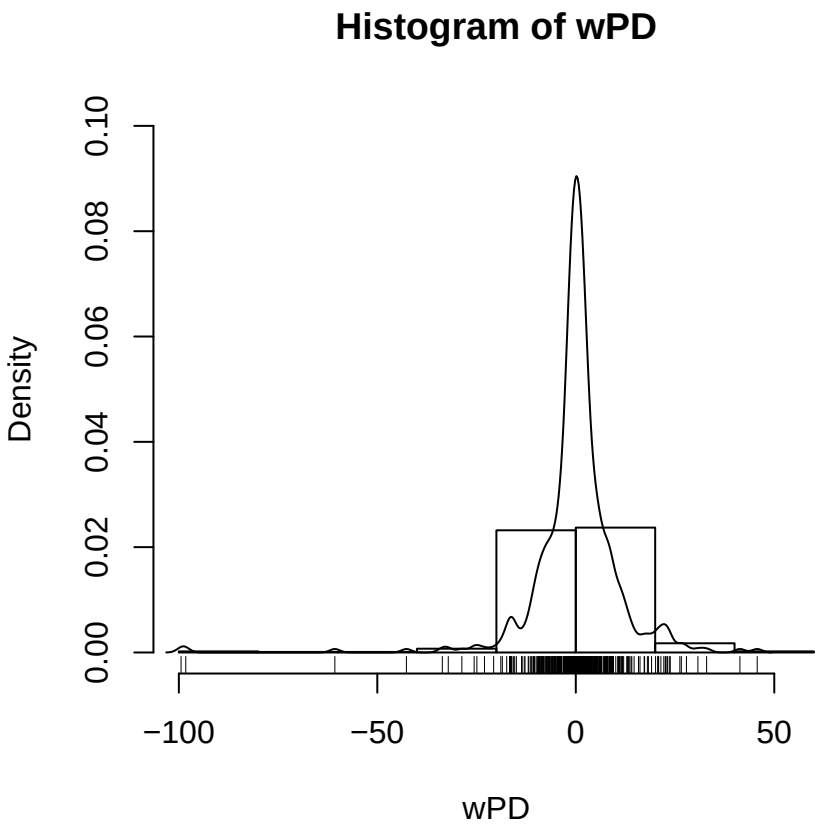

Figure 3.14: Basic Weighted Data for Analysis

Null Hypothesis:

Mean value of the weighted percent difference between the FAST detector flow rates and the video counted rates is zero.

To perform the hypothesis testing, we will use the t-test. For the data that we have, we get the t-statistic as given by

$$t = \frac{\overline{wPD}}{\sigma/\sqrt{N}} \tag{3.15}$$

Here, we have for sample mean

$$\overline{wPD} = \frac{\sum_{i=1}^{N} wPD_i}{N} \tag{3.16}$$

and for sample variance

$$\sigma = \frac{\sum_{i=1}^{N} (wPD_i - \overline{wPD})^2}{N-1} \tag{3.17}$$

The application of the t-test to the wPD data gives the result shown in Listing 18. The result shows a p-value of 0.7084 which clearly shows that the null hypothesis cannot be rejected. Hence, we accept the null hypothesis, which means that we claim that the flow

detector data has been validated by the video counted data.

Listing 18 T-test of wPD Data

```
> t.test(wPD)

        One Sample t-test

data:  wPD
t = 0.3742, df = 486, p-value = 0.7084
alternative hypothesis: true mean is not equal to 0
95 percent confidence interval:
 -0.8172784  1.2017711
sample estimates:
mean of x
0.1922463
```

The confidence interval, at the confidence level, γ for the population mean, μ is given by Equation 3.18.

$$\overline{wPD} - \frac{c\sigma}{\sqrt{n}} \leq \mu \leq \overline{wPD} + \frac{c\sigma}{\sqrt{n}} \tag{3.18}$$

Listing 18 gives the 95% confidence interval for the population mean as $(-0.8172784, 1.2017711)$.

3.8.1.2 Confidence Interval for the Variance for the Weighted Data

In this subsection, we will estimate the confidence interval for the variance of the percent error for the weighted data that we expect from the population. This will indicate to us what performance can be expected from flow detectors of the type that were tested using the enhanced method.

The steps applied to the analysis of the wPD data produce the following.

First Step

$\gamma = 0.95$.

Second Step

We get $F(c_1) = (1 - 0.95)/2 = 0.025$, and $F(c_2) = (1 + 0.95)/2 = 0.975$

For $F(c_1) = 0.025$, $c_1 = (h - 1.96)^2/2$, where $h = \sqrt{2m - 1}$, m being the number of degrees of freedom, i.e. $m = n - 1$. For our data, $n = 487$, which gives $c_1 = 426.3455$.

Similarly, for $F(c_2) = 0.975$, $c_2 = (h + 1.96)^2/2$, which gives $c_2 = 548.4961$.

Third Step

Variance of the wPD data is 128.5585. Hence, $(n - 1)s^2 = 62479.45$.

Fourth Step

Now, $k_1 = (n - 1)s^2/c_1 = 146.5465$ and $k_2 = (n - 1)s^2/c_2 = 113.9105$.

Fifth Step

Hence, the confidence interval for the variance is $113.9105 \leq \sigma^2 \leq 146.5465$. This implies that the confidence interval for the standard deviation is $(10.67289, 12.10564)$.

3.8.1.3 Normalized Plot of Percent Errors and Analysis

Based on the sample mean and the sample variance, we can create a normal curve to show the approximate performance in terms of the weighted percent difference for the flow detectors. The code for this plot is shown in Listing 19, and the corresponding plot is shown in Figure 3.15.

Listing 19 Code for Normal Curve for wPD Data

```
> mean <- mean(wPD)
> sd <- sd(wPD)
> x <- seq(-4,4,length=100)*sd + mean
> hx <- dnorm(x,mean,sd)
> plot(x, hx, type="l", xlab="wPD", ylab="Density",main="Percent Error Plot")
```

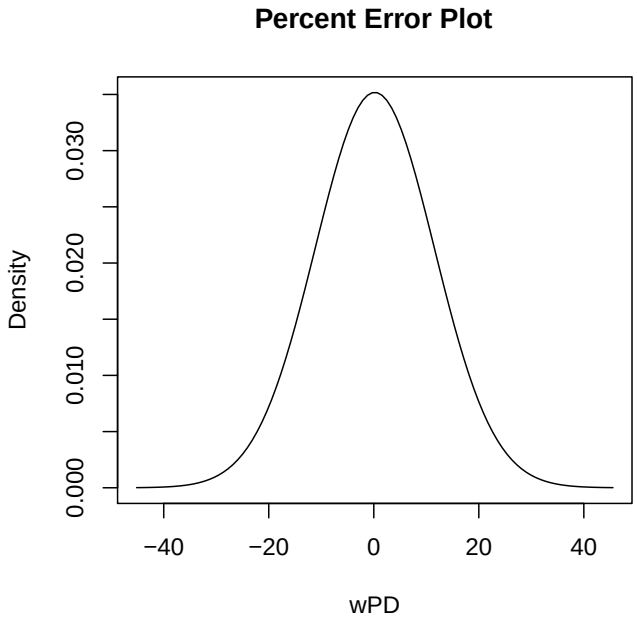

Figure 3.15: Normal Plot for Weighted Percent Errors

We can use this plot for some basic approximate analysis. For instance, if we want to find out what percentage we get errors between the values of $(-5\%, +5\%)$, we use the p norm function in R, and obtain the answer of 35.3%. Similarly, for errors between the values of $(-10\%, +10\%)$, we get 63.13%, and for errors between the values of $(-15\%, +15\%)$, we get 81.97%. The R-code for this analysis and the corresponding results are shown in Listing 20.

Listing 20 Code for Analysis of wPD Data

```
> 2*(0.5 - pnorm(-5,mean,sd))
[1] 0.3530016
> 2*(0.5 - pnorm(-10,mean,sd))
[1] 0.631303
> 2*(0.5 - pnorm(-15,mean,sd))
[1] 0.8197213
```

3.9 Analysis of the Data with the Best Rating

In this section we present analysis of the data that has 0 rating, which means it is the data where the video quality was the best. We use the variable $PD0$ for the percent difference for this data. The statistics for the percent difference are shown in Listing 21.

Listing 21 Summary Statistics for the Weighted Difference

```
> inputdata<-read.table(file = "clipboard")
> PD0 <- inputdata$V1
> summary(PD0)
    Min.  1st Qu.   Median     Mean  3rd Qu.     Max.
-51.5400  -3.7560   0.2212  -0.3035   4.3060  21.4300
```

The code for plotting $PD0$ data is shown in Listing 22. The plot itself of the $PD0$ data is shown in Figure 3.16.

Listing 22 R-code for $PD0$ Plotting

```
hist(PD0, freq = FALSE, ylim = c(0, 0.08))
lines(density(PD0))
rug(PD0, side=1)
```

Now, 95% of the sample data is between -19.06819% and 14.53804%. This is obtained using the R-code shown in Listing 23.

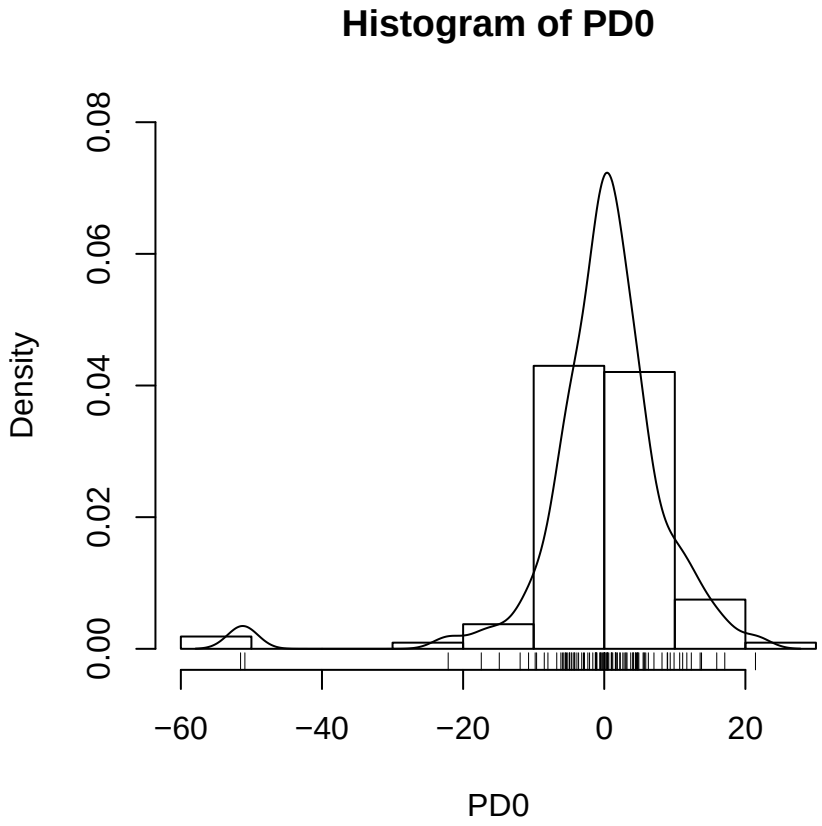

Figure 3.16: Basic Best Rated Data for Analysis

Listing 23 Summary of $PD0$ Data

```
> quantile(PD0, probs=.025)
     2.5%
-19.06819
> quantile(PD0, probs=.975)
   97.5%
14.53804
```

3.9.0.4 Hypothesis Testing and Confidence Intervals for the Mean for the Best Rated Data

We hypothesize that the $PD0$ data is coming from a population of zero mean. This is our null hypothesis. This indicates that the percentage error in the detectors is unbiased, and that essentially the detectors and the video data are compatible.

Null Hypothesis:

Mean value of the percent difference between the FAST detector flow rates and the video counted rates is zero for the Best Rated Data.

To perform the hypothesis testing, we will use the t-test. For the data that we have, we get the t-statistic as given by

$$t = \frac{\overline{PD0}}{\sigma/\sqrt{N}} \tag{3.19}$$

Here, we have for sample mean

$$\overline{PD0} = \frac{\sum_{i=1}^{N} PD0_i}{N} \tag{3.20}$$

and for sample variance

$$\sigma = \frac{\sum_{i=1}^{N}(PD0_i - \overline{PD0})^2}{N-1} \tag{3.21}$$

The application of the t-test to the $PD0$ data gives the result shown in Listing 24. The result shows a p-value of 0.749 which clearly shows that the null hypothesis can not be rejected. Hence, we accept the null hypothesis, which means that we claim that the flow detector data has been validated by the video counted data.

Listing 24 T-test of $PD0$ Data

```
> t.test(PD0)

        One Sample t-test

data:  PD0
t = -0.3208, df = 106, p-value = 0.749
alternative hypothesis: true mean is not equal to 0
95 percent confidence interval:
 -2.179141  1.572207
sample estimates:
 mean of x
-0.3034671
```

The confidence interval, at the confidence level, γ for the population mean, μ is given by Equation 3.22.

$$\overline{PD0} - \frac{c\sigma}{\sqrt{n}} \leq \mu \leq \overline{PD0} + \frac{c\sigma}{\sqrt{n}} \tag{3.22}$$

Listing 24 gives the 95% confidence interval for the population mean as $(-2.179141, 1.572207)$.

3.9.0.5 Confidence Interval for the Variance for the Weighted Data for the Best Rated Data

In this subsection, we will estimate the confidence interval for the variance of the percent error for the data that we expect from the population using the Best Rated Data. This will indicate to us what performance can be expected from flow detectors of the type that were tested using the enhanced method.

The steps applied to the analysis of the $PD0$ data produce the following.

First Step

$\gamma = 0.95$.

Second Step

We get $F(c_1) = (1 - 0.95)/2 = 0.025$, and $F(c_2) = (1 + 0.95)/2 = 0.975$

For $F(c_1) = 0.025$, $c_1 = (h - 1.96)^2/2$, where $h = \sqrt{2m - 1}$, m being the number of degrees of freedom, i.e. $m = n - 1$. For our data, $n = 107$, which gives $c_1 = 426.3455$.

Similarly, for $F(c_2) = 0.975$, $c_2 = (h + 1.96)^2/2$, which gives $c_2 = 548.4961$.

Third Step

Variance of the $PD0$ data is 95.77. Hence, $(n - 1)s^2 = 10151.62$.

Fourth Step

Now, $k_1 = (n - 1)s^2/c_1 = 23.81078$ and $k_2 = (n - 1)s^2/c_2 = 18.5081$.

Fifth Step

Hence, the confidence interval for the variance is $18.5081 \leq \sigma^2 \leq 23.81078$. This

implies that the confidence interval for the standard deviation is $(4.302104, 4.879629)$.

3.9.0.6 Normalized Plot of Percent Errors and Analysis for the Best Rated Data

Based on the sample mean and the sample variance, we can create a normal curve to show the approximate performance in terms of the percent difference for the flow detectors using the Best Rated Data. The code for this plot is shown in Listing 25, and the corresponding plot is shown in Figure 3.17.

Listing 25 Code for Normal Curve for $PD0$ Data

```
> mean <- mean(PD0)
> sd <- sd(PD0)
> x <- seq(-4,4,length=100)*sd + mean
> hx <- dnorm(x,mean,sd)
> plot(x, hx, type="l", xlab="PD0", ylab="Density",main="Percent Error Plot")
```

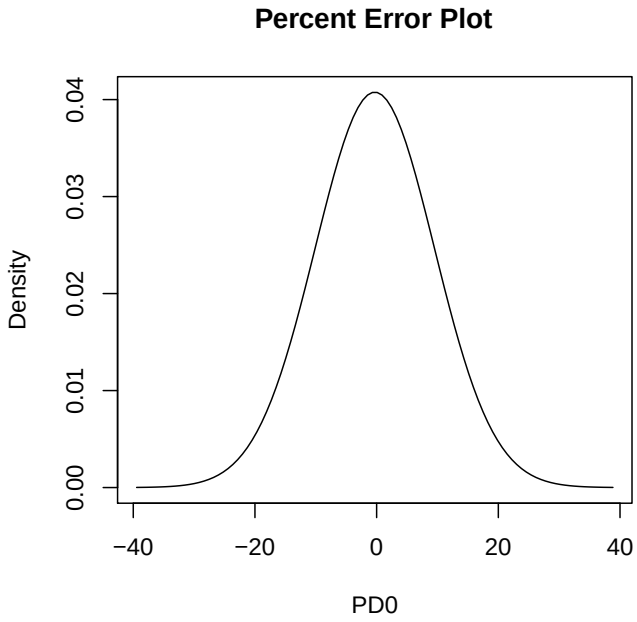

Figure 3.17: Normal Plot for Weighted Percent Errors

We can use this plot for some basic approximate analysis. For instance, if we want to find out what percentage we get errors between the values of $(-5\%, +5\%)$, we use the norm function in R, and obtain the answer of 36.87%. Similarly, for errors between the values of $(-10\%, +10\%)$, we get 67.82%, and for errors between the values of $(-15\%, +15\%)$, we get 86.68%. The R-code for this analysis and the corresponding results are shown in Listing 26.

Listing 26 Code for Analysis of $PD0$ Data

```
> 2*(0.5 - pnorm(-5,mean,sd))
[1] 0.3687108
> 2*(0.5 - pnorm(-10,mean,sd))
[1] 0.6782343
> 2*(0.5 - pnorm(-15,mean,sd))
[1] 0.8668406
```

3.10 Summary of the Results

The following are the main results for the data analysis performed that consisted of the following:

- Data analysis without considering video ratings
- Potentially Faulty detectors:
- Data analysis considering video ratings

3.10.1 Percent Errors Without Using Video Ratings

Listing 27 demonstrates the statistics for the percent difference obtained.

Listing 27 Summary Statistics for the Difference

```
Min.    1st Qu.     Median       Mean    3rd Qu.       Max.
-1067.000    -4.822     0.495    -3.187     6.351    82.070
```

The performance of the errors are depicted in the Figure 3.18.

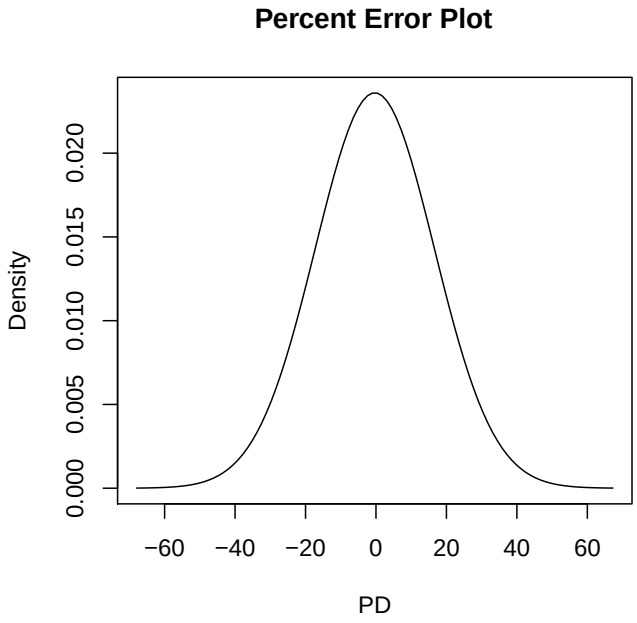

Figure 3.18: Normal Plot for Percent Errors

3.10.2 Potentially Faulty Detectors

The detectors listed in Table 3.5 are the potential faulty detectors identified by the algorithm developed in section 3.7.

3.10.3 Percent Errors Using Video Ratings

Listing 28 demonstrates the statistics for the percent weighted difference obtained.

Table 3.5: Potential faulty detectors identified using developed algorithm

RoadID	**SegID**
56	2
49	2
102	1
103	1
103	1
41	1
57	1
61	1
65	1
190	1
125	2
126	1
8	2
29	2
405	1
327	1
329	2
129	2

Listing 28 Summary Statistics for the Weighted Difference

```
    Min.  1st Qu.   Median     Mean  3rd Qu.     Max.
-99.4400  -2.6450   0.2636   0.1922   3.7390  45.7000
```

1. 95% of the sample data errors are between -18.33740% and 22.49848%.

2. 95% confidence interval for the population mean is $(-0.8172784\%, 1.2017711\%)$.

3. 95% confidence interval for the population standard deviation is $(10.67289\%, 12.10564\%)$.

4. 35.3% of the data is in between $(-5\%, +5\%)$, 63.13% between $(-10\%, +10\%)$, and 81.97% between $(-15\%, +15\%)$.

The performance of the errors can be seen in the Figure 3.19.

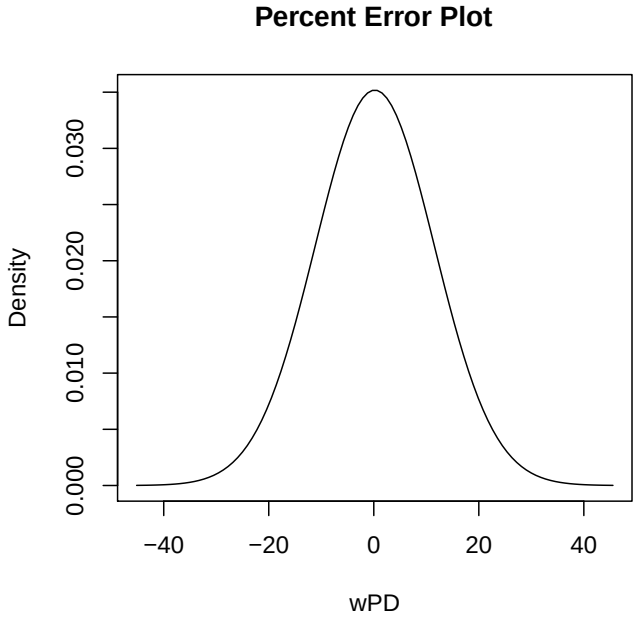

Figure 3.19: Normal Plot for Weighted Percent Errors

3.10.4 Recommendations

The following recommendations are based on the analysis performed:

1. The analysis presented in this study identified some detectors that could be potentially faulty, and those must be tested further.

2. An automated method of data verification should be developed so that on a regular basis faulty detectors can be identified.

3. The method for the verification should be further developed. If video will be used for verification, then the requirements for the video quality that includes its location, angle, zoom etc. will have to be specified.

4. Some detectors should be tested thoroughly in a highly controlled environment to see what the accuracy is when the actual counts can be compared with the detector counts. The controlled environment can be a location where the researchers can drive vehicles to see how the detectors are responding.

3.11 Conclusions

In this chapter, we examine the detectors that were used in order to collect most of the data on the roadway network treated in this research. The detectors' counts are compared with manual video counts. T-statistics was used since both sets of data are experimental and the actual mean is not available. A weighted statistical approach is developed in order to give more weight to data obtained from clear videos. Additional statistical processing is performed in order to remove the bias of the video ratings since they are assigned by different people. This study compares the flow detector volume data to manual counted traffic video volume data. Since, traffic videos can have varying levels of clarity depending on different factors such as the angle, distance, occlusion, and clarity due to environment, a new technique for statistical analysis for comparison was developed. This technique used clarity ratings of the manual counters. Analysis was performed to obtain a model relating the rating numbers to consistency variation, which was then used for paired t-test for final comparison. This technique was used on data collected and the results were presented. Finally, specific recommendations were made based on the results obtained in this project.

Part III

Reliability

CHAPTER 4

Classical Reliability

4.1 Overview

This chapter discusses the classical reliability which treats the performance measures aspect of networks as shown in Figure 4.1. In this chapter, some classical reliability measures are introduced and investigated. Travel time data is used along Interstate 15 along the South as well as the North bounds. Mainly, normalized standard deviation analysis, the 95th percentile, and reliability as non-failure analysis are used in conducting the reliability day-to-day and within the day analysis.

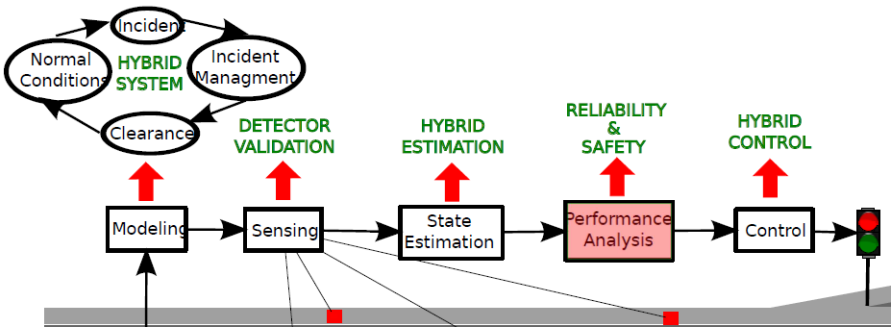

Figure 4.1: Overall research work

4.2 Introduction

In this chapter, the classical methods of measuring travel time reliability are presented. Traffic conditions caused by non-recurring events are highly unpredictable, causing unexpected delays that directly affect travel times. This uncertainty results in variable traffic

conditions, and is measured by "travel time reliability." The uncertainty associated with travel times is of major importance to drivers: in fact, it is highly ranked among all influential factors that affect the choice of departure time choice of travelers [35]. The inconsistency of travel times inflict a scheduling cost, where commuters have to budget extra time when traveling a certain route [36]. Also, manufacturing operations give travel time reliability more importance than delayed trips [37]. Therefore, travel time reliability is an crucial measure in transportation system management [38]. Lomax [37] recognizes some of the possible sources for inconsistency, such as incidents, work zones, weather, fluctuations in demand, special events, traffic control, and inadequate capacity. He also argues that reliability measures should indicate how much each source contributes to the inconsistencies, when possible; this is highly dependent on the measure used as well as on the available data.

4.3 Background

4.3.1 Reliability in the Transportation Sense

The reliability of transportation systems mainly quantifies the consistency of travel times of a certain trip or route. "Travel time" is the time that takes users of the road system to commute from an origin to a certain destination. Considering a fixed length of a highway section, travel times directly reflect traffic conditions, such as congestion due to recurring or nonrecurring events. Overall transportation reliability research has come to agree on the importance of measuring inconsistency of travel times for certain trips as well as inconsis-

tency of performance. Many reliability measures were developed and shown to be "good measures." However, as stated in Lint's work [39], all these measures have been proven to be inconsistent with each other: they do not accurately measure inconsistency and, as a whole, are inadequate measures for the performance of the transportation network.

4.3.2 Classical Reliability Measures

Traditionally, travel time reliability can be evaluated using various quantitative measures, all of which differ to a certain degree in the information they contain. The appropriate measure to be chosen depends on the evaluation criteria. Most researchers as well as transportation entities use standard statistical methods when defining reliability.

Lomax [37] recognizes that the common definition for reliability used in transportation is the level of consistency in travel times. In this context, reliability allows assessment of the performance of certain elements of transportation systems, such as a mode, trip, route, or a corridor.

Bogers [35] recognizes the various reliability measures that have been used, and stresses that the reliability analysis method depends on the application. Nie and Fan [40] developed an adaptive routing strategy, named the stochastic on-time arrival (SOTA) algorithm, to target least-expected travel time as a mechanism to address the performance measure of reliability. Oh and Chung [38] studied travel time variability by using data from Orange County, California. They studied travel time variability that was computed in terms of day-to-day variability, within-day variability, and spatial variability. They concluded that

travel time is correlated with standard deviation. Chen et. al. [36] demonstrated the relationship between travel time and level of service. They show how the 90th percentile travel incorporates the mean and variability into a single measure; they also studied how travel time information using ITS can reduce travel uncertainty.

The median of travel times as a measure of reliability was used in Lam's study [41] [35]. Black [42] defines a travel time reliability ratio that gives an assessment of the extra time that commuters must account for, based on variance [35]. Van Lint [43] defined "skew" as a measure of the asymmetry of the travel time distribution, and claimed that skew was important in travel time reliability. Cambridge Systematic [44] used planning time, planning time index, and buffer index to measure reliability; they found that buffer and planning time indices are very useful statistical measures. The buffer index is defined as the extra time needed to accomplish a certain trip with respect to the mean travel time, where planning time index is an indication of the deviation of the buffer size from the ideal travel time [44].

Classical reliability measure can be categorized into four classes, as depicted in Figure 4.2: statistical range, buffer time, tardy trip, and probabilistic. Clearly, the main focus of these measures are travel time reliability.

4.3.2.1 Statistical Range

Statistical range relies on expected value (average travel time) as well as standard deviation calculations upon which the following measures are based: travel time window, percent

Class	Measures	Formula	Description
Statistical Range	Travel Time Window	$TTW = TT_{Avg} \pm \sigma$	The expected travel time range experienced by travelers.
	Percent Variation	$PV = \frac{\sigma}{TT_{Avg}} \times 100\%$	The percentage of variation in travel time with respect to average travel time.
	Variability Index	$V_I = \frac{(U_{95\%} - L_{95\%})_{Peak}}{(U_{95\%} - L_{95\%})_{Off-Peak}}$	The percentage of travel time range (inconsistency level) during peak hours with respect to off peak hours.
Buffer Time	Buffer Time	$BT = PT - TT_{Avg}$	The difference between the expected travel time and the 95th percentile travel time (the extra travel time cause by variability)
	Buffer Time Index	$BT_I = \frac{BT}{TT_{Avg}}$	The percentage of buffer time with respect to the expected travel time
	Planning Time Index	$PT_I = PT/TT_{Id}$	The percentage of the planning time (95th percentile) with respect to the ideal travel time
Tardy Trip	Florida Reliability Method	$FR = (1 - \frac{n_{Tr(TR>TR_{Avg})}}{N_{Tr}}) \times 100\%$	The percentage of trips where travel times are less or equal to expected travel time.
	On Time Arrival	$OTA = (1 - \frac{n_{TR(TR>110\%TR_{Avg})}}{N_{TR}}) \times 100\%$	The percentage of time where travel times are less or equal to expected travel time.
	Misery Index	$M_I = \frac{TR_{Avg_{(Longest\ 20\%\ trips)}} - TR_{Avg}}{TR_{Avg}}$	The ratio of the difference between the average travel rate for the longest 20% of total trips and average travel rate of total trips.
Probabilistic	Travel Time Unreliability	$P(TT \geq \alpha \cdot TT_{th})$	The probability that the travel time is larger than a certain threshold recognized as the upper limit for success.

Acronyms

$TT - TravelTime$ $Avg - Average$ $\sigma - S\tan dardDeviation$ $U - Upper$ $L - Lower$ $Id - Ideal$ $PT - PlanningTime(95^{th}\ Percentile)$ $n_{Tr} - NumberOfTrips$ $N_{Tr} - TotalNumberOfTrips$ $TR - TravelRate$ $TT_{th} - TravelTimeThreshold$

Figure 4.2: Classical reliability measures summary

variation, and variability index. The travel time window indicated the expected travel time range that is experienced by travelers. Percent variation is the percentage of variation in travel time with respect to average travel time. The variability index is the percentage of the range of travel time, and indicates the inconsistency level during peak hours with respect to off-peak hours.

4.3.2.2 Buffer Time Measures

Buffer time measures are also based on average travel time. In their calculations, this class of measures uses percentiles, defined as planning time, and ideal travel times. They indicate the extra amount of time that the traveler must allow to reach the desired destination at the desired time. The most common set of measures that are based in buffer time are buffer time, buffer time index, and planning time. Basically, buffer time is the difference between the expected travel time and the 95th percentile travel time. In other words, it is the extra travel time caused by variability. The buffer time index is the percentage of buffer time with respect to the expected travel time. The planning time index is the percentage of the planning time with respect to the ideal travel time.

4.3.2.3 Tardy Trips

Tardy trips is a class of measures that indicate how often travelers are late. This measure is based on thresholds that are preset in order to define what is considered to be late; in the previous measure, buffer time, calculations are mostly based on averages. Tardy trip measures are also based on the extra delay incurred during the worst trips [39]. Florida

reliability, on time arrival, and misery index are examples of reliability measures of this class. The Florida reliability method gives the percentage of trips where the travel times are less than or equal to the expected travel time. "On time arrival" indicates the percentage of time where travel times are less than or equal to the expected travel time. The ratio of the difference between the average travel time rate for the longest 20% of total trips and average travel rate of total trips is given by the misery index.

4.3.2.4 Probabilistic Measures

Probabilistic measures are based on the distribution fitting of the random variable. The transportation component's reliability to be measured becomes the random variable for which the appropriate distribution is determined, based on the nature of the component. This measure indicates the probability of success based on a threshold set by the evaluator, for instance, the probability that the travel time is greater than a certain threshold. The distribution that is used can vary based on what is being measured. The following are common distributions used for extreme event failure, such as incidents and failure of traffic control devices: gamma, Weibull, normal, exponential, log normal, Poisson process, and truncated normal.

4.4 Reliability Measures and Technical Methods

The term "reliability" suggests repeatability or dependability. For a random experiment this would mean that the results of an experiment are repeatable. In terms of travel-time,

this would mean that if travel time is measured repeatedly on a section, we obtain comparable values. In general, repeatability of travel time could be framed in terms of time-of-day, day of the week, etc. Thus, travel time reliability is determined by conducting analysis on data measured for a certain roadway segment.

In this chapter, the following approaches are used in obtaining various reliability measures:

- Classical Method: Planning Time, Planning Time Index, Buffer Index
- Variability, Based on Normalized Standard Deviation,
- Analysis of Variance ANOVA
- Travel Time Mean Estimation using t Statistics,
- Reliability as a Measure of Non-failures, and

4.4.1 Classical Method: Planning Time, Planning Time Index, Buffer Index

Traditionally, reliability is measured through calculating planning time (the buffer) and two indices: planning time index and buffer index through analyzing the travel time frequency distribution. Planning time or the buffer is calculated as the 95th percentile of travel time as demonstrated in Equation 4.1. The planning time buffer indicates the extra time travelers should account for in order to guarantee on time arrival. Planning time index is the ratio of the planning time to the ideal travel time (free flow) which indicates how planning time compares to ideal travel. Planning time provides more information about the severity of

the conditions. The cheer buffer size (planning time) indicates consistency of travel times. Buffer index is the ratio of the difference between planning time and average travel time to the average travel time as demonstrated in Equation 4.2.

$$\tau_{pi} = \tau_p / \tau_f \tag{4.1}$$

$$B_i = \frac{\tau_p - \tau_A}{\tau_A} \tag{4.2}$$

where

τ_p : planning time (the 95^{th} percentile)

τ_{pi} : planning time index

τ_f : free flow travel time

τ_A : average travel time

B_i : buffer index

4.4.2 Variability, Based on Normalized Standard Deviation

For a given set of travel time data on a freeway section, statistical mean can be calculated by Equation 4.3; however, travel time mean is not sufficient since it does not convey any

information about how volatile the travel times are on the studied highway segment. Therefore, calculations of the standard deviation given in Equation 4.5 are necessary in order to understand the distributive nature of travel times [45]. Clearly, a lower standard deviation indicates a higher concentration of data about the mean illustrating closer values to the mean; thus a more reliable highway segment.

$$\bar{\tau} = \frac{\sum_{i=0}^{n} \tau_i}{N} \tag{4.3}$$

$$\sigma = \sqrt{\frac{\sum_{i=0}^{n} (\tau_i - \bar{\tau})^2}{N-1}} \tag{4.4}$$

$$\sigma_n = \sigma / \bar{\tau} \tag{4.5}$$

where

τ_n : travel time on a certain highway segment

$\bar{\tau}$: Average travel time for the given data set

σ : Standard deviation of travel times for the given data set

N : Total number of data points in the data set

σ_n :Normalized standard deviation

4.4.3 Analysis of Variance (ANOVA)

Using ANOVA, the means of various data sets were compared for hypothesis testing. A null hypothesis is defined by determining a desired α value representing the variation between the groups tested. If the ratio of the variance among the samples means to the variance within the samples, F, is less than critical value (F_α), then the null hypothesis (H_0) is accepted indicating that the variation in mean falls within the desired regions. Otherwise, the alternate hypothesis (H_1)is accepted indicating higher variability thereof lower reliability.

$$\begin{aligned} H_0 &: F \leq F_\alpha \\ H_1 &: F > F_\alpha \end{aligned} \tag{4.6}$$

where:

H_0 : Null hypothesis

H_1 : Alternative hypothesis

4.4.4 Travel Time Mean Estimation Using t-Statistics

Average of measured travel times of the sample data $\bar{\tau}$ may or may not reflect an accurate measure of the actual population mean μ. The actual travel time mean can be estimated

using T distribution, since actual population variance is unknown, with a certain confidence interval 4.7. Travel time mean estimation with the specified confidence intervals delivers a practical measure that could be easily understood by the general public. Furthermore, this measure can be used for the day to day operations of emergency responders in the private and public sectors as well as general drivers. An automated statistical technique can be developed to reflect travel times given certain settings such as day, time, and location based on real time data.

$$
\begin{gathered}
1-\alpha = 90\% \\
t = \frac{\bar{\tau}-\mu}{\sigma/\sqrt{n}} \\
\text{The 90th percentile:} \\
\Pr(\bar{\tau} - t_{\alpha/2}\frac{\sigma}{\sqrt{n}} < \mu < \bar{\tau} + t_{\alpha/2}\frac{\sigma}{\sqrt{n}}) = 0.9
\end{gathered}
\tag{4.7}
$$

where

$\bar{\tau}$: Average travel time for the given data set

σ : Standard deviation of travel times for the given data set

4.4.5 Reliability as a Measure of Non-Failures

One can perceive travel time reliability, R, as the probability of success of a certain route. This method provides probability of the extremes, pass or fail, defined in Equation 4.9. Success can take various meanings; in terms of travel time. Success of a highway segment can be defined as whether the actual travel time is below or above a desired travel time τ_d as defined in Equation 4.8. This measure is a representation of the percentage of time a certain link is at a desired condition, for instance free flow. It is easily understood by the general public and could be expanded further to measure reliability of complex networks. This measure is different from the meaning of traditional reliability since it indicates the success of the transportation system of maintaining travel times at free flow. This measure is more useful for transportation engineers, and policy makers.

$$\tau_d = \tau_{ff} + \tau_{th} \tag{4.8}$$

$$R_i = \frac{S_T}{N} \tag{4.9}$$

where

τ_d : Desired Travel Time

τ_{ff} : Free Flow Travel Time

τ_{th} : Travel Time Threshold, ex: 5 min

N : Sample size

S_T : Total number of successes, where $\tau < \tau_d$

Using this method, reliability of a highway segment R_s that consists of multiple contagious segments R_1, R_2 ... R_n is determined as implied by Equation 4.10 [46]

$$R_s = \prod_{i=1}^{n} R_i \tag{4.10}$$

4.4.6 Issues with Classical Reliability Measures

By carefully examining the classical reliability measures, one can obtain far more information from the values other than pure inconsistency. For instance, the tardy trip and the probabilistic class of measures deliver reliability with respect to a certain threshold that determines the success rate and/or the failure rate. Even though this meaning of "reliability" is not touched upon by the classical definition, it is of major interest to researchers as well as to transportation systems evaluators because it is a vital indicator of the system's performance.

Inadequacy is another issue with the classical reliability measures. Lint [39] highlighted that classical measures are highly inconsistent in providing conclusions regarding the reliability of a certain trip or roadway segment. This is a predictable result since all of these measures

use various thresholds. Another flaw in using these measures is that most of them assume a symmetrical distribution in calculating the variability ranges; this is inaccurate, particularly because symmetrical distributions are not the most appropriate for extreme event analysis. Therefore, a measure of inconsistency needs to be developed irrespective of any threshold or distribution.

The lack of equipment in order to measure network reliability is another issue. Lint argues that these measures are inadequate in terms of cost for evaluating the performance of the system. Such evaluation is crucial for policy makers and for the optimization of budget allocation in transportation projects. In order for a certain value to serve as a good performance measure, it must capture such information as the safety of the link, emissions, and incident rates. Thus, the development of network reliability measures is highly necessary.

Issues with the classical reliability measures can be summarized as follows:

1. Inadequacy
2. Inconsistency
3. Inability of expansion to Network Reliability

4.5 Results and Discussion

Two types of analysis were conducted, day-to-day and within the day reliability, on the DMS data obtained from FAST using the six proposed methods.

4.5.1 Variability, Based on Normalized Standard Deviation (NSTD)

Tables 4.1(a) and 4.1(b) list the obtained NSTD for both signs.

Table 4.1: Normalized Standard Deviation

(a) Day to day

Std. Statistics	Sign 13				Sign 17			
	Average	Variance	Std	N-Std	Average	Variance	Std	N-Std
Monday	13.37	3.12	1.77	0.13	13.86	0.62	0.79	0.06
Tuesday	14.43	3.48	1.87	0.13	13.10	0.42	0.65	0.05
Wednesday	14.97	3.17	1.78	0.12	13.57	0.52	0.72	0.05
Thursday	14.44	4.09	2.02	0.14	12.52	0.69	0.83	0.07
Friday	14.88	6.30	2.51	0.17	14.14	1.32	1.15	0.08
Saturday	11.32	0.92	0.96	0.08	9.67	1.16	1.08	0.11
Sunday	10.30	0.03	0.17	0.02	9.25	1.11	1.05	0.11

(b) Within the day

Std. Statistics	Sign 13				Sign 17			
	Average	Variance	Std	N-Std	Average	Variance	Std	N-Std
6am-8am	12.84	5.78	2.40	0.19	12.36	14.81	3.85	0.31
8am-10am	13.69	8.51	2.92	0.21	12.29	12.62	3.55	0.29
10am-12am	12.97	5.45	2.33	0.18	12.26	13.15	3.63	0.30
12am-2pm	15.02	10.99	3.31	0.22	14.54	26.69	5.17	0.36
2pm-4pm	22.97	56.59	7.52	0.33	17.00	28.71	5.36	0.32
4pm-5pm	22.07	49.84	7.06	0.32	17.82	40.12	6.33	0.36

Figures 4.3(a) and 4.3(b) show the normalized standard deviation trends for signs 13 and 17.

The data was processed in two different ways day to day and within the day. Day to day processing aggregates travel times for a one day at a time which allows comparison of aggregated travel times between different days of the week as well as weekends.

Examining the obtained results for day to day analysis for sign 13 (north bound direction of the I15), higher variability is noted during week days. Yet, lower overall NTSD was obtained for sign 17 (I-15 south bound) compared to sign 13. However, results of the processed data during weekends show a higher variability for I-15 south bound (sign 17) than I-15 North

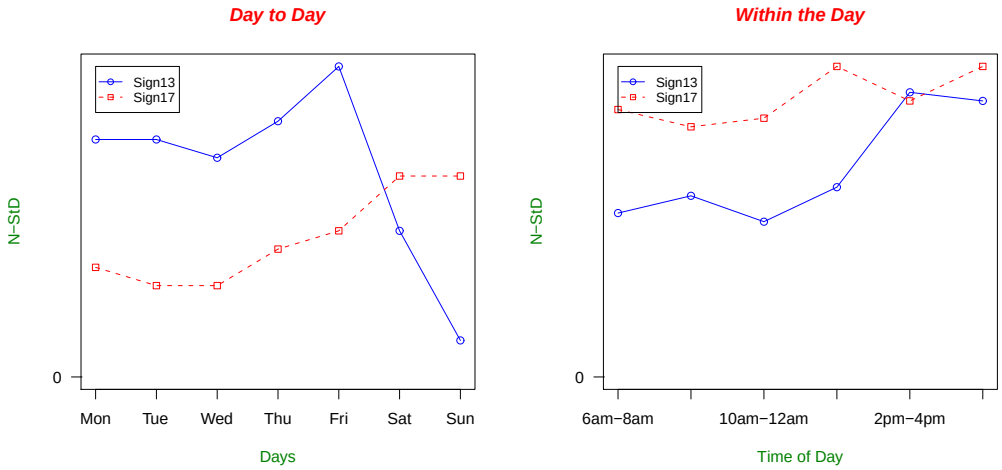

(a) Day to Day (b) Within the Day

Figure 4.3: Normalized Standard Deviation Analysis

bound (sign 13). This phenomenon may be caused by the fact that drivers' destination for that section of the freeway is most likely to be in the south direction during weekends since it leads to the center of the town. Overall reliability is not very high which means that traffic conditions on that segment are somewhat inconsistent.

From analyzing the obtained values of the normalized standard deviation for within the day processing, it is noted that the values are higher than the values obtained for day to day analysis. This was expected since traffic conditions vary tremendously from throughout the day taking into consideration traffic demand during peak hours as well as off peak hours; however, aggregating the values to represent a day as whole will result in a more consistent travel times. Less consistency is noted when travel times are compared for all days vs. when only alike days are compared. This emphasizes the importance of data processing methods and how different processing can give different meanings. Overall, higher reliability is noted on I-15 North which is inconsistent with day to day analysis.

The same data will be analyzed in the subsections to follow using the various proposed methods in order to extract the information that each one provides.

4.5.2 Analysis of Variance ANOVA

Tables 4.2(a) and 4.2(b) show the F value obtained from the ANOVA hypothesis test with $\alpha = 0.05$. The F values obtained from ANOVA analysis for both signs and the two types of analysis (day to day and within the day) are greater than the critical value F_α which indicates rejection of the null hypothesis. These results show low consistency in travel times for the studied freeway section; thus, low reliability.

Table 4.2: Normalized Standard Deviation

(a) Day to day

	F	P-Value	F_α
Sign13	59.56	6.95E-51	2.12
Sign17	253.12	2.6E-125	2.12

(b) Within the Day

	F	P-Value	F_α
Sign13	193.2	1.8E-151	2.22
Sign17	56.45	7.88E-53	2.12

4.5.3 Travel Time Mean Estimation

Tables 4.3(a) and 4.3(b) illustrate the average travel time with 95 percent confidence. Depicted in Figures 4.4(a) and 4.4(b)the 95th percentile for both signs.

As expected, the 95 th percentile averages approximately 18 and 14 minutes for sign 13 and 17, respectively during week days; however, it is much lower on weekends. Analyzing within the day values, it is noticeable that travel times are much higher in the afternoon than it is in the mornings as shown in Figures 4.4(a) and 4.4(b).

Table 4.3: Anaysis of Variance (ANOVA)

(a) Day to day

Confidence Intervals	Sign13		Sign 17	
	Time	Percentile	Time	Percentile
Monday	$12.96 < t < 13.78$	16.44	$13.68 < t < 14.04$	15.06
Tuesday	$13.99 < t < 14.86$	17.92	$13.41 < t < 13.74$	14.98
Wednesday	$14.29 < t < 15.46$	17.92	$13.41 < t < 13.74$	14.98
Thursday	$13.97 < t < 14.91$	17.87	$12.32 < t < 12.71$	14.06
Friday	$14.29 < t < 15.46$	18.81	$13.87 < t < 14.41$	16.16
Saturday	$11.09 < t < 11.54$	12.91	$9.42 < t < 9.92$	11.48
Sunday	$10.26 < t < 10.34$	10.62	$9.00 < t < 9.49$	10.76

(b) Within the day

Confidence Intervals	Sign13		Sign 17	
6am-8am	$12.56 < t < 13,12$	16.35	$11.92 < t < 12.81$	18.75
8am-10am	$13.35 < t < 14.02$	18.82	$11.87 < t < 12.70$	19.59
10am-12am	$12.70 < t < 13.24$	17.93	$11.84 < t < 12.68$	18.68
12am-2pm	$14.64 < t < 15.41$	20.57	$13.94 < t < 15.14$	25.37
2pm-4pm	$22.10 < t < 23.84$	32.84	$16.38 < t < 17.62$	26.92
4pm-5pm	$21.25 < t < 22.89$	32.71	$17.09 < t < 18.56$	30.32

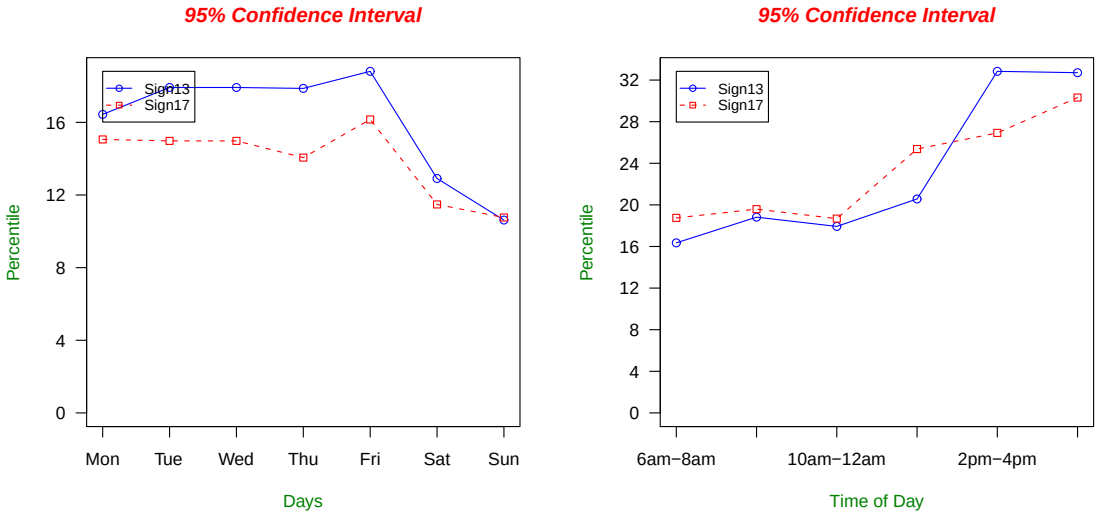

(a) Day to Day

(b) Within the Day

Figure 4.4: The 95th percentile

4.5.4 Reliability as a Measure of Non-failures

Tables 4.4(a) and 4.4(b) show the results obtained when non-failure analysis is used in determining reliability. Figures 4.5(b) and 4.5(a) illustrate the trend for both day to day and within the day.

Table 4.4: Reliability as a measure of non-failure analysis

(a) Day to day

Failure Anlys	Min		Max		Range		Threshold	Success		Failure		R	
Sign(S)	S13	S17	S13	S17	S13	S17	S13/17	S13	S17	S13	S17	S13	S17
Monday	10.58	11.83	16.51	15.10	5.94	3.27	11	3	0	49	52	0.06	0
Tuesday	10.94	11.59	17.68	14.31	6.74	2.72		1	0	51	52	0.02	0
Wednesday	11.72	12.34	17.99	15.02	6.27	2.67		0	0	52	52	0	0
Thursday	10.71	10.73	17.93	14.09	7.22	3.36		3	2	49	50	0.06	0.04
Friday	10.67	12.48	18.85	16.18	8.18	3.71		3	0	49	52	0.06	0
Saturday	10.33	8.26	12.94	11.59	2.61	3.33		25	43	27	9	0.49	0.83
Sunday	10.07	8.19	10.62	10.77	0.55	2.57		52	52	0	0	1	1

(b) Within the day

Failure Anlys	Min		Max		Range		Threshold	Success		Failure		R	
Sign(S)	S13	S17	S13	S17	S13	S17	S13/17	S13	S17	S13	S17	S13	S17
6am-8am	9	7.63	31.1	30.98	22.10	23.35	11	52	97	151	105	0.26	0.48
8am-10am	9.63	7.63	22.94	24.73	13.31	17.1		48	94	155	108	0.24	0.47
10am-12am	9.63	7.63	24.29	25.71	14.67	18.08		32	94	171	108	0.16	0.47
12am-2pm	9.83	8.6	30.67	33.42	20.83	24.81		20	65	183	137	0.1	0.32
2pm-4pm	9.63	8.63	38.85	37.23	29.23	28.6		14	21	189	181	0.07	0.10
4pm-5pm	10.17	8.08	42.40	32.81	32.23	24.73		3	27	200	175	0.02	0.13

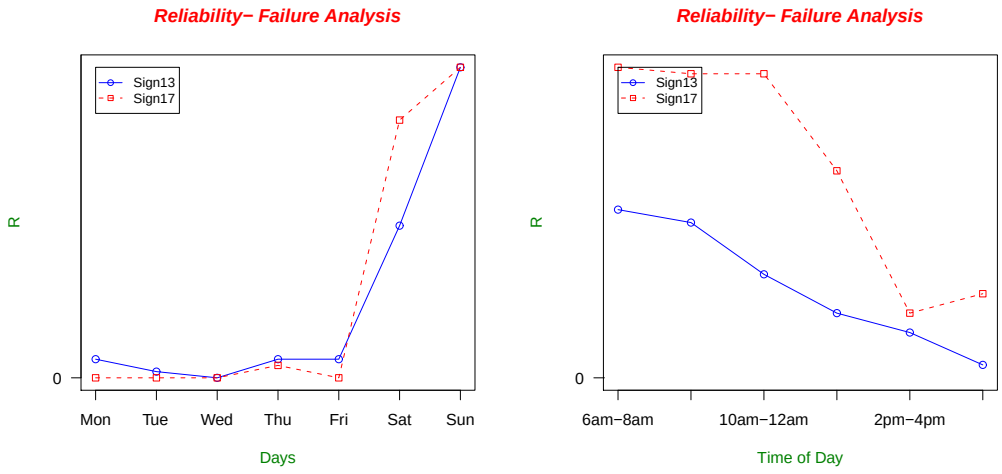

(a) Day to Day (b) Within the Day

Figure 4.5: Reliability as non-failure Analysis

Data was compared to an eleven minute threshold based on a free flow speed of 65 mph

as well as segment length which is approximately 10.5 and 7.7 miles for signs 13 and 14, respectively. The results show a higher overall reliability for sign 17 (south bound) than it is for sign 13 (north bound). The studied freeway section is unreliable in the afternoon as well as weekends for both directions. In this case reliability indicates whether travel times are above or below the desired travel time.

4.6 Conclusion

In this chapter, some classical reliability measures are introduced and investigated. Travel time data is used along Interstate 15 along the South as well as the North bounds. Mainly, normalized standard deviation analysis, the 95th percentile, and reliability as non-failure analysis are used in conducting the reliability day-to-day and within the day analysis.

CHAPTER 5

Entropy-based Reliability

5.1 Overview

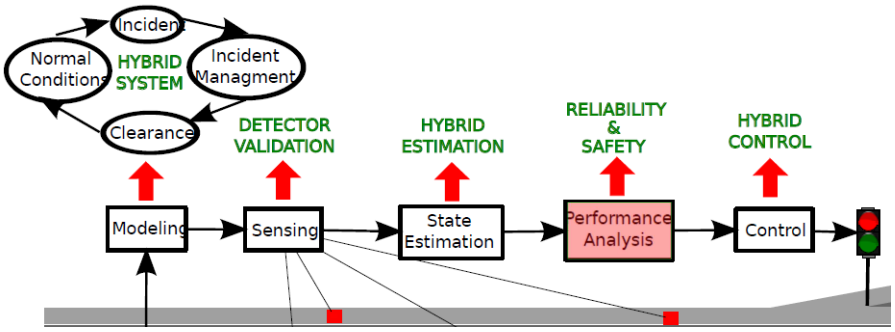

Figure 5.1: Overall research work

This chapter discusses a novel reliability measure which treats the performance measures aspect of networks as shown in Figure 5.1. In this chapter, a novel travel time reliability measure is proposed. The developed measure is based on entropy from information theory. In this chapter, some classical reliability measures are introduced and investigated. Travel time data is used along Interstate 15 along the South as well as the North bounds in order to conduct within the day analysis.

5.2 Introduction

Classical reliability measures rely fundamentally on the statistical standard deviation quantity. However, entropy is a direct tool to measure the uncertainty present in any random

variable. The quantity of entropy not only contains the standard deviation but also all other moments. Based on this, a novel travel time reliability measure is constructed that can be applied to any random variable regardless of its distributional characteristics. Then the use of the proposed novel travel time reliability measure is demonstrated by applying it to travel time data obtained from stationary detectors. The developed measure herein can be also used in various cyber complex networks such as manufacturing, power, and communication system specifically when the goal is to assess uncertainty.

Information theory has successfully demonstrated tools and formulations that are used in many disciplines such as data compression and coding in communications. Information theory introduced a number of equations that quantify information. One of the most important quantity in information theory is entropy. Entropy is the measure of uncertainty present in a random variable. Since travel time can be considered as a random variable, this study proposes developing a travel time reliability measure based on entropy.

5.3 THEORETICAL BACKGROUND

5.3.1 Information Theory

Information theory quantifies information based on probability theory and statistics. Much of the mathematics behind it was developed in order to quantify entropy in thermodynamics. Nyquist has developed a similar relation in order to quantify telegraph speed. The

information theory field was established later on by Claude E. Shannon. He introduced qualitative and quantitative models for communications based on information theory. This was considered revolutionary in the field of communications. Information theory had many applications, such as data compression. In order to understand better how information theory can be used to measure reliability, one must understand the various concepts as well as the various properties that this theory provides. Various quantities of information can be measured, most importantly, entropy and mutual information. In this study, the entropy measure will be considered since it is the most relevant measure to reliability.

5.3.1.1 The Concept of Entropy

Entropy is the measure of uncertainty that is embedded in a random variable. A high level of uncertainty in a random variable indicates high information content since it cannot be easily predicted, and vise versa. Low level of uncertainty indicates low information content. The ability to measure information content in this manner provides a powerful tool in many applications, such as message compression. Likewise, one can quantify the level of information in any set of data and, more generally, in any random variable.

Generally speaking, random variables can be discrete or continuous. The entropy measure formulation is developed for both cases. Even though they might seem similar, some properties may hold in one case but not the other.

5.3.1.2 Discrete Entropy

Equation (5.1) presents the discrete formulation of entropy [47][48][49].

Definition: Let X be a discrete random variable where $\{x_1, x_2, \cdots, xn\}$ is the set of all possible events, and let $P(x)$ be the probability of x $\forall x \in X$. Then, the entropy of X is defined as the expected value E_x of the self information $I(x)$:

$$H(x) = E_x[I(x)] = -\sum_{x \in X} P(x) log P(x) \tag{5.1}$$

where $I(x)$ is the entropy contribution of a single member of X.

Note that entropy is maximized when $P(x) = \frac{1}{n} \forall x \in X$. In other words, uncertainty is at its highest when the random variable has uniformly distributed probability mass function (PMS) since equiprobable events have high **unpredictability**. This gives the following result [47][48][49]:

$$\begin{aligned} H(x) = E_x[I(x)] &= -\sum_{x \in X} \frac{1}{n} log \frac{1}{n} \\ &= n(-\frac{1}{n} log \frac{1}{n}) = log(n) \end{aligned} \tag{5.2}$$

This result will be used in normalizing the formulation of the reliability measure.

5.3.1.3 Differential Entropy

Differential entropy is the quantity obtained when measuring the uncertainty of a continuous random variable. This is defined by (5.3). **Definition:** Let X be a continuous random

variable, and let $f(x)$ be the probability density function (pdf) of x such that the support of f lies in X. Then, the differential entropy of X is defined as [47][48][49]:

$$h(x) = -\int_X P(x) log P(x) \tag{5.3}$$

It is important to note that there are fundamental differences in the properties between entropy and differential entropy. Some of these differences are as follows:

- Normal distribution is maximized in differential entropy, whereas uniform distribution is maximized in discrete entropy.
- Differential entropy can take negative values.
- Differential entropy is not invariant under change of variables.

The last two properties mentioned in the list are undesired properties. This is resolved by introducing the relative entropy or the Kullback-Leibler divergence, which includes the invariant measure factor and is based on the limiting density of discrete points. In this chapter, the main focus will be on the discrete formulation of reliability based on information theory.

5.3.2 Entropy as a "Measure"

One can consider entropy to be a signed measure. The results in (5.2) and (5.3) can be expressed in one generalized form using relative entropy or Kullback-Leibler divergence. It is clear that the integration in the differential entropy is taken with respect to the Lebesgue

measure $\mu(x)$. Therefore, differential entropy in (5.3) can be expressed as (5.4) [47][48][49]:

$$h(x) = -\int_X f(x) log f(x) d\mu(x) \tag{5.4}$$

where $f(x)$ is the probability density function.

Likewise, the entropy measure for a discrete random variable can also be expressed as integration instead of summation; however, the integration, in this case, is with respect to the counting measure $v(x)$. In this case, (5.2) can be expressed as in (5.5) [47][48][49]:

$$h(x) = -\int_X f(x) log f(x) dv(x) \tag{5.5}$$

Note that in both (5.4) and (5.5), the probability density function f is the Radon-Nikodym derivative of the probability measure with respect to their associated measures. For example, $f = \frac{dP}{d\mu}$ in (5.4) where $f = \frac{dP}{dv}$ in (5.5). This realization leads to generalizations of the entropy concept, regardless of the nature of the space of random variables. Generalization is accomplished by introducing the following proposition:

Proposition: Let P and Q be probability measures defined on the same space. Assume that P is absolutely continuous with respect to Q, that is $P << Q$. Then , by the Radon-Nikodym theorem, the Radon-Nikodym derivative $\frac{dP}{dQ}$ exists.

This allows us to extract the relative entropy or the Kullback-Leibler divergence as it is expressed in its most general form as follows [47][48][49]:

$$\begin{aligned} D_{KL}(P||Q) &= \int_{supp(P)} \frac{dP}{dQ} log \frac{dP}{dQ} dQ \\ &= \int_{supp(P)} log \frac{dP}{dQ} dP \end{aligned} \tag{5.6}$$

Practically, this quantity represents the additional uncertainty involved when using one probability measure versus another probability measure.

In some cases, the quantity in (5.6), or the relative entropy, can be more fundamental to use than entropy, particularly, in the continuous case, for the same reasons mentioned the Differential Entropy Section. This is induced from the "nice" properties of (5.6) such as:

- Non-negative, also called Gibb's inequality
- Invariant under parameter transformation
- Additive for independent distributions

5.4 ENTROPY AS A MEASURE OF RELIABILITY

The purpose of the transportation systems reliability is to quantify the consistency of travel times of a certain trip or route. Consistency can also be thought of as redundancy or certainty. As mentioned previously, entropy is a measure of uncertainty in a random variable,

where high entropy in a random variable indicates a high level of uncertainty and low entropy indicates a low level of uncertainty. In order to relate the both concepts, a number of issues must be discussed, such as:

- What are the desired properties in a reliability measure?
- How can one use entropy to measure reliability?
- What is the reasoning behind using information theory versus using any other classical reliability measure?
- How can the new measure be applied to data?

5.4.1 Desired Properties of the Reliability Measure

Properly defining the properties of interest, is the key to developing the appropriate measure. Properties of the desired travel time reliability measure can be categorized into two categories qualitative and quantitative. Let $R(x)$ be the reliability measure and X be the random variable.

5.4.1.1 Qualitative Properties:

- $R(x)$ has to effectively quantify certainty of travel times.

5.4.1.2 Quantitative Properties:

- $R(x) : X \rightarrow [0, 1]$

5.4.2 Entropy based Reliability Construction

One can view the reliability of a certain segment of freeway as a random variable since it has uncertainty associated with it. Entropy is a well established measure of uncertainty for messages, data, and random variables in general. This information theory quantity provides a fundamental tool in quantifying uncertainty in travel time as a random variable. **Definition:**Let TT be the probability mass function of a discrete random variable, representing travel time on a given roadway segment. Then, from (5.2) the entropy TT_e or the uncertainty of the travel time on a given segment is given by (5.7):

$$TT_e(x) = -\sum_{x \in X} TT(x) log(TT(x)) \tag{5.7}$$

As mentioned in the properties, it is desired that the reliability value is less than 1 and larger than 0. Even though in its raw form TT_e is not the reliability measure, normalizing it can simplify later derivation. In order to normalize the quantity TT_e, the fact that entropy is maximized under uniform distribution (5.2) is used as shown in (5.8).

Proposition: Let TT_{ne} be the normalized travel time entropy, and let n be the total number of allowable discrete travel time values. Then,

$$TT_{ne}(x) = \frac{-\sum_{x \in X} TT(x) log(TT(x))}{log(n)} \tag{5.8}$$

Equation (5.8) provides us with a normalized value of the uncertainty present in a unit travel time. However, as stated in the qualitative properties, the reliability measure has to quantify predictability or in other words certainty. Therefore, it is proposed that this quantity is obtain by (5.9).

Proposition: Let R_{TT} be the travel time reliability for a given roadway segment. Then,

$$R_{TT}(x) = 1 - TT_{ne}(x) \tag{5.9}$$

Note that the reliability measure satisfies the qualitative as well as the quantitative measure properties that are desired.

5.4.3 Why Information Theory?

Information theory provides a direct measure of uncertainty from which the reliability measure can be easily derived. To indicate variability, classical reliability measures mainly use statistical variance as well as its different forms. There is no doubt that these measures somewhat represent certainty; however, the proposed entropy based reliability considers not only variance but also all statistical moments of a probability density function. This follows from the fact that the entropy formulation uses the probability density function as a whole

in order to extract the certainty associated with the travel time.

5.4.4 Travel Time Reliability Analysis Using Entropy

In order to demonstrate the proposed reliability measure, travel time data was obtained from The Freeway Arterial System of Transportation (FAST), an integrated Intelligent Transportation System organization in the Las Vegas area. FAST has approximately 21 Dynamic Message Signs (DMS) mostly distributed along the I-15, as depicted in Figure 5.2. Travel times are computed by means of the Incident Processing Module (IPM) in the Freeway Management System (FMS). The detector data from traffic detector stations on the freeways is processed and then displayed on the DMS [50] [51].

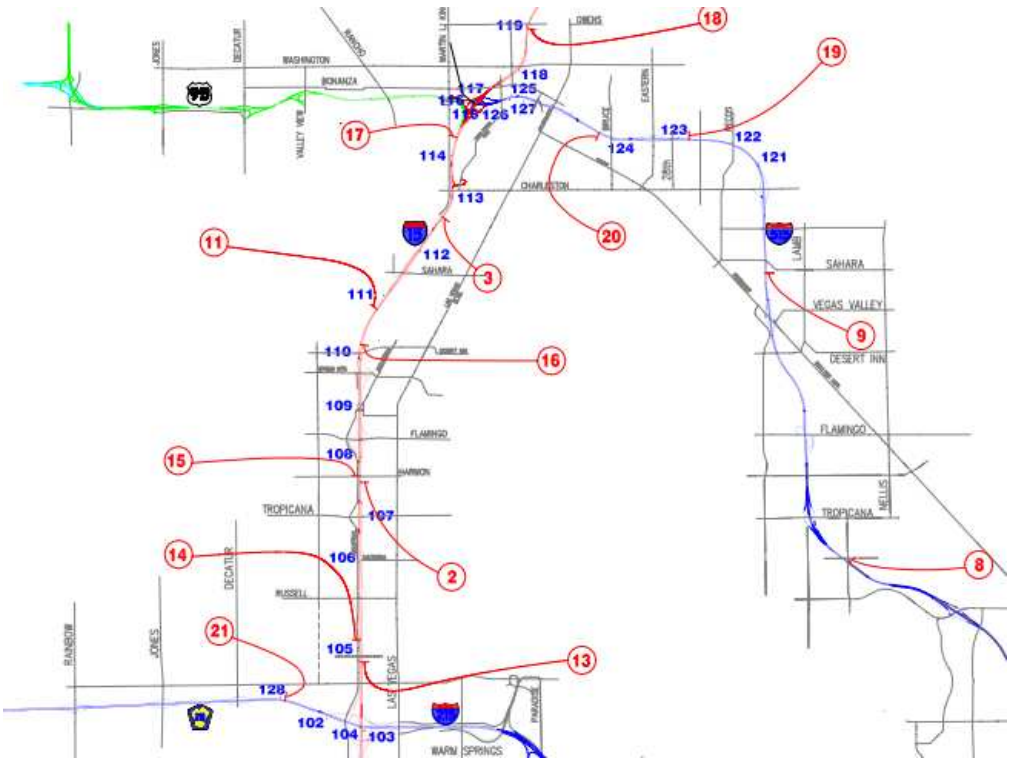

Figure 5.2: DMS on the I-15 corridor in Las Vegas from FAST

The travel time data that was obtained spanned a period of eight months, from October

Table 5.1: Sample Data Analysis using Information Theory

Time of Day	R_{Sign13}	R_{Sign17}
6am-8am	0.75	0.45
8am-10am	0.63	0.48
10am-12pm	0.75	0.47
12pm-2pm	0.56	0.37
2pm-4pm	0.27	0.33
4pm-5pm	0.26	0.26

2008 through May 2009. Sign identifiers 13 and 17 were selected for analysis since they are located on main thorofares that are frequently traversed. Sign identifier 17, located on the southbound I-15 freeway, records the travel time from US-95 to the I-215. Sign identifier 13, located on the northbound I-15, records the travel time from I-215 to US-95. The stretch of freeway covered by the chosen signs witnesses a high percentage of commuters daily, which emphasizes the importance of studying it.

Reliability calculations for the obtained data were performed using the new proposed information theory based reliability measures presented in (5.9). After further discretization of the data, the frequency distribution was obtained from which the probability density function was attained.

Analysis results are presented in Table 5.1 and Figure 5.3. Both sets of data from Sign 13 and Sign 17 show higher reliability during morning hours and much lower reliability during afternoon peak hours. This is consistent with what is expected.

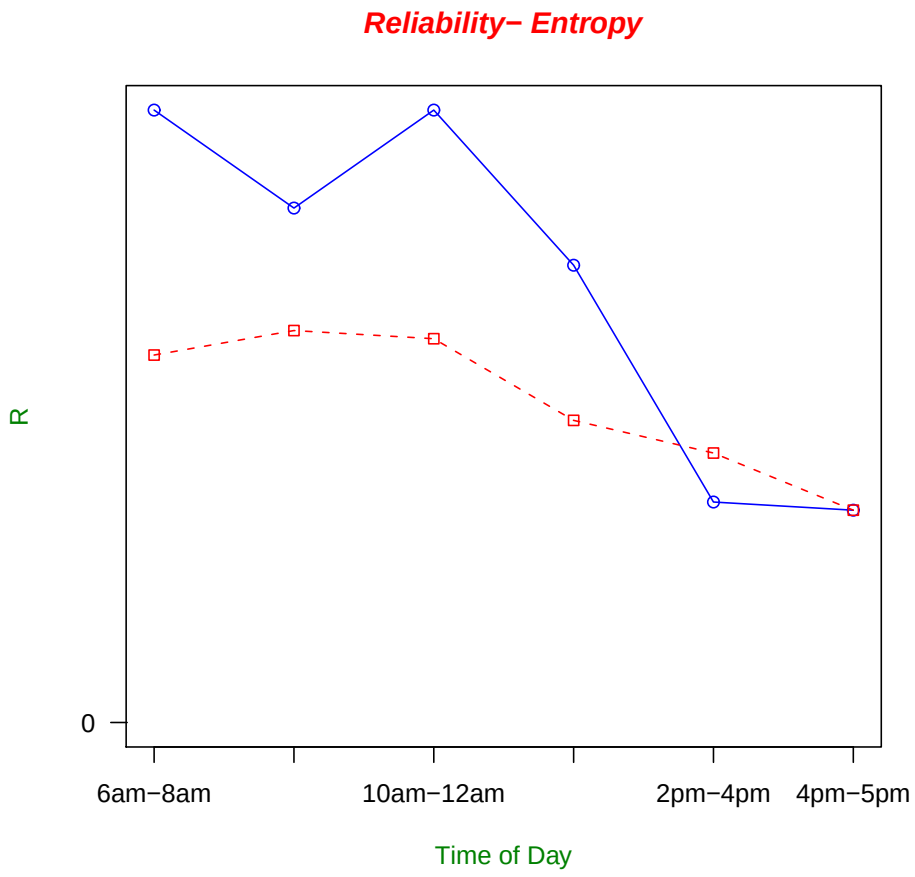

Figure 5.3: Sample Data Analysis using Information Theory

5.5 Conclusion

In this chapter, a novel travel time reliability measure is proposed. The developed measure is based on entropy from information theory. In this chapter, some classical reliability measures are introduced and investigated. Travel time data is used along Interstate 15 along the South as well as the North bounds in order to conduct within the day analysis. The reliability measure proposed in this study measures pure consistency of travel time data, which is exactly what is needed. This measure can also be used in other cyber complex system such as communication, power, and manufacturing systems.

CHAPTER 6

Min-Plus Semi-ring Algebraic Structure of Network Reliability

6.1 Overview

This chapter discusses the expansion of link reliability to complex networks which treats the performance measures aspect of networks as shown in Figure 6.1.

In this chapter, we investigate the measure of network reliability when link reliability is provided. Various approaches are introduced using the max-plus algebraic structure using reliability, unreliability, and Bellman's principle of optimality.

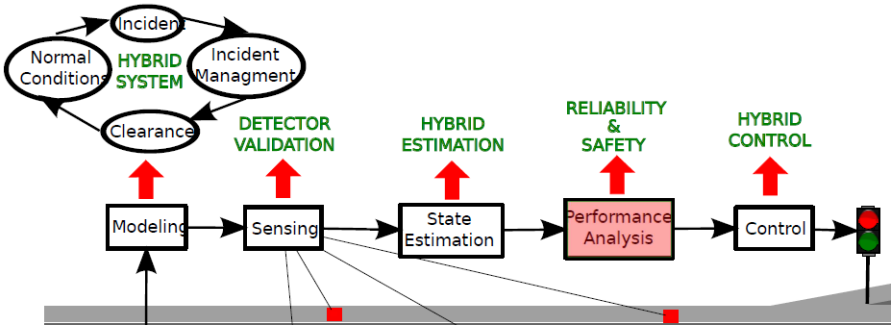

Figure 6.1: Overall research work

6.2 Introduction

This chapter demonstrates measuring the reliability of networked roadway segments or any networked system such as communications, sensor, and power networks. In this study, it

is found that the algebraic structure of the reliability of a network is consistent with the semi-ring min-plus algebraic structure. This provides us with well established properties that can simplify the algebra over networks' reliability. This study discovers the structure of the algebraic space when reliability is measured for a network.

Generally speaking, the reliability of a complex network is multilayered. As in the Open Systems Interconnection (OSI) model described in Figure 6.2, this study develops a similar model for the transportation system. Each layer of the OSI network model is responsible for a specific functionality of the networked system where information is passed to subsequent layers once data is processed [52][53].

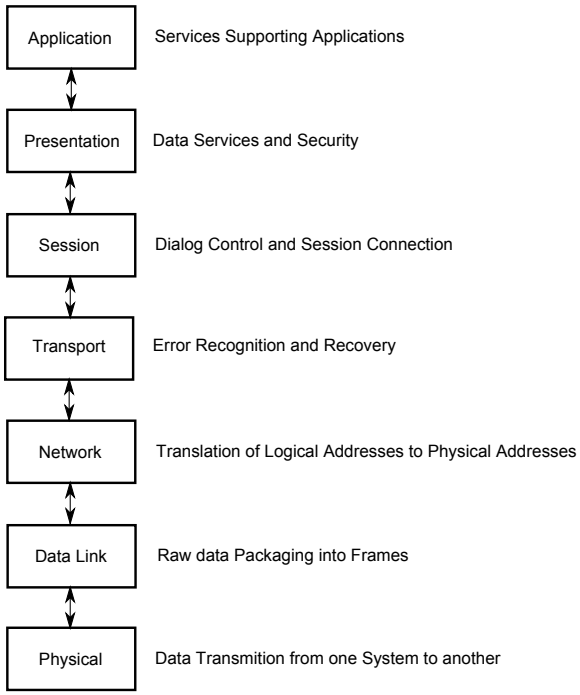

Figure 6.2: Open System Interconnection (ISO/OSI) model

Figure 6.3 describes the proposed Transportation Network Hierarchical Layer Model. Each layer is composed of elements and components residing in a layer at a lower level.

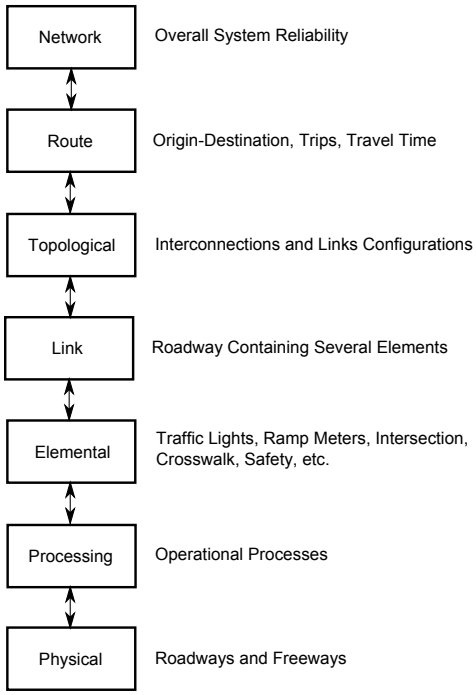

Figure 6.3: Transportation Network Hierarchical Layer Model

The Physical Layer is the most basic component of the network which consists of the connections between nodes such as roadways, highways, and freeways.

The Processing Layer is responsible for the traffic operations including traffic management strategies such as traffic management centers and intelligent transportation systems.

The Elemental Layer is responsible for the operations, safety, and reliability of the various physical components of the network such as traffic lights, ramp meters, intersections, and crosswalks.

The Elemental Layer is responsible for the operations, safety, and reliability of the various physical components of the network such as traffic lights, ramp meters, intersections, and crosswalks.

The Link Layer is responsible for the operations, safety, and reliability of a link which is composed of various physical components of the network such as traffic lights, ramp meters, intersections, crosswalks, and roadways.

The Topological Layer is the reliability of a certain topological structure composed of a number of links in the network.

The Route Layer is the reliability of a trip specified by an origin and destination. A route is composed of various lower level components.

The Network Layer is the highest level in the hierarchy. The network reliability must be composed of a quantitative integration or mapping of all reliabilities that compose the overall system.

6.3 Network Reliability

Transportation systems are composed of many components that are highly networked. Components of the transportation system can be chosen based on the criteria of the system's performance evaluation. For instance, a transportation system can be viewed as a network of the most common trip routes. A Network Structure Map (NSM) can be developed based on the network's actual topology, based on which the overall reliability of the transportation system can be measured. It is evident that the operation of some components is essential for the operation of other components. Therefore, components of the transportation network may have two possible connections: a series connection or a parallel connection. Two

components are connected in series if the operation of one depends on the operation of the other; parallel connections take place when the operation of one component is independent of the operation of the other [54].

6.3.1 Discovering the Space

An NSM can represent all the physical relations present in a transportation system. Roadway segments are mainly connected either in parallel or in series. A Network Structure Function (NSF) must be developed that allows the aggregation of the reliability measures of individual components in order to be able to quantify the reliability of the network as a whole.

6.3.1.1 Parallel Components

Given a transportation network with n components connected in parallel, as shown in Figure 6.4, let $R = \{R_1, R_2, \cdots, R_n\}$ be the set of reliability values of the segments. Since the segments are connected in parallel, there is a possibility that the driver takes any of the available components or roadway segments. Therefore, in order to obtain the total reliability of the network, more information is needed, such as the probability of taking a certain route. This leads to introducing a new set of values $W = \{w_1, w_2, \cdots, w_n\}$ or the probability mass function of the parallel segments, where w_i is the probability of taking route or segment i. Note that $\sum_{i=1}^{n} w_i = 1$.

Proposition 6.3.1. *The total parallel reliability network value R_P is given by the expected*

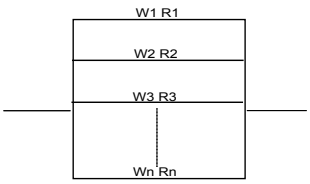

Figure 6.4: Reliability of the parallel network

value of the segmental reliability set R with respect to their probability mass function, as given in Equation 6.1.

$$R_P = \sum_{i=1}^{n} w_i R_i \tag{6.1}$$

Definition 6.3.1. *Define* $R_i^{'} \equiv w_i R_i$. *In which case (6.2) becomes:*

$$R_P = \sum_{i=1}^{n} R_i^{'} \tag{6.2}$$

This quantity will be used later to establish the algebra of reliability measure on networks.

Rewriting (6.1) in a matrix form, we obtain the following:

$$R_P = \grave{W} R \tag{6.3}$$

6.3.1.2 Series Components

Given a transportation network with n components connected in series, as shown in Figure 6.5, let $R = \{R_1, R_2, \cdots, R_n\}$ be the set of reliability values of the segments. Since the segments are connected in series, the driver must go through all the available components or roadway segments. Therefore, the total reliability of a series network is given by the minimum reliability out of all segments, as presented in Equation 6.4.

Figure 6.5: Reliability of the series network

Proposition 6.3.2. *The total series network reliability value R_s is given by the minimum of $\{R_1, R_2, \cdots, R_n\}$ as presented in Equation 6.4.*

$$R_s = min\{R_1, R_2, \cdots, R_n\} \tag{6.4}$$

6.3.1.3 Desired Properties

Based on (6.2) and (6.4), we are mainly interested in performing two operations on the real numbers: the minimum and the addition operations. This constructs a semi-ring algebraic structure that is consistent with the min-plus algebra [55].

6.3.2 Min-Plus Algebra

Definition 6.3.2. *Min-plus algebra is a semi-ring algebraic structure defined on the set $R_{min} = \{\infty\} \cup \Re$ together with two operations [56]:*

1. $a \oplus b = min(a, b)$

2. $a \otimes b = a + b$

6.3.3 Reliability of a Network

Now, we are ready to redefine the algebraic structure of the reliability of a network for parallel and series connections based on min-plus algebra.

Proposition 6.3.3. *Let $R_i^{'} \equiv w_i R_i$. Then, the total parallel reliability network value R_P is given by (6.5).*

$$R_P = \otimes_{i=1}^{n} R_i^{'} \tag{6.5}$$

Proposition 6.3.4. *The total series network reliability value R_s is given by (6.6).*

$$R_s = \oplus_{i=1}^{n} R_i \tag{6.6}$$

6.3.4 Reliability of General Networks

Given a general network, as in Figure 6.6, that has a mixed parallel and series connections. In order to analyze the reliability of the network, one must parse the overall system in terms of Origin-Destination (OD) routes. Then one must recognize all possible OD routes

as demonstrated in Figures 6.7 and 6.8. If more than one route can be assigned for the same OD pair then the routes are considered to have parallel connection.

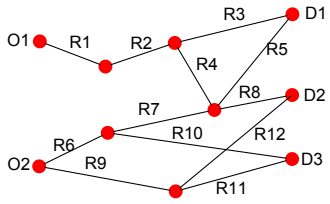

Figure 6.6: Transportation network

The next step in determining the reliability of the network is to determine the reliability of each route. By parsing the network into OD routes, each route simply becomes composed of links that are connected in series. In each case, the reliability of the route is determined by the minimum reliability among all links. Table 6.1 states the reliability for all possible OD pairs shown in Figures 6.7 and 6.8.

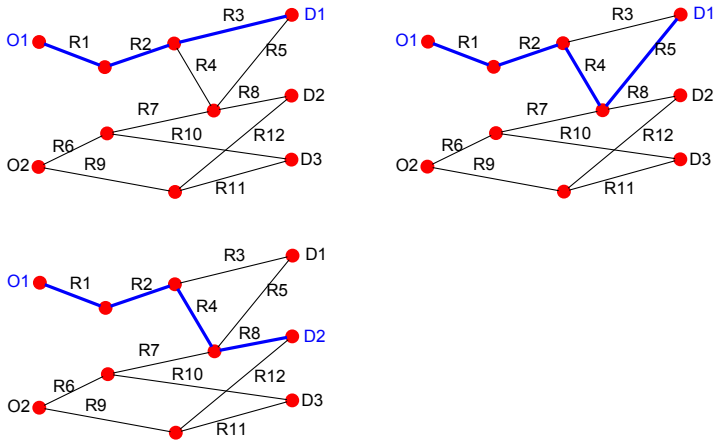

Figure 6.7: Possible routes for O1

In order to determine the reliability associated with a certain OD pair, additional information is needed on the network that indicates the possibility of taking a certain route as indicated in Equation 6.1. However, from this point forward, it will be assumed that the routes are equi-probable. This results in the following:

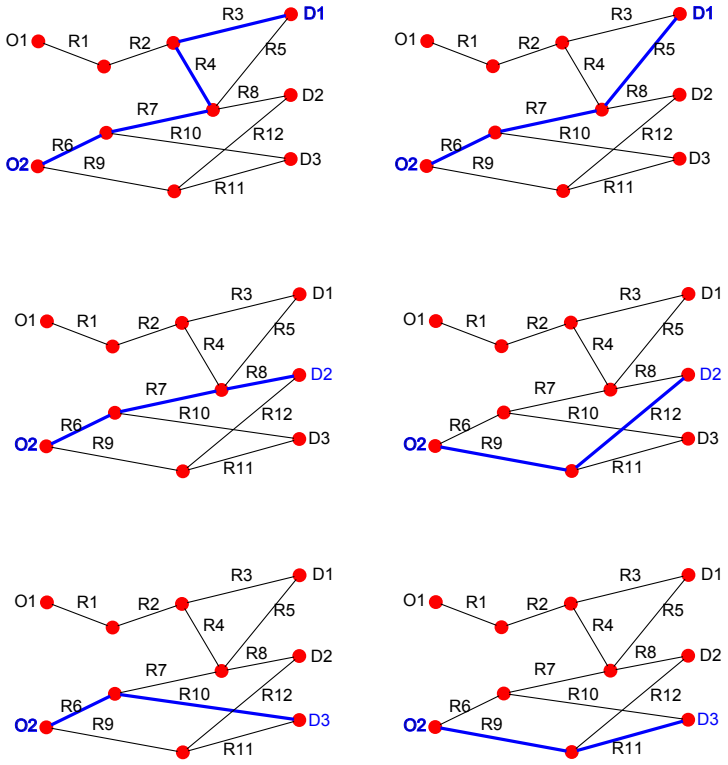

Figure 6.8: Possible routes for O2

Table 6.1: Reliability of all possible routes

OD Pair	**Route Reliability**
O1 to D1	$R_{11a} = R_1 \oplus R_2 \oplus R_3 = \min\{R_1, R_2, R_3\}$ $R_{11b} = R_1 \oplus R_2 \oplus R_4 \oplus R_5 = \min\{R_1, R_2, R_4, R_5\}$
O1 to D2	$R_{12} = R_1 \oplus R_2 \oplus R_4 \oplus R_8 = \min\{R_1, R_2, R_4, R_8\}$
O2 to D1	$R_{21a} = R_6 \oplus R_2 \oplus R_7 \oplus R_4 \oplus R_3 = \min\{R_6, R_7, R_4, R_3\}$ $R_{21b} = R_6 \oplus R_7 \oplus R_5 = \min\{R_6, R_7, R_5\}$
O2 to D2	$R_{22a} = R_6 \oplus R_7 \oplus R_8 = \min\{R_6, R_7, R_5\}$ $R_{22b} = R_9 \oplus R_{12} = \min\{R_9, R_{12}\}$
O2 to D3	$R_{23a} = R_6 \oplus R_{10} = \min\{R_6, R_{10}\}$ $R_{23b} = R_9 \oplus R_{12} = \min\{R_9, R_{11}\}$

$$R_P = \frac{1}{n}\sum_{i=1}^{n} R_i \tag{6.7}$$

where n is the number of routes connected in parallel.

Based on this assumption, the reliability of the ODs in Figures 6.7 and 6.8 is presented in Table 6.2

Table 6.2: Reliability of all OD pairs

OD Pair	**OD Reliability**
O1 to D1	$R_{11} = \frac{1}{2}\left(R_{11a} \otimes R_{11b}\right)$
O1 to D2	R_{12}
O2 to D1	$R_{21} = \frac{1}{2}\left(R_{21a} \otimes R_{21b}\right)$
O2 to D2	$R_{22} = \frac{1}{2}\left(R_{22a} \otimes R_{22b}\right)$
O2 to D3	$R_{23} = \frac{1}{2}\left(R_{23a} \otimes R_{23b}\right)$

Generalizing these results, when computing the reliability of a given network, OD pairs are first recognized, then the reliability of all routes that connect a certain OD are computed Each route is composed of roadway segments that are connected in series. In general, the reliability associated with a certain route R_r is given as the minimum of the reliability of all segments R_s composing it as in the following equation:

$$R_r = min\{R_s\} \tag{6.8}$$

where $s = 1 \cdots n$ and

n = number of segments connected in series that compose the route.

When the reliability of each possible route of an OD is determined and assuming that the probability of taking each route is equal, then the total reliability of an OD R_{od} is determined as indicated in Equation 6.7.

$$R_{od} = \otimes_1^n(\oplus_1^{i,j,..l} R_{rs}) = \\ \frac{1}{n}(min\{R_{11}, R_{12}, \cdots R_{1i}\} + min\{R_{21}, R_{22}, \cdots R_{2j}\} + \cdots + min\{R_{n1}, R_{n2}, \cdots R_{nl}\}) \tag{6.9}$$

The network reliablity can then be repsented as a system of equations as follows:

$$\begin{aligned} R_{od1} &= \frac{1}{a} \otimes_{r=1}^{a} (\oplus_{s=1}^{i} R_{rs}) \\ R_{od2} &= \frac{1}{b} \otimes_{r=1}^{b} (\oplus_{s=1}^{j} R_{rs}) \\ R_{od3} &= \frac{1}{c} \otimes_{r=1}^{c} (\oplus_{s=1}^{k} R_{rs}) \\ R_{od4} &= \frac{1}{d} \otimes_{r=1}^{d} (\oplus_{s=1}^{l} R_{rs}) \\ &\vdots \end{aligned} \tag{6.10}$$

The system of equations in 6.10 describes the proposed network reliability. However, the algebra over the min-plus algebraic structure is developed for problems that are of the form:

$$
\begin{aligned}
y_1 &= \oplus_{r=1}^{a}(\otimes_{s=1}^{i} x_{rs}) \\
y_2 &= \oplus_{r=1}^{b}(\otimes_{s=1}^{j} x_{rs}) \\
y_3 &= \oplus_{r=1}^{c}(\otimes_{s=1}^{l} x_{rs}) \\
y_4 &= \oplus_{r=1}^{d}(\otimes_{s=1}^{k} x_{rs}) \\
&\vdots
\end{aligned}
\tag{6.11}
$$

Therefore, in order to solve the system in 6.10, a new algebra must be developed. Alternatively, one can consider the dual problem for network reliability using unreliability as presented in the next section.

6.4 Alternative View of Network Reliability using Unreliability

In order to be able to take advantage of the algebra developed for min-plus problems, network reliability is defined slightly different than it is in the last section.

Definition 6.4.1. *Let R be the reliability of a roadway segment where $0 \leq R \leq 1$, then the unreliability $U \equiv 1 - R$.*

6.4.1 Min-Plus Algebra

As it is for network reliability, network unreliability has the min-plus algebraic as well.

Definition 6.4.2. *Min-plus algebra is a semi-ring algebraic structure defined on the set $U_{min} = \{\infty\} \cup \Re$ together with two operations [56]:*

1. $a \oplus b = min(a, b)$

2. $a \otimes b = a + b$

6.4.2 Series Components

Given a transportation network with n components connected in series, as shown in Figure 6.5, let $U = \{U_1, U_2, \cdots, U_n\}$ be the set of unreliability values of the segments. Since the segments are connected in series, the driver must go through all the available components or roadway segments. Therefore, the normalized total reliability of a series network is given by the addition of unreliability of all segments, as presented in (6.12)

.

Proposition 6.4.1. *The total series network unreliability value U_s is given by the addition of $\{U_1, U_2, \cdots, U_n\}$ as presented in Equation 6.12.*

$$U_s = \otimes_{i=1}^{n} U_i = \frac{1}{n}\left(U_1 + U_2 + \cdots + U_n\right) \tag{6.12}$$

6.4.3 Parallel Components

Given a transportation network with n components connected in parallel, as shown in Figure 6.4, let $U = \{U_1, U_2, \cdots, U_n\}$ be the set of unreliability values of the segments. Since the segments are connected in parallel, the driver can chose to go through any roadway segments. Therefore, the total unreliability of a parallel network is given by the minimum unreliability

out of all segments, as presented in Equation 6.13.

Proposition 6.4.2. *The total parallel network unreliability value U_p is given by the minimum of $\{U_1, U_2, \cdots, U_n\}$ as presented in Equation 6.13.*

$$U_p = \oplus_{i=1}^{n} U_i = min\{U_1, U_2, \cdots, U_n\} \tag{6.13}$$

6.4.4 Network Unreliability

using the unreliability concept, the network unreliability can then be represented as a system of equations as follows:

$$\begin{aligned} U_{od1} &= \frac{1}{i} \oplus_{r=1}^{a} (\otimes_{s=1}^{i} U_{rs}) \\ U_{od2} &= \frac{1}{j} \oplus_{r=1}^{b} (\otimes_{s=1}^{j} U_{rs}) \\ U_{od3} &= \frac{1}{k} \oplus_{r=1}^{c} (\otimes_{s=1}^{k} U_{rs}) \\ U_{od4} &= \frac{1}{l} \oplus_{r=1}^{d} (\otimes_{s=1}^{l} U_{rs}) \\ &\vdots \end{aligned} \tag{6.14}$$

6.5 Network Reliability as the Optimal Path Problem

Optimal path problems are special discrete, deterministic, Optimal Control problems [57]. One can consider network reliability to be the "most" reliable path connecting an origin

and a destination. In which case, the network reliability becomes an optimization problem.

6.5.1 Bellman's Principle of Optimality

"An optimal policy has the property that whatever the initial state and initial decision are, the remaining decisions must constitute an optimal policy with regard to the state resulting from the first decision." [58]

6.5.2 Application of the Bellman's Principle

Consider the network in Figure 6.9. The performance function in the considered case is given to be reliability.

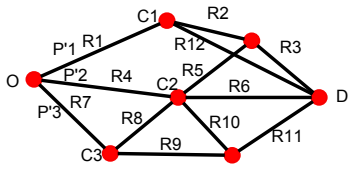

Figure 6.9: A given network to be used in the optimal path problem

Assuming one has the reliability values of all links or link value. Then, the shortest path will be the path with the maximum reliability. In this optimization problem it is desired to maximize the performance function which in this case it is reliability. Therefore, solving the deterministic maximum reliability problem is equivalent to solving the maximal weight paths tree problem [57]. It is convenient to introduce the completed max-plus semi-ring, as defined earlier, in order to characterize the optimal path problem.

According to the principle of optimality, the optimal path in the given network for a certain

set of OD is provided by:

$$R^* = \max\{P_1, P_2, P_3\} = \bigoplus_{k=1}^{3} P_k^{'} \otimes C_k$$

where:

$$P_1 = R_1 \otimes \{P_{11} \oplus P_{12}\}$$

$$P_2 = R_4 \otimes \{P_{21} \oplus P_{22} \oplus P_{23}\}$$

$$P_3 = R_7 \otimes \{P_{31} \oplus P_{32} \oplus P_{33}\}$$

$$P_{11} = R_2 \otimes R_3, P_{12} = R_{12}$$

$$P_{21} = R_5 \otimes R_3, P_{22} = R_6, P_{23} = R_{10} \otimes R_{11}$$

$$P_{31} = R_8 \otimes R_6, P_{32} = R_8 \otimes R_{10} \otimes R_{11}, P_{33} = R_9 \otimes R_{11}$$

This formulation of the network reliability problem clearly transforms it into a discrete, linear optimal path problem which we know how to solve using dynamic programming methods.

6.5.3 Link Reliability Dependency

The network reliability formulation developed earlier in this chapter assumes independency between all the links in the network. However, this might not always be the case. It highly depends on the type of reliability considered. For instance, if the reliability is measured

by considering the number of incident on each link, then one can assume the links are independent. Note that this is an approximation since an incident on one link can play a role in causing incidents in subsequent links causing secondary incidents. However, in the case were dependency cannot be ignored, such as travel time reliability, it is vital to extract the independent reliability of each link before proceeding with the network reliability calculations demonstrated above.

6.6 Introduction

This chapter demonstrated measuring the reliability of networked roadway segments. In this study it is found that the algebraic structure of the reliability of a network is consistent with the semi-ring min-plus algebraic structure. This provides us with well established properties that can simplify the algebra over networks' reliability. This study discovers the structure of the algebraic space when reliability is measured for a network.

6.7 Conclusion

In this chapter, we investigated the measure of network reliability when link reliability is provided. Various approaches are introduced using the max-plus algebraic structure using reliability, unreliability, and Bellman's principle of optimality.

In the future, the minimal path problem using a probabilistic approach based on failure analysis will be considered. Dependency of roadway links is a major issue that will also be

considered in future studies.

Part IV

Safety

CHAPTER 7

Bayesian Safety Analyzer

7.1 Overview

This chapter discusses the safety aspect of complex networks as shown in Figure 7.1. In the future, the minimal path problem using a probabilistic approach based on failure analysis will be considered. Dependency of roadway links is a major issue that will also be considered in future studies.

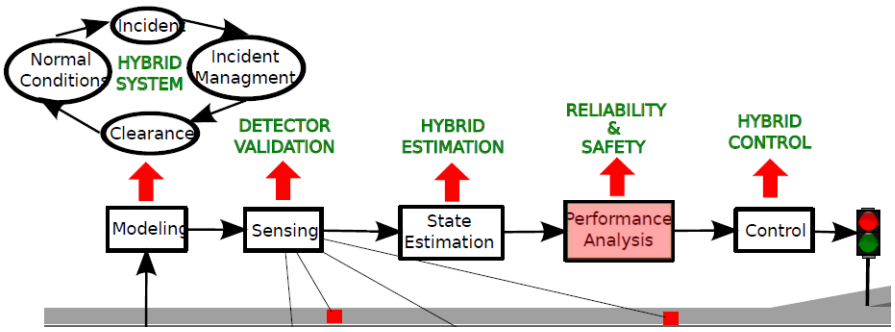

Figure 7.1: Overall research work

7.2 Introduction

In this study, the development of a Bayesian Safety Analyzer (BSA) using multiple accident data sources as well as traffic flow data is demonstrated. Simulations of the developed model are conducted using MATLAB FullBNT toolbox where different parameter estimations are used. This study demonstrates the efficiency as well as flexibility of using Bayesian analysis

on large data sets containing a large number of attributes. The developed BSA can be used in the incident management process. It can assist decision makers in estimating the severity of a certain incident based on given attributes for better preparedness. BSA can also be used in order to assess the safety transportation system.

This study presents a very important tool in data integration, analysis, and probability theory [59] [60]. Bayesian theory is used in order to build a probabilistic data structure that can be used to extract likelihood information about various pieces of parameters that are updated through the enormous amount of data [61] [62]. A given data set usually has a number of attributes where the relationship between them is not well defined. When constructing a Bayesian structure over the available data set, each attribute becomes a node. The links between the nodes can be determined by the nature of the problem, for instance bad weather conditions can impact the probability of incidents hence causing congestion. This leads to a nodal structure that has a topological order where ancestor nodes must precede descendant nodes [59]. The Bayesian Safety Analyzer (BSA) is designed based on an integration of multiple traffic and crash data sources. The BSA tool allows structuring the available data into a Bayesian Network. Based on the content of the data, the occurrence likelihood of different components in the system can be extracted. Data for the BSA networks developed herein is obtained from Freeway and Arterial System of Transportation (FAST), Nevada Highway Patrol (NHP), and Nevada Department of Transportation (NDOT).

7.3 Literature Review

7.3.1 Bayesian in Action

Bayesian analysis methods are used in many areas in transportation. Ozbay et. al. in [63] uses Bayesian networks to analyze incidents in order to improve decision making during the incident management process. In another work of his, Ozbay uses Bayesian networks in order to estimate incident duration [64]. Lee in his dissertation work used Bayesian sampling methodology in order to extend Simultaneous Perturbation Stochastic Approximation for calibration of traffic simulation models [65]. Tuze et. al. [66] uses hierarchical Bayesian mixed logit approach in order to estimate the value of travel time. Rongmei [67] introduces an intelligent transportation system for traffic accident processing where key influence factors are analyzed using case base Bayesian networks and provides conclusions using Bayesian network Reasoning. Traffic flow forecasting based on Bayesian networks is developed by Sun et. al. [68].

7.3.2 Accidents Analysis

When it comes to accidents analysis, researchers have used various analysis methodologies. Tian in [69], employed data mining theories in order to analyze causes of accidents. Ma in [70], uses Gray relations in order to identify the nature of traffic accidents and their relation to pre-defined factors. SongBai et. al. [71] built a multidimensional association rule model of traffic accidents, a data mining methodology, in order to develop the analysis system of association factors in traffic accidents. Hwang et. al. uses a system that is

based on hierarchical probabilistic network for detection of traffic accidents on intersections [72]. Fuzzy distribution fitting is employed by Lurong in order to study the rules of traffic accidents and hazards [73].

7.3.3 Why Bayesian?

Bayesian methods have proven to be very effective when large amount of data attributes are involved in analysis. In this research, a Bayesian Safety Analyzer (BSA) is developed. The BSA allows isolation and identification of likelihood of occurrence of the various data attributes.

7.4 Theoretical Background

7.4.1 Bayes' Theorem

In probability theory, Bays theorem is used to calculate the inverse conditional probability or the posterior probability of a certain event A given another event B [74] [75]. Bay's theorem requires the knowledge of the prior probabilities of A and B (also called marginal probability) and the likelihood of A given B which is obtained by calculating the conditional probability of B given A.

$$P(A|B) = \frac{P(B|A)\,P(A)}{P(B)}$$

In order to calculate the conditional probabilities, the following equation is used:

$$P(A|B) = \frac{P(A \cap B)}{P(B)}$$

Where:

$P(A)$: is the prior probability of A.

$P(B)$: is the prior or the marginal probability of B.

$P(A|B)$: is the posterior probability of A given B.

$P(B|A)$: is the likelihood of A given B.

7.4.2 Bayesian Inference

Bayesian inference is a method of statistical inference. Data is used to calculate the probability that a hypothesis may be true, or it could be used to update its previously calculated probability [76]. Bayesian inference uses the prior probability over a certain hypotheses to determine the likelihood of a particular hypothesis given some observed data.

Definition:

Let S be a finite parents space containing n members given by $s_1, s_2, \ldots, s_n$. $\forall s_i \in S, m(s_i) \equiv$ the number of states each parent s_i can take.

Proposition:

The number of all possible combinations of states for which the children's probability dis-

tribution must be defined is given by:

$$m(S) = \prod_{i=1}^{n} m(s_i)$$

This clearly indicates that the distribution tables' size increase tremendously for each node based on the number of parents nodes and the number of their states.

7.5 Available Data

The BSA structure presented in this study is based on traffic data as well as crash data from multiple sources. The data is collected from multiple agencies Freeway and Arterial System of Transportation (FAST), Nevada Highway Patrol (NHP), and Nevada Department of Transportation (NDOT). FAST collects traffic data on the freeways, mainly the I-15. In addition, FAST collects accident data observed through their video cameras. Additional Crash or accident data is also collected from NHP and NDOT. Obtaining crash data from multiple sources is important since different agencies collect different attributes. For instance, FAST is the only agency that collects the number of lane closure; however, FAST does not collect other information such as weather conditions or clearance times.

The following is a list of the various attributes collected by the different agencies:

- **FAST detector data:** Time stamp, Location, Cumulative Volume, Volume by Ve-

hicle size, Speed.

- **FAST accident compile:** Date and time, Location, Lanes Blocked.
- **NHP:** Date and time, Location, Incident Type, Receive Time, Dispatch Time, En-route Time, Onsite Time, Clearance Time
- **NDOT Crash Data:** Date and time, Location, Weather, Number of vehicles, Type of vehicles.

7.6 Proposed Bayesian Safety Analyzer Model

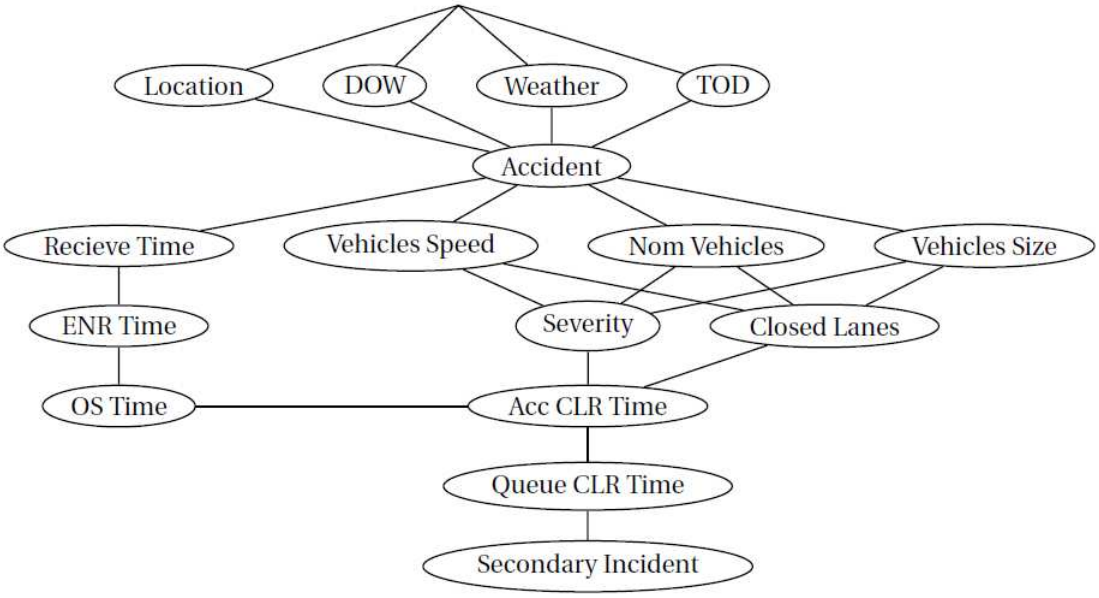

Figure 7.2: Proposed Bayesian Model

The Bayesian model in Figure 7.2 is formed via eight hierarchical levels. The increase of hierarchy level may reduce direct dependencies between parents' nodes and immediate children which implies simpler distribution tables for each node. However, the number of hierarchical levels is constrained by the nature of the problem being modeled since certain

parameters directly depend on multiple parameters simultaneously.

Table 7.1: Terms Definitions

Term	**Definition**
TOD	Time of day
DOW	Day of week
ENR Time	Enroute time
OS Time	Onsite time
CLR Time	Clearance Time

The distribution tables for the BSA model introduced in this work are presented in Tables 7.3(a), 7.3(b), 7.3(c), 7.4(a), 7.5(a), 7.5(b), 7.6(a), and 7.6(b).

The hierarchal structure of the BSA has eight stages corresponding to the data presented in Table 7.2.

7.7 Constructing Bayesian Model and Simulations in MATLAB - FullBNT-1.0.4

7.7.1 Nodes and Relations Assignment

Bayesian construction of the analyzer through nodes assignment and their relations is created in MATLAB using FullBNT tool box as demonstrated in 9.

When displaying the network at this stage, the following is obtained:

bnet =

Program 9 Bayesian Structure Construction

```
N   = 16;
dag = zeros(N,N);

%Assign nodes in the Bayesian Structure
Location = 1; DOW = 2; Weather = 3; TOD = 4;
Accident = 5;
RecieveTime = 6;  VehiclesSpeed = 7; NomVehicles = 8; VehiclesSize = 9;
ENR = 10; Severity = 11; ClosedLanes = 12;
OSTime = 13;
AccCLRTime = 14;
QueueCLRTime = 15;
SecondaryIncident = 16;

%Assign relations between nodes
dag(Location,Accident)=1;
dag(DOW,Accident)=1;
dag(Weather,Accident)=1;
dag(TOD,Accident)=1;
dag(Accident,[RecieveTime VehiclesSpeed NomVehicles VehiclesSize])=1;
dag(RecieveTime,ENR)=1;
dag(VehiclesSpeed,[Severity ClosedLanes])=1;
dag(NomVehicles,[Severity ClosedLanes])=1;
dag(VehiclesSize,[Severity ClosedLanes])=1;
dag(ENR,OSTime)=1;
dag(Severity,AccCLRTime)=1;
dag(ClosedLanes,AccCLRTime)=1;
dag(OSTime,AccCLRTime)=1;
dag(AccCLRTime,QueueCLRTime)=1;
dag(QueueCLRTime,SecondaryIncident)=1;

%Determine size of nodes
discrete_nodes = 1:N;
node_sizes     = [2 2 3 2 2 2 2 4 3 2 4 4 4 4 4 2];
onodes         = 1:N;

%Make BayNet
bnet = mk_bnet(dag, node_sizes, 'names', 'Location', 'DOW', 'Weather', 'TOD','Accident',

'RecieveTime','VehiclesSpeed','NomVehicles','VehiclesSize','ENR', 'Severity','ClosedLanes','OSTime',
'AccCLRTime','QueueCLRTime','SecondaryIncident', 'discrete', discrete_nodes, 'observed', onodes);

%Display BayNet
bnet
```

$equiv\_class$: [12345678910111213141516]

$dnodes$: [12345678910111213141516]

$observed$: [12345678910111213141516]

$names$: [$1x1assocarray$]

$hidden$: [$1x0double$]

$hidden\_bitv$: [0000000000000000]

dag : [$16x16double$]

$node\_sizes$: [2232222432444442]

$cnodes$: [$1x0double$]

$parents$: $1x16cell$

$members\_of\_equiv\_class$: $1x16cell$

CPD : $1x16cell$

rep_of_eclass : [12345678910111213141516]

$order$: [43215987121161013141516]

7.7.2 Distribution Assignment

Distributions assignment of the nodes is performed as well as inference creation. Initially, uniform distribution is assumed for all the parameters. The Bayesian structure can learn using data and accordingly adjust the given distributions. The probability distributions describe the direct relationship between parents nodes and immediate children nodes.

Program 10 Distribution assignment of nodes

```
%Assigning Destribution
bnet.CPDLocation= tabular_CPD(bnet, Location, [0.5 0.5]);
bnet.CPDDOW     = tabular_CPD(bnet, DOW, [0.5 0.5]);
bnet.CPDWeather = tabular_CPD(bnet, Weather, [0.3 0.3 0.4]);
bnet.CPDTOD     = tabular_CPD(bnet, TOD, [0.5 0.5]);
bnet.CPDAccident= tabular_CPD(bnet, Accident, [0.5 0.5 0.5
0.5 0.5 0.5 0.5 0.5 0.5 0.5 0.5 0.5 0.5 0.5 0.5 0.5 0.5 0.5 0.5 0.5
0.5 0.5 0.5 0.5 0.5 0.5 0.5 0.5 0.5 0.5 0.5 0.5 0.5 0.5 0.5
0.5 0.5 0.5 0.5 0.5 0.5 0.5 0.5 0.5 0.5 0.5 0.5 0.5]);
bnet.CPDRecieveTime= tabular_CPD(bnet, RecieveTime, [0.5 0.5 0.5 0.5]);
bnet.CPDVehiclesSpeed= tabular_CPD(bnet, VehiclesSpeed, [0.5 0.5 0.5 0.5]);
bnet.CPDNomVehicles  = tabular_CPD(bnet, NomVehicles, [0.25 0.25 0.25 0.25 0.25 0.25 0.25 0.25]);
bnet.CPDVehiclesSize = tabular_CPD(bnet, VehiclesSize, [0.33 0.33 0.33 0.33 0.33 0.33]);
bnet.CPDENR      = tabular_CPD(bnet, ENR, [0.5 0.9 0.5 0.1]);
bnet.CPDSeverity = tabular_CPD(bnet, Severity, [0.25 0.25 0.25 0.25
0.25 0.25 0.25 0.25 0.25 0.25 0.25 0.25 0.25 0.25 0.25 0.25 0.25 0.25
0.25 0.25 0.25 0.25 0.25 0.25 0.25 0.25 0.25 0.25 0.25 0.25 0.25 0.25
0.25 0.25 0.25 0.25 0.25 0.25 0.25 0.25 0.25 0.25 0.25 0.25 0.25 0.25
0.25 0.25 0.25 0.25 0.25 0.25 0.25 0.25 0.25 0.25 0.25 0.25 0.25 0.25
0.25 0.25 0.25 0.25 0.25 0.25 0.25 0.25 0.25 0.25 0.25 0.25 0.25 0.25
0.25 0.25 0.25 0.25 0.25 0.25 0.25 0.25 0.25 0.25 0.25 0.25 0.25 0.25
0.25 0.25 0.25 0.25 0.25 0.25 0.25 0.25]);

bnet.CPDClosedLanes  = tabular_CPD(bnet, ClosedLanes, [0.25 0.25
0.25 0.25 0.25 0.25 0.25 0.25 0.25 0.25 0.25 0.25 0.25 0.25 0.25 0.25
0.25 0.25 0.25 0.25 0.25 0.25 0.25 0.25 0.25 0.25 0.25 0.25 0.25 0.25
0.25 0.25 0.25 0.25 0.25 0.25 0.25 0.25 0.25 0.25 0.25 0.25 0.25 0.25
0.25 0.25 0.25 0.25 0.25 0.25 0.25 0.25 0.25 0.25 0.25 0.25 0.25 0.25
0.25 0.25 0.25 0.25 0.25 0.25 0.25 0.25 0.25 0.25 0.25 0.25 0.25 0.25
0.25 0.25 0.25 0.25 0.25 0.25 0.25 0.25 0.25 0.25 0.25 0.25 0.25 0.25
0.25 0.25 0.25 0.25 0.25 0.25 0.25 0.25 0.25 0.25]);
bnet.CPDOSTime       = tabular_CPD(bnet, OSTime, [0.25 0.25 0.25 0.25
0.25 0.25 0.25 0.25]);
bnet.CPDAccCLRTime   = tabular_CPD(bnet, AccCLRTime, [0.25 0.25 0.25
0.25 0.25 0.25 0.25 0.25 0.25 0.25 0.25 0.25 0.25 0.25 0.25 0.25 0.25
0.25 0.25 0.25 0.25 0.25 0.25 0.25 0.25 0.25 0.25 0.25 0.25 0.25 0.25
0.25 0.25 0.25 0.25 0.25 0.25 0.25 0.25 0.25 0.25 0.25 0.25 0.25 0.25
0.25 0.25 0.25 0.25 0.25 0.25 0.25 0.25 0.25 0.25 0.25 0.25 0.25 0.25
0.25 0.25 0.25 0.25 0.25 0.25 0.25 0.25 0.25 0.25 0.25 0.25 0.25 0.25
0.25 0.25 0.25 0.25 0.25 0.25 0.25 0.25 0.25 0.25 0.25 0.25 0.25 0.25
0.25 0.25 0.25 0.25 0.25 0.25 0.25 0.25 0.25 0.25 0.25 0.25 0.25 0.25
0.25 0.25 0.25 0.25 0.25 0.25 0.25 0.25 0.25 0.25 0.25 0.25 0.25 0.25
0.25 0.25 0.25 0.25 0.25 0.25 0.25 0.25 0.25 0.25 0.25 0.25 0.25 0.25
0.25 0.25 0.25 0.25 0.25 0.25 0.25 0.25 0.25 0.25 0.25 0.25 0.25 0.25
0.25 0.25 0.25 0.25 0.25 0.25 0.25 0.25 0.25 0.25 0.25 0.25 0.25 0.25
0.25 0.25 0.25 0.25 0.25 0.25 0.25 0.25 0.25 0.25 0.25 0.25 0.25 0.25
0.25 0.25 0.25 0.25 0.25 0.25 0.25 0.25 0.25 0.25 0.25 0.25 0.25 0.25
0.25 0.25 0.25 0.25 0.25 0.25 0.25 0.25 0.25 0.25 0.25 0.25 0.25 0.25
0.25 0.25 0.25 0.25 0.25 0.25 0.25 0.25 0.25 0.25 0.25 0.25 0.25 0.25
0.25 0.25 0.25 0.25 0.25 0.25 0.25 0.25 0.25 0.25 0.25 0.25 0.25 0.25
0.25 0.25 0.25 0.25 0.25 0.25 0.25 0.25 0.25 0.25 0.25 0.25 0.25 0.25
0.25 0.25 0.25 0.25 0.25 0.25 0.25 0.25 0.25 0.25 0.25 0.25 0.25 0.25
0.25]);
bnet.CPDQueueCLRTime = tabular_CPD(bnet, QueueCLRTime, [0.25 0.25 0.25
0.25 0.25 0.25 0.25 0.25 0.25 0.25 0.25 0.25 0.25 0.25 0.25 0.25]);
bnet.CPDSecondaryIncident= tabular_CPD(bnet, SecondaryIncident, [0.5 0.5 0.5 0.5 0.5 0.5 0.5 0.5]);

%creating inference
engine = jtree_inf_engine(bnet);
```

7.7.3 Marginal Distribution Computation

In order to demonstrate how to calculate marginal distributions, consider the example where the evidence consists of the fact that 'SecondaryIncident' takes the value 2, meaning that a secondary incident has occurred. Then, to compute the probability that 'Severity' is at level 2, indicating injury, given that 'Secondary ncident' is 2. Running the code gives $p = 0.25$ which makes sense since the distributions are uniform by assumption. The graph in Figure 7.3 displays the marginal distributions of the 'Severity' being at level 1, 2, 3, or 4, respectively given that a secondary incident has occurred.

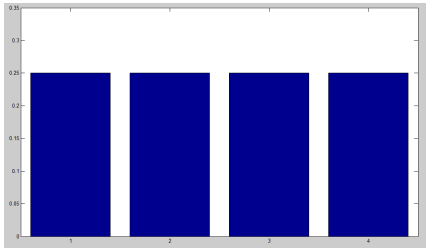

Figure 7.3: Marginal Distributions

7.8 Bayesian Parameter Learning

There are four types of parameter estimation:

1. **Fully observed point estimate:** Maximum likelihood parameter estimation from complete data, command: $learn - params$
2. **Partially observed point estimate:** Maximum likelihood parameter estimation with missing values, command: $learn - params - em$

Program 11 Distribution assignment of nodes

```
 %creating inference
%%%%%%%%%%%%%%%%%%%
engine = jtree_inf_engine(bnet);


%Computing Marginal Distributions

%%%%%%%%%%%%%%%%%%%%%%%%%%%%%%%%

%The evidence consists of the fact that Secondary Incident=2

%All the other nodes are hidden (unobserved)

evidence = cell(1,N);

evidenceSecondaryIncident = 2;


%add the evidence to the engine.

[engine, loglik] = enter_evidence(engine, evidence);
%compute p=P(Severity=2|SecondaryIncident=2) as follows.

marg = marginal_nodes(engine, Severity);

marg.T

p = marg.T(2)


%add the evidence that 3 lanes were closed

evidenceClosedLanes = 3;

[engine, loglik] = enter_evidence(engine, evidence);

marg = marginal_nodes(engine, Severity);


% Find p = P(Severity=2|SecondaryIncident=2,ClosedLanes=3)

p = marg.T(2)


%plot a marginal distribution over a discrete variable as a barchart

bar(marg.T)
```

3. **Fully observed full Bayesian:** (Sequential) Bayesian parameter updating from complete data, $bayes - update - params$

4. **Partially observed full Bayesian:**Not supported

Fully observed indicates that all the variables are observed, whereas partially observed indicates that there is missing or hidden data. Full Bayesian computes the full posterior over the parameters. However, point estimate computes Maximum Likelihood or a Maximum A Posteriori.

7.8.1 Loading Data

Data is needed in order to perform parameter learning on the Bayesian structure. For testing purposes, data can be generated using forward sampling. However, in this study, a sample data file is created which corresponds to the parameters and values specified in Tables 7.2. Various file formats are supported including txt and xls. The data is then loaded as shown in Program 12 and used to update the distributions of each parameter in the Bayesian structure. The original data must be processed and formatted in order to be read by the structure.

7.8.2 Maximum Likelihood Parameter Estimation from Complete Data

Program 13 demonstrates how parameter learning is accomplished. After the data is loaded from the sample file, it is used to find the maximum likelihood estimates. The learnt param-

Program 12 Loading data from a file

```
data = load('DataRdTr.txt', '-ascii');
data   = xlsread('AccidentPredict.xls')

ncases = size(data, 1) % each row of data is a training case

cases  = cell(16, ncases);

cases([1 2 3 4 5 6 7 8 9 10 11 12 13 14 15 16], :) =
num2cell(data') % each column of cases is a training case

%%%%%%%%%%%%%%%%%%%%%%%%%%%%%%%%
```

eters can be viewed using a MAT LAB trick as shown in the program below. For instance, after updating the structure in this study using a sample data file of 20 entries, the following is obtained when node 4 is viewed:

1 : 0.4500

2 : 0.5500

Note that the distribution is not uniform anymore for this node which indicates that the distributions of the nodes are updated using the new data.

7.8.3 Partial Parameter Learning

When data is incomplete or has missing values, the Maximum Likelihood Estimates (MLEs) values are computed using the EM algorithm. An inference algorithm is used in order to compute the expected sufficient statistics as shown in Program 14. Dipected in Figure 7.4

Program 13 Parameter Learning

```
%Parameter Learning

%%%%%%%%%%%%%%%%%%%
% find the maximum likelihood estimates

bnet3 = learn_params(bnet2, cases);

bnet3


%To view the learned parameters

CPT3 = cell(1,N);

for i=1:N

  s=struct(bnet3.CPDi);
  CPT3i=s.CPT;

end


%Here are the parameters learned for node 4.
dispcpt(CPT34)
```

is the plot of the log-likelihood at the i^{th} iteration.

7.9 Conclusions and Future Work

7.9.1 Conclusions

In this study, a Bayesian Safety Analyzer (BSA) is constructed based on various data sources including crash data and traffic data. It is demonstrated how posterior probabilities can be computed and how data can be used to train the Bayesian structure composed of a large amount of parameters. Bayesian analysis is proved to be a very efficient probabilistic method for analyzing a large set of data in order to better estimate dependencies and likelihood of occurrence of various events. The developed BSA can be used in the incident

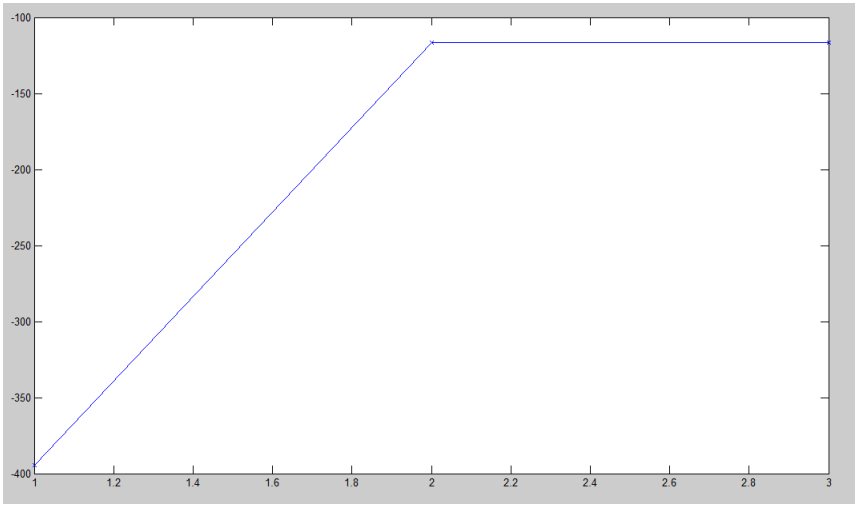

Figure 7.4: The log-likelihood at the i^{th} iteration

Program 14 Partial Parameter Learning

```
%Partial Parameter Learning

%%%%%%%%%%%%%%%%%%%%%%%%%%

engine2 = jtree_inf_engine(bnet2);

max_iter = 10;

[bnet4, LLtrace] = learn_params_em(engine2, cases, max_iter);


%LLtrace(i) is the log-likelihood at iteration i

plot(LLtrace, 'x-')
```

management process. It can assist decision makers in estimating the severity of a certain incident based on given attributes in order to better prepare. BSA can also be used in order to assess the transportation system's safety.

7.9.2 Future Work

Future work includes developing algorithms in order to automate data formatting from multiple sources into one file that integrates all required data and feeds into the developed BSA.

Table 7.2: State Description of Parameters

Parameter	**States Description**	**State**	**States Values**
Location	Freeway or Arterial	Fr	2=Freeway, 1=Arterial
DOW	Weekday or Weekend	Wd	2= Weekday 1= Weekend
Weather	Rain, Fog, or Clear	Wth	3= Rain, 2= Fog, 1= Clear
TOD	Peak-hour or Regular	Pk	2=Peakhour, 1= Regular
Accident	Accident Occurred	Ac	2= True, 1= False
Receive Time	Informing response agency took greater than 1 minute	Rc	2= True, 1= False
Vehicles Speed	Vehicles involved were going higher than the speed limit	Vs	2= True, 1= False
Nom Vehicles	1, 2, 3, or more vehicles were involved	Vn	4= more than 3, 3= 3, 2= 2, 1= 1
Vehicles Size	At least one of the vehicles involved was of compact, medium, or large size	Vsz	Large= 3, Medium = 2, Compact= 1
ENR Time	The responding unit was on its way to the scene after more than 1 minute of being informed	En	2= True, 1= False
Severity	Property damage(Pd), Injury (In), Hit and Run (HR), or Fatality (Ft)	Pd	4= Ft, 3= HR, 2= In, 1= Pd
Closed Lanes	1, 2, 3, or all lanes were closed	L	4= All lanes, 3= 3, 2= 2, 1= 1
OS Time	The responding unit was on-scene within 5, 10, 15, or more minutes from being informed	Os	4 = more than 15 min, 3= 15, 2= 10, 1= 5
Acc CLR Time	Accident cleared within 30, 60, 90, or more minutes	Acl	4 = more than 90 min, 3= 90, 2= 60, 1= 30
Queue CLR Time	Queue due to accident was cleared within 30, 60, 90, or more minutes	Qcl	4 = more than 90 min, 3= 90, 2= 60, 1= 30
Secondary Incident	A secondary incident occurred	S	2= True, 1= False

Table 7.3: Hierarchical Initial Probability Distributions of Parameters

(a) Hierarchy level 1

Fr=2	**Fr=1**	**Wd=2**	**Wd=1**	**Wth=3**	**Wth=2**	**Wth=1**	**Pk=2**	**Pk=1**
0.5	0.5	0.5	0.5	$0.\dot{3}$	$0.\dot{3}$	$0.\dot{3}$	0.5	0.5

(b) Hierarchy level 2

Fr	**Wd**	**Wth**	**Pk**	**Ac=2**	**Ac=1**
1	1	1	1	0.5	0.5
1	1	1	2	0.5	0.5
1	1	2	1	0.5	0.5
1	1	2	2	0.5	0.5
1	1	3	1	0.5	0.5
1	1	3	2	0.5	0.5
1	2	1	1	0.5	0.5
1	2	1	2	0.5	0.5
1	2	2	1	0.5	0.5
1	2	2	2	0.5	0.5
1	2	3	1	0.5	0.5
1	2	3	2	0.5	0.5
2	1	1	1	0.5	0.5
2	1	1	2	0.5	0.5
2	1	2	1	0.5	0.5
2	1	2	2	0.5	0.5
2	1	3	1	0.5	0.5
2	1	3	2	0.5	0.5
2	2	1	1	0.5	0.5
2	2	1	2	0.5	0.5
2	2	2	1	0.5	0.5
2	2	2	2	0.5	0.5
2	2	3	1	0.5	0.5
2	2	3	2	0.5	0.5

(c) Hierarchy level 3

Ac	**Rc=2**	**Rc=1**	**Vs=2**	**Vs=1**	**Vn=4**	**Vn=3**	**Vn=2**	**Vn=1**	**Vsz=3**	**Vsz=2**	**Vsz=1**
1	0.5	0.5	0.5	0.5	0.25	0.25	0.25	0.25	$0.\dot{3}$	$0.\dot{3}$	$0.\dot{3}$
2	0.5	0.5	0.5	0.5	0.25	0.25	0.25	0.25	$0.\dot{3}$	$0.\dot{3}$	$0.\dot{3}$

Table 7.4: Hierarchical Initial Probability Distributions of Parameters

(a) Hierarchy level 4

Rc	**En=2**	**En=1**	**Vs**	**Vn**	**Vsz**	**Pd=4**	**Pd=3**	**Pd=2**	**Pd=1**	**L=4**	**L=3**	**L=2**	**L=1**
1	0.5	0.5	1	1	1	0.25	0.25	0.25	0.25	0.25	0.25	0.25	0.25
2	0.5	0.5	1	1	2	0.25	0.25	0.25	0.25	0.25	0.25	0.25	0.25
			1	1	3	0.25	0.25	0.25	0.25	0.25	0.25	0.25	0.25
			1	2	1	0.25	0.25	0.25	0.25	0.25	0.25	0.25	0.25
			1	2	2	0.25	0.25	0.25	0.25	0.25	0.25	0.25	0.25
			1	2	3	0.25	0.25	0.25	0.25	0.25	0.25	0.25	0.25
			1	3	1	0.25	0.25	0.25	0.25	0.25	0.25	0.25	0.25
			1	3	2	0.25	0.25	0.25	0.25	0.25	0.25	0.25	0.25
			1	3	3	0.25	0.25	0.25	0.25	0.25	0.25	0.25	0.25
			1	4	1	0.25	0.25	0.25	0.25	0.25	0.25	0.25	0.25
			1	4	2	0.25	0.25	0.25	0.25	0.25	0.25	0.25	0.25
			1	4	3	0.25	0.25	0.25	0.25	0.25	0.25	0.25	0.25
			2	1	1	0.25	0.25	0.25	0.25	0.25	0.25	0.25	0.25
			2	1	2	0.25	0.25	0.25	0.25	0.25	0.25	0.25	0.25
			2	1	3	0.25	0.25	0.25	0.25	0.25	0.25	0.25	0.25
			2	2	1	0.25	0.25	0.25	0.25	0.25	0.25	0.25	0.25
			2	2	2	0.25	0.25	0.25	0.25	0.25	0.25	0.25	0.25
			2	2	3	0.25	0.25	0.25	0.25	0.25	0.25	0.25	0.25
			2	3	1	0.25	0.25	0.25	0.25	0.25	0.25	0.25	0.25
			2	3	2	0.25	0.25	0.25	0.25	0.25	0.25	0.25	0.25
			2	3	3	0.25	0.25	0.25	0.25	0.25	0.25	0.25	0.25
			2	4	1	0.25	0.25	0.25	0.25	0.25	0.25	0.25	0.25
			2	4	2	0.25	0.25	0.25	0.25	0.25	0.25	0.25	0.25
			2	4	3	0.25	0.25	0.25	0.25	0.25	0.25	0.25	0.25

Table 7.5: Hierarchical Initial Probability Distributions of Parameters

(a) Hierarchy level 5

En	Os=4	Os=3	Os=2	Os=1
1	0.25	0.25	0.25	0.25
2	0.25	0.25	0.25	0.25

(b) Hierarchy level 6

Os	Pd	L	Acl=4	Acl=3	Acl=2	Acl=1	Os	Pd	L	Acl=4	Acl=3	Acl=2	Acl=1
1	1	1	0.25	0.25	0.25	0.25	3	1	1	0.25	0.25	0.25	0.25
1	1	2	0.25	0.25	0.25	0.25	3	1	2	0.25	0.25	0.25	0.25
1	1	3	0.25	0.25	0.25	0.25	3	1	3	0.25	0.25	0.25	0.25
1	1	4	0.25	0.25	0.25	0.25	3	1	4	0.25	0.25	0.25	0.25
1	2	1	0.25	0.25	0.25	0.25	3	2	1	0.25	0.25	0.25	0.25
1	2	2	0.25	0.25	0.25	0.25	3	2	2	0.25	0.25	0.25	0.25
1	2	3	0.25	0.25	0.25	0.25	3	2	3	0.25	0.25	0.25	0.25
1	2	4	0.25	0.25	0.25	0.25	3	2	4	0.25	0.25	0.25	0.25
1	3	1	0.25	0.25	0.25	0.25	3	3	1	0.25	0.25	0.25	0.25
1	3	2	0.25	0.25	0.25	0.25	3	3	2	0.25	0.25	0.25	0.25
1	3	3	0.25	0.25	0.25	0.25	3	3	3	0.25	0.25	0.25	0.25
1	3	4	0.25	0.25	0.25	0.25	3	3	4	0.25	0.25	0.25	0.25
1	4	1	0.25	0.25	0.25	0.25	3	4	1	0.25	0.25	0.25	0.25
1	4	2	0.25	0.25	0.25	0.25	3	4	2	0.25	0.25	0.25	0.25
1	4	3	0.25	0.25	0.25	0.25	3	4	3	0.25	0.25	0.25	0.25
1	4	4	0.25	0.25	0.25	0.25	3	4	4	0.25	0.25	0.25	0.25
2	1	1	0.25	0.25	0.25	0.25	4	1	1	0.25	0.25	0.25	0.25
2	1	2	0.25	0.25	0.25	0.25	4	1	2	0.25	0.25	0.25	0.25
2	1	3	0.25	0.25	0.25	0.25	4	1	3	0.25	0.25	0.25	0.25
2	1	4	0.25	0.25	0.25	0.25	4	1	4	0.25	0.25	0.25	0.25
2	2	1	0.25	0.25	0.25	0.25	4	2	1	0.25	0.25	0.25	0.25
2	2	2	0.25	0.25	0.25	0.25	4	2	2	0.25	0.25	0.25	0.25
2	2	3	0.25	0.25	0.25	0.25	4	2	3	0.25	0.25	0.25	0.25
2	2	4	0.25	0.25	0.25	0.25	4	2	4	0.25	0.25	0.25	0.25
2	3	1	0.25	0.25	0.25	0.25	4	3	1	0.25	0.25	0.25	0.25
2	3	2	0.25	0.25	0.25	0.25	4	3	2	0.25	0.25	0.25	0.25
2	3	3	0.25	0.25	0.25	0.25	4	3	3	0.25	0.25	0.25	0.25
2	3	4	0.25	0.25	0.25	0.25	4	3	4	0.25	0.25	0.25	0.25
2	4	1	0.25	0.25	0.25	0.25	4	4	1	0.25	0.25	0.25	0.25
2	4	2	0.25	0.25	0.25	0.25	4	4	2	0.25	0.25	0.25	0.25
2	4	3	0.25	0.25	0.25	0.25	4	4	3	0.25	0.25	0.25	0.25
2	4	4	0.25	0.25	0.25	0.25	4	4	4	0.25	0.25	0.25	0.25

Table 7.6: Hierarchical Initial Probability Distributions of Parameters

(a) Hierarchy level 7

Acl	P(Qcl=4)	Qcl=3	Qcl=2	Qcl=1
1	0.25	0.25	0.25	0.25
2	0.25	0.25	0.25	0.25
3	0.25	0.25	0.25	0.25
4	0.25	0.25	0.25	0.25

(b) Hierarchy level 8

Qcl	S=2	S=1
1	0.5	0.5
2	0.5	0.5
3	0.5	0.5
4	0.5	0.5

Part V

Control

CHAPTER 8

Hybrid Modeling and Control of Ramps

8.1 Overview

This chapter discusses the modeling, parameter estimation, and development of control schemes for switching hybrid systems as shown in Figure 8.1.

This chapter presents a feedback control design for an isolated freeway ramp that utilizes a hybrid dynamical model for the traffic using Godunov's numerical technique. Ramp-metering is the primary means of controlling highway networks.

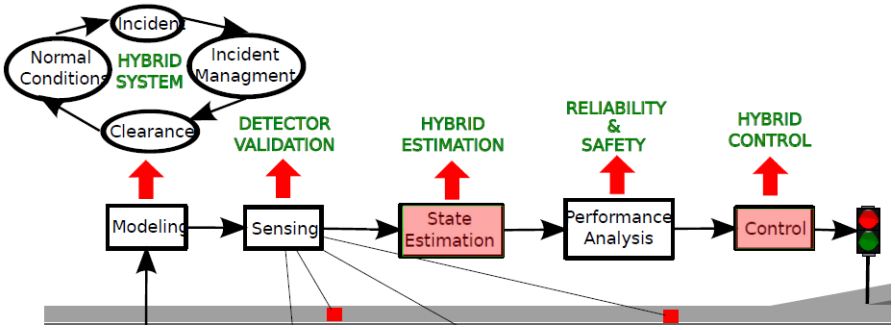

Figure 8.1: Overall research work

8.2 Introduction

Feedback ramp metering designs in the past have relied on either discretized linearized method such as ALINEA, or nonlinear feedback designs based on ordinary differential

equations for the traffic model. However, lumped parameter models fail to represent the rarefaction wave phenomenon of the distributed model. This study uses Godunov based hybrid lumped model based on which feedback control design is proposed, and simulation results for the model are presented. Ramp metering is designed to improve the traffic flow on the freeways by controlling the allowable rate of flow into the freeway at the entrance ramp. Ramp metering has been studied and implemented for more than 45 years, see for instance [77], [78], [79], and [80] for some early references. The handbook [81] provides a nice general overview of the ramp metering methods. Some optimization based methods on ramp metering are presented in [82], [83], and [84]. Simulation based analysis of ramp metering is covered in many papers such as [85], and [86]. A local feedback ramp control designed based on discretized linearization of the traffic dynamics is presented in [87]. A fuzzy logic based local ramp controller is presented in [88], a neural network based in [89], and a decentralized one in [90]. Ramp meters have been deployed in many different countries, such as in U.S.A [91], France [92], Italy [93], Germany [94], New Zealand [95], U.K. [96], and Netherlands [97]. Feedback ramp metering controllers based on nonlinear lumped parameter model are detailed in [98]. Model formulations in different settings such as the distributed model, lumped model, and their continuous and discrete time versions are shown in [99] and [100].

8.3 Background

Ramp meters are designed to control the inflow into freeways to reduce congestion on the highways. Ramp meters can be pre-timed, or can be operated in an actuated way. Feedback

control theory can be used to design real-time ramp meters so that the ramp flows can be made dependent on the current traffic conditions. Figure 8.2 shows a freeway with an entrance ramp being controlled by a traffic light.

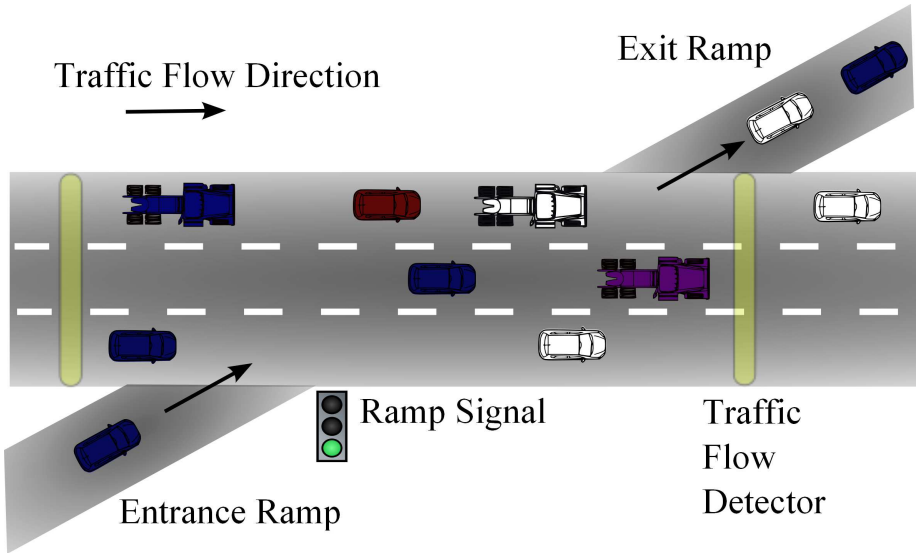

Figure 8.2: Ramp Metering

Ramp metering models that have been used for feedback control design that utilize lumped parameter model have used dynamics that do not reproduce the rarefaction behavior of traffic. In those models, when the traffic is at jam density the outflow from a section becomes zero. However, this would mean that the traffic would never come out of the jam. This research uses a Godunov based model in the lumped setting which reproduces the rarefaction behavior. The study then presents a feedback control design for ramp metering that provides asymptotic stable behavior for the closed loop system.

The next section presents the mathematical model for the system, followed by a section on control design, and finally the section that presents simulation results.

8.4 Mathematical Model

The LWR (Lighthill-Whitham-Richards) model, named after the authors in [101] and [102], is a macroscopic one-dimensional traffic model. The conservation law for traffic in one dimension is given by

$$\frac{\partial}{\partial t}\rho(t,x) + \frac{\partial}{\partial x}f(t,x) = 0 \tag{8.1}$$

In this equation ρ is the traffic density and f is the flux which is the product of traffic density and the traffic speed v, i.e. $f = \rho v$. There are many models researchers have proposed for how the flux should be dependent on traffic conditions. Greenshield's model (see [103]) uses a linear relationship between traffic density and traffic speed.

$$v(\rho) = v_f(1 - \frac{\rho}{\rho_m}) \tag{8.2}$$

where v_f is the free flow speed and ρ_m is the maximum density. Free flow speed is the speed of traffic when the density is zero. This is the maximum speed. The maximum density is the density at which there is a traffic jam and the speed is equal to zero.

A space discretized model of Equation 8.1 for the ramp metering is presented in Figure 8.3. Here, $u(t)$ is the ramp inflow into the freeway.

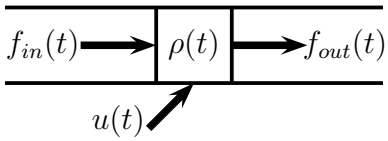

Figure 8.3: Discretized Model

The ordinary differential equation (ODE) model from the figure for the ramp metering, assuming unit length for the section, is given by

$$\frac{d\rho(t)}{dt} = f_{in}(t) + u(t) - f_{out}(t) \tag{8.3}$$

The outflow traffic using Greenshield's model is given by

$$f_{out}(t) = v_f \rho(t)(1 - \frac{\rho(t)}{\rho_m}) \tag{8.4}$$

Now, substituting Formula 8.4 for the outflow into the conservation Equation 8.3 shows that when the traffic density is equal to the jam density, and the value of $u(t)$ is zero, the rate of increase in the traffic density is non-negative. In fact, for positive inflow, the density can increase according to the equation. Hence, there are two issues with this model that need to be fixed. When the traffic density is equal to jam density for the section,

1. the inflow from upstream can increase the density above the jam value, and

2. the outflow is zero from the section not allowing for the traffic to be dissipated to downstream.

The original distributed LWR model given by Equation 8.1 using the Greenshield's fundamental relationship 8.2 does not have these limitations. This can be seen by studying the characteristics emanating from an initial value problem for a Riemann's problem where the upstream traffic density is lower (see [104], [105], and [106]). Figure 8.4 shows the characteristics of traffic where the initial traffic data is shown on the x-axis, where the traffic density is piecewise constant. The middle section has the jam density ρ_m, the upstream has a lower density ρ_0 and the downstream has zero density. As time increases, as shown on the y-axis, the shock wave travels upstream and at the same time the jam dissipates as a rarefaction onto the downstream.

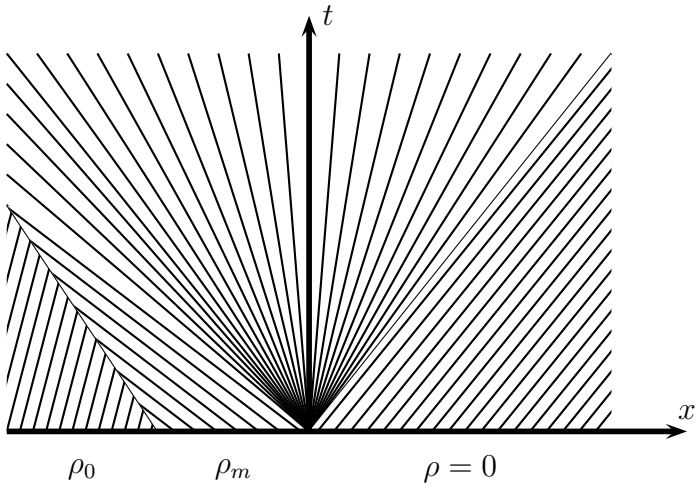

Figure 8.4: Traffic Characteristics

We can use Godunov's model to fix these two issues in the ODE model, and use the Godunov model as our nominal model for the control design. Note that we could also take model

given by Equation 8.3 as the nominal model for the feedback control design and let the closed loop system provide performance via its robustness for the real system. However, we choose the Godunov based nominal model so as to have better representation of the system in the nominal model.

8.4.1 Godunov based Model

The Godunov method is based on solving the Riemann problem where the initial condition is a piecewise constant function with two values ρ_ℓ and ρ_r for the upstream (left) and downstream (right) densities (see [107]). From the junction of the two densities either a shockwave or a rarefaction wave can emanate. A shockwave develops if $f'(u_\ell) > f'(u_r)$ (see [108]).

(a) Left (b) Right

Figure 8.5: Shockwaves moving Upstream (left) and Downstream (right)

The speed of the shockwave is given by Equation 8.5. In this equation, $x_s(t)$ is the position of the shockwave as a function of time. If the shock speed is positive then the inflow at junction between the two traffic densities will be a function of upstream traffic density, whereas if the shock speed is negative, then the inflow at junction between the two traffic densities will be a function of downstream traffic density.

$$s = \frac{dx_s(t)}{dt} = \frac{[f(u_\ell) - f(u_r)]}{u_\ell - u_r} \tag{8.5}$$

A rarefaction develops if $f'(u_\ell) < f'(u_r)$. The rarefaction can be entirely to the left, or to the right or in the middle.

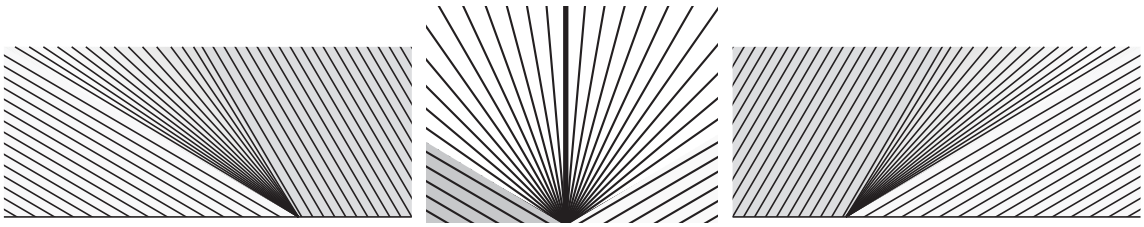

(a) Left (b) Middle (c) Right

Figure 8.6: Rarefaction Solution

The analysis of the shockwave and rarefaction conditions gives us the Godunov based ODE model for traffic. The ODE for Godunov method is the same as the conservation law, and is give by Equation 8.6, where we have assumed unit length for the section. To derive the rest of the model, please consider Figure 8.7.

$$\frac{d\rho(t)}{dt} = f_{in}(t) - f_{out}(t) + u(t) \tag{8.6}$$

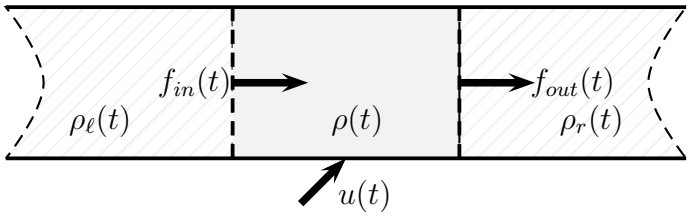

Figure 8.7: Godunov Dynamics

Now, the inflow $f_{in}(t)$ will be a function of upstream density ρ_ℓ and downstream density ρ_r. Here upstream and downstream are with respect to the left junction. Hence we have

the relationship given by Equation 8.7 where we have used the function $F(\cdot, \cdot)$ that will be obtained from the Godunov method.

$$f_{in}(t) = F(\rho_\ell, \rho) \tag{8.7}$$

Similarly, for the right junction, the outflow $f_{out}(t)$ is given by Equation 8.8.

$$f_{out}(t) = F(\rho, \rho_r) \tag{8.8}$$

The function $F(\rho_\ell, \rho_r)$ in terms of its arguments is given by the Godunov method as follows (see [107]).

$$F(\rho, \rho_r) = f(\rho^*(\rho_\ell, \rho_r)) \tag{8.9}$$

Here, the flow-dictating density ρ^* is obtained from the following (see [107]):

1. $f'(\rho_\ell), f'(\rho_r) \geq 0 \Rightarrow \rho^* = \rho_\ell$
2. $f'(\rho_\ell), f'(\rho_r) \leq 0 \Rightarrow \rho^* = \rho_r$
3. $f'(\rho_\ell) \geq 0 \geq f'(\rho_r) \Rightarrow \rho^* = \rho_\ell$ if $s > 0$, otherwise $\rho^* = \rho_r$

4. $f'(\rho_\ell) < 0 < f'(\rho_r) \Rightarrow \rho^* = \rho_s$

Here, ρ_s is obtained as the solution to $f'(\rho_s) = 0$.

Physically, the Gordunov conditions have the following meanings:

1. $f'(\rho_\ell), f'(\rho_r) \geq 0 \Rightarrow \rho^* = \rho_\ell$: If the densities on the left and right of the boundary are less than the critical density $rho_m/2$, then the inflow is determined by the density on the left. This is due to the fact that the segment on the right , in this case, can absorb additional flow until it reaches the maximum flow possible.

2. $f'(\rho_\ell), f'(\rho_r) \leq 0 \Rightarrow \rho^* = \rho_r$: If the densities in both sections are close to jam density, particularly, higher than the critical density, then the flow at the boundary is determined by the density on the right since the segment on the right cannot handle additional vehicle flow.

3. $f'(\rho_\ell) \geq 0 \geq f'(\rho_r) \Rightarrow \rho^* = \rho_\ell$ if $s > 0$, otherwise $\rho^* = \rho_r$ If the density in the segment on the left is less than critical density and the density in the right segment is higher than the critical density then the density that is used to determine flow at the boundary depends on the speed of the shockwave. This is determined by noting that in this case the density on the left is always less than the density on the right then by using Equation 8.5 in order to determine the direction of the shockwave as follows:

    - if the flow on the left is less than it is on the right, then the shockwave is traveling to the right. In which case, the density at the boundary is determined

by the density on the left.

- if the flow on the left is higher than it is on the left, then the shockwave is traveling to the right. In which case, the density at the boundary is determined by the density on the right.

4. $f'(\rho_\ell) < 0 < f'(\rho_r) \Rightarrow \rho^* = \rho_s$: If the density on the left is higher than the critical density and the density on the right is less than the critical density then the critical density is used to determine the flow at the boundary which is the maximum flow possible.

8.5 Hybrid Dynamic Model and Control Design

The ODE model for the ramp metering system can be written as

$$\frac{d\rho(t)}{dt} = F(\rho_\ell, \rho) - F(\rho, \rho_r) + u(t) \tag{8.10}$$

This is a switched hybrid system (see [109]), where the switching happens autonomously based on the values of ρ_ℓ, ρ, and ρ_r. The function $F(\rho_\ell, \rho)$ can have three distinct values, $f(\rho_\ell)$, $f(\rho)$, or $f(\rho_s)$. Similarly, $F(\rho, \rho_r)$ can have three distinct values. Hence, the dynamics can be written as

$$\frac{d\rho(t)}{dt} = G_q(\rho_\ell, \rho, \rho_r) + u(t) \tag{8.11}$$

where $q \in \{1, 2, \cdots, 9\}$ and the different G_q functions can be obtained from Equations 8.9, 8.10, and 8.11.

We propose the following feedback linearization based model for the ramp metering control that attempts to keep the mainline traffic density at ρ_c, which is taken to be the flow maximizing density. For the Greenshield's model this critical density is $\rho_m/2$.

$$u(t) = -G_q(\rho_\ell, \rho, \rho_r) - k(\rho(t) - \rho_c),\ k > 0 \tag{8.12}$$

The closed loop dynamics obtained by using this control law (if the prevalent traffic conditions are enabling) provide an exponentially decaying error, i.e.

$$e(t) = [\rho(t) - \rho_c] \to 0, \text{as } t \to \infty \tag{8.13}$$

The enabling conditions for the performance are obviously important, since if there are no vehicles at the ramp, then the control rate will not be achieved. Moreover, there is a maximum possible ramp inflow rate. In addition vehicles cannot be taken out of the freeway using an entrance ramp. Hence, only those values of the ramp flow are practically implemented that are in the range of $[0, u_{max}]$.

8.6 Simulations

The control developed in this study is implemented using the open source software scilab. The simulated model is consistent with the conservation law as well as the Gordunov conditions that make up the hybrid system. The model is first validated, then the control scheme is added and various scenarios are simulated in order to test the control rule developed. In this particular simulation model, the parameters used are as follows:

- Jam density: 80 vehicles/mile
- Critical Density: 40 vehicles/mile
- Free Flow Speed: 60 miles/hour

8.6.1 Simulation Model

The code presented in Program 15 is the implementation of Godunov conditions.

Program 15 Implementation of the Godunov Conditions in Scilab

```
// ---------- Hybrid Godunov-Based Feedback Ramp Control
clear;
clc;

function rhog = Godunov(rl,rr)
rhos = 40;
rhom = 80;
vf = 60;
ul =  vf .* (1-rl/rhom);
ur =  vf .* (1-rr/rhom);
s = (ul.*rl - ur.*rr)/(rl - rr);
dfl = vf .* (1-2.*rl/rhom);
dfr = vf .* (1-2.*rr/rhom);
case1 = dfl >= 0 & dfr >= 0;
case2 = dfl <= 0 & dfr <= 0;
case3 = dfl >= 0 & dfr <= 0 & s > 0;
case4 = dfl >= 0 & dfr <= 0 & s <= 0;
case5 = dfl <= 0 & dfr >= 0;
//~(case1 | case2);
rhog = (case1 + case3) .* rl + (case2 + case4) .* rr + case5 .* rhos;

endfunction;
```

The Scilab code in Program 16 describes the ordinary differential equation (ode) given in Equation 8.10 which uses the hybrid control scheme developed in this study. In addition, a lower limit of zero and an upper limit of 0.75 of the maximum flow is applied on the in-flow of the control.

Program 16 Implementation of the Conservation Law in Scilab

```
function dx = RampControl(t,x)
vf = 60;
rhom = 80;
rhos = 40;
rhol = 20;
rhor = 20;
k=0.5;
fmax = vf*(1-rhos /rhom).*rhos;
umax = 0.75 .* fmax;
umin = 0;
rfout = Godunov(x,rhor);
rfin = Godunov(rhol,x);
fin = vf*(1-rfin /rhom).*rfin;
fout = vf*(1-rfout /rhom).*rfout;
up = fout - fin - k .* (x - rhos);
case1 = up <= umax & up >= 0;
case2 = up > umax;
case3 = up < 0;
u = up .* case1 + umax .* case2 + 0 .* case3;
dx = fin - fout + u;
//dx = fin - fout

endfunction
```

The code presented in Program 17 describes the implementation of the ode solver combined with the hybrid control law and Godunov's conditions.

Program 17 Implementation of the Ramp Hybrid Control in Scilab

```
k=0.5;
vf = 60;
rhom = 80;
rhos = 40;
rhol = 20;
rhor = 20;
fmax = vf*(1-rhos /rhom).*rhos;
umax = 0.75 .* fmax;
umin = 0;

t = 0:0.0001:0.7;
x0 = [10];
x = ode(x0,0,t,RampControl);

e = x - 40;
rfout = Godunov(x,rhor);
rfin = Godunov(rhol,x);
fin = vf*(1-rfin /rhom).* rfin;
fout = vf*(1-rfout /rhom).* rfout;
up = fout - fin - k .* (x - rhos);
case1 = up <= umax & up >= 0;
case2 = up > umax;
case3 = up < 0;
u = up .* case1 + umax .* case2 + 0 .* case3;

subplot(221);
plot(t,x(1,:));xgrid;
xlabel("time");
title('Density in the middle section ');

subplot(222);
plot(t,rfin);xgrid;
xlabel("time");
title('In Density used');

subplot(224);
plot(t,e);xgrid;
xlabel('time');
title('Error');

subplot(223);xgrid;
plot(t,u);
xlabel('time');
title('Control');
```

8.6.2 Simulation Model Validation

Before applying the control scheme developed in this study, the model was validated in order to verify its consistency with the conservation law based on Godunov boundary conditions. Therefore, different scenarios for boundary as well as initial conditions where carefully chosen to cover all possibilities as stated in Table 8.1 which also states the figures associated with each scenario.

Table 8.1: Scenarios Tested

ρ_l	ρ_0	ρ_r	Figure
20	10	20	8.8
20	30	20	8.9
20	50	20	8.10
20	60	20	8.11
20	60	70	8.13
20	70	20	8.12
50	20	70	8.14
60	50	60	8.16
60	70	60	8.17
70	20	50	8.15

Note that when $\rho_l = 20$, $\rho_0 = 10$, and $\rho_r = 20$, then at both boundaries, the conditions should satisfy Godunov's first condition since all the given densities are less than the critical density. Figures 8.8 and 8.9 clearly show that at the first boundary, the density on the left ρ_l was used as indicated by the "In Density Plot" which is consistent with Gardanov's first condition. Similarly, the "Out Density" plot is following exactly the density in the middle section which is again consistent with Godunov's first condition.

When $\rho_l = 20$, $\rho_0 = 50$, and $\rho_r = 20$, the first boundary condition must satisfy Godunov's third condition since the density on the left is lower than the density on the right of the boundary. However, in a very small amount of time the density in the middle section

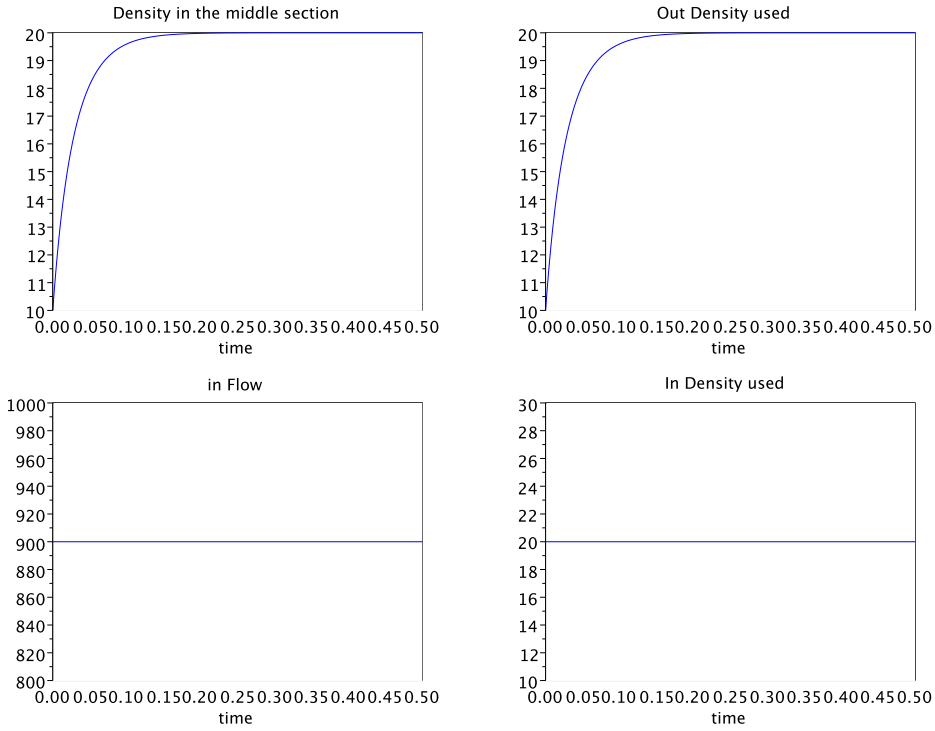

Figure 8.8: Results when $\rho_l = 20$, $\rho_0 = 10$, and $\rho_r = 20$

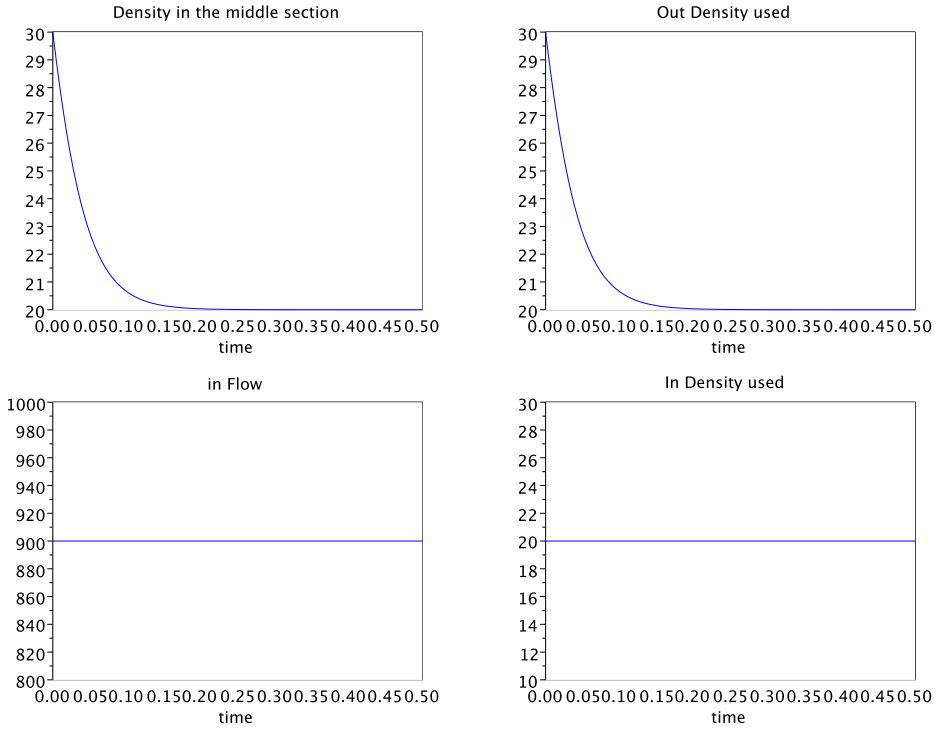

Figure 8.9: Results when $\rho_l = 20$, $\rho_0 = 30$, and $\rho_r = 20$

reduces and becomes lower than the critical density. Therefore, for the most part, the first boundary condition needs to be consistent with the first Godunov condition which takes on the density on the left as demonstrated in the "In Density used" plot in Figure 8.10. The second boundary, however, must satisfy the fourth Godunov's condition since the density on the right is lower than the critical density and the density on the left is higher than the critical density. This holds until the density in the center segment becomes lower than the critical density then Godunov's first condition must be satisfied where the density on the left of the boundary is used as shown in the "Out Density used" plot in Figure 8.10. identical behaviour is also observed in Figures 8.11 and 8.12.

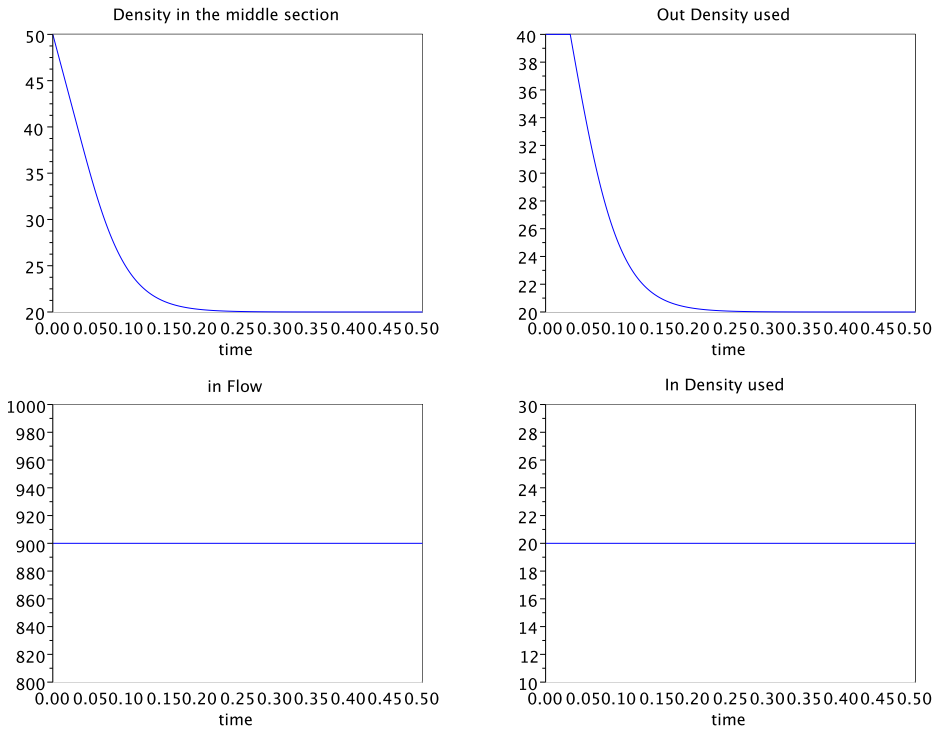

Figure 8.10: Results when $\rho_l = 20$, $\rho_0 = 50$, and $\rho_r = 20$

When $\rho_l = 20$, $\rho_0 = 60$, and $\rho_r = 70$, the left boundary must satisfy Godunov's third condition since the density on the left is less than the critical density and the density on

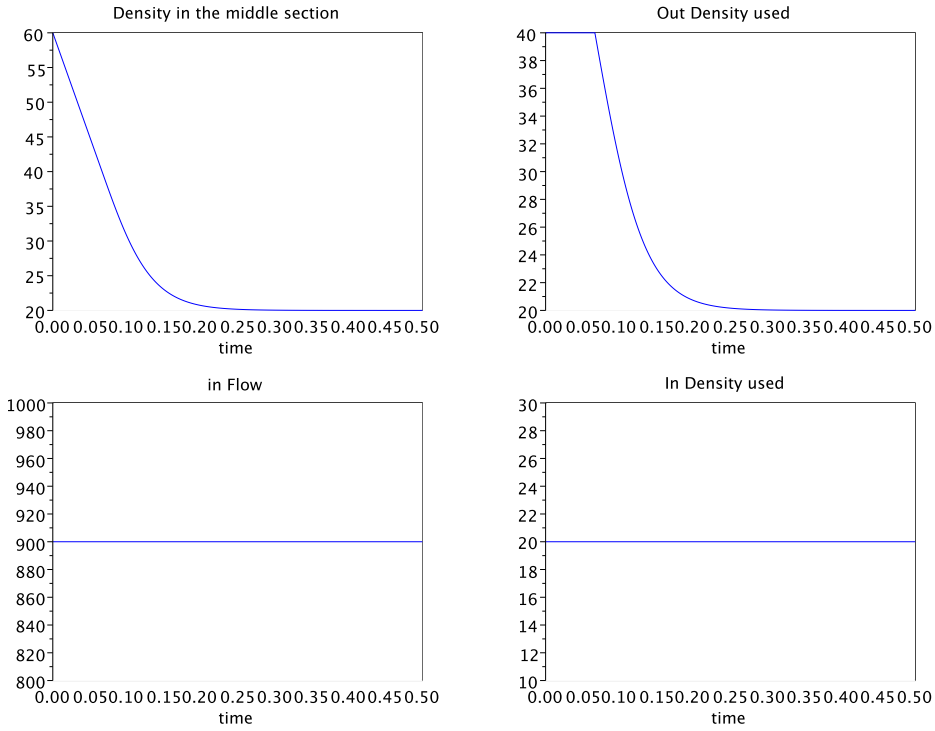

Figure 8.11: Results when $\rho_l = 20$, $\rho_0 = 60$, and $\rho_r = 20$

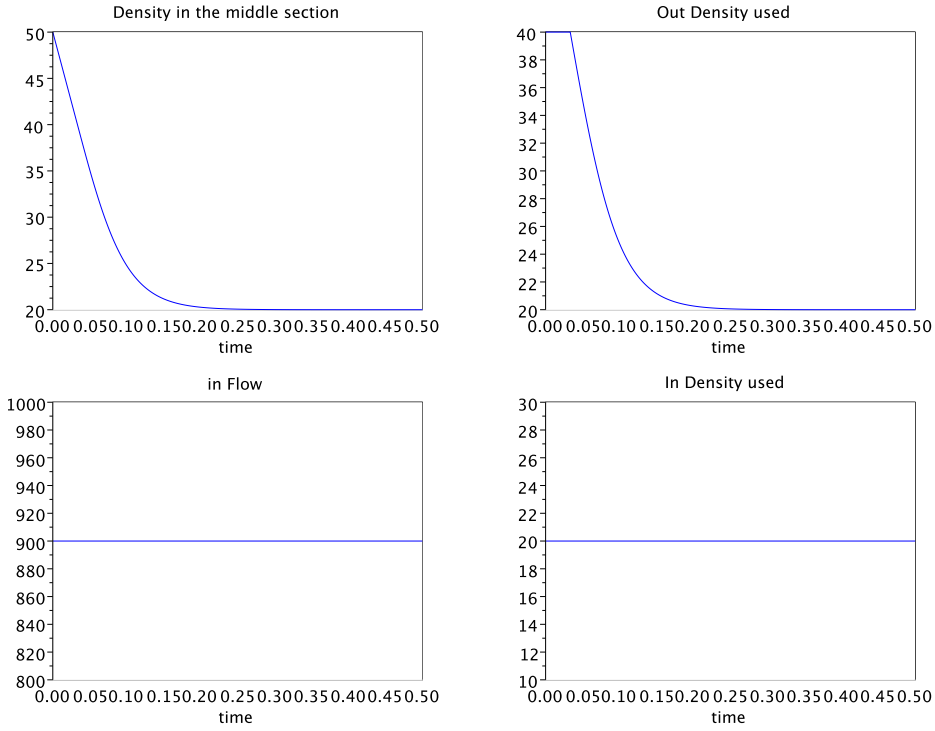

Figure 8.12: Results when $\rho_l = 20$, $\rho_0 = 70$, and $\rho_r = 20$

the right is higher than the critical density. However, note that the flow at both sides of the boundary is equal; therefore, according to Godunov's third condition, the density on the right is used at the boundary as shown in the "In Density used" plot in Figure 8.13. The right boundary, however, must be consistent with Godunov's second condition since both densities are higher than the critical density in which case the density on the right of the boundary is used as shown in the "Out Density used" in Figure 8.13.

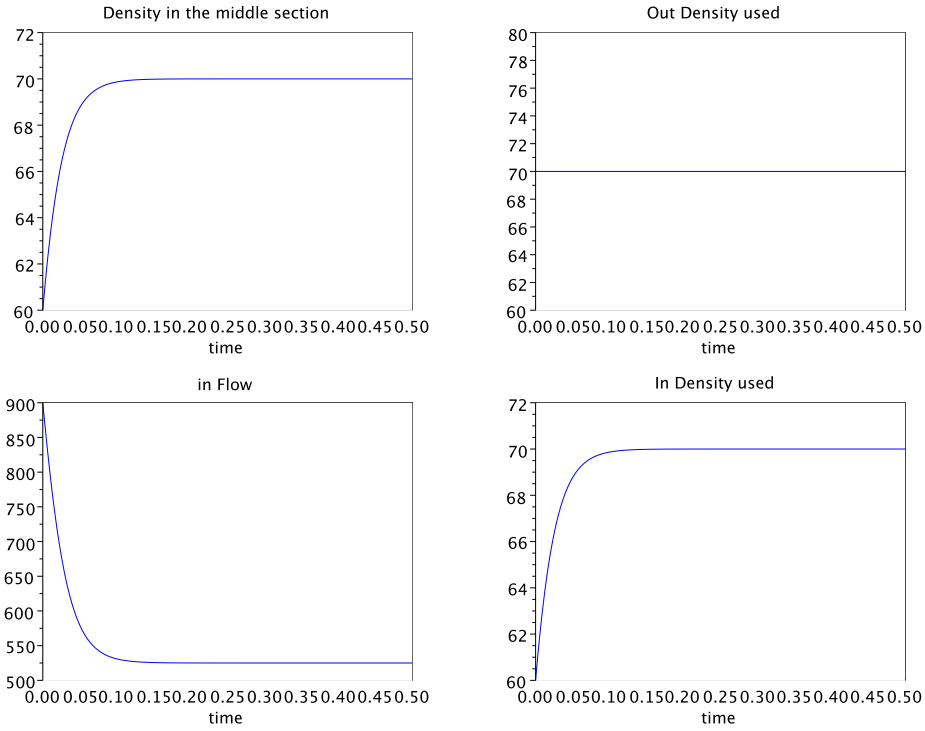

Figure 8.13: Results when $\rho_l = 20$, $\rho_0 = 60$, and $\rho_r = 70$

When $\rho_l = 50$, $\rho_0 = 20$, and $\rho_r = 70$, the density on the left of the first boundary is higher than the critical density where the density on the right boundary is lower than the critical density. In this case, the density used at the boundary in order to determine the flow is the critical density, that is the maximum flow, as shown in the "in Density used" plot in Figure 8.14 which stays at 40 until the center density becomes higher than the critical density.

At this point, Godunov's second condition is applied where the density on the right of the boundary is used. However, initially, the second boundary must satisfy Godunov's third condition with a negative shock speed which uses the density on the left of the boundary until the density on the left becomes higher than the critical density. In this case, Godunov's second control law must be followed which also uses the density on the right of the boundary as shown in the "Out Density used" plot in Figure 8.14. Similar reasoning also applies to results in Figure 8.15

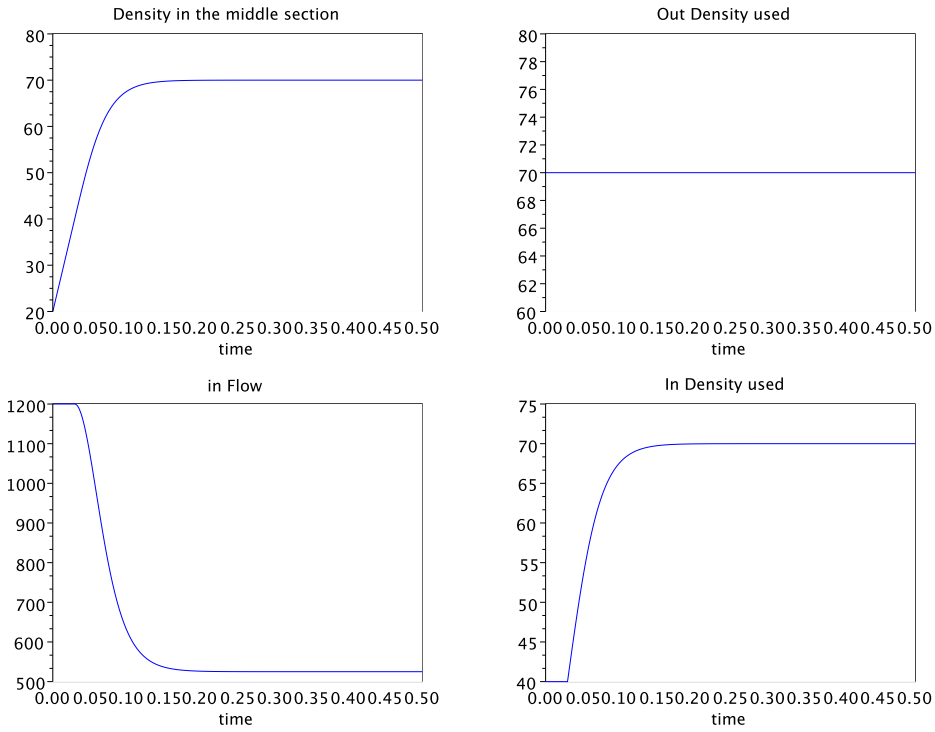

Figure 8.14: Results when $\rho_l = 50$, $\rho_0 = 20$, and $\rho_r = 70$

When $\rho_l = 50$, $\rho_0 = 60$, and $\rho_r = 50$, Godunov's second condition must be satisfied at both boundaries. In this case, the densities on the right of the boundaries are used as show in the plots in Figure 8.16. The same reasoning applies to the results in Figure 8.17

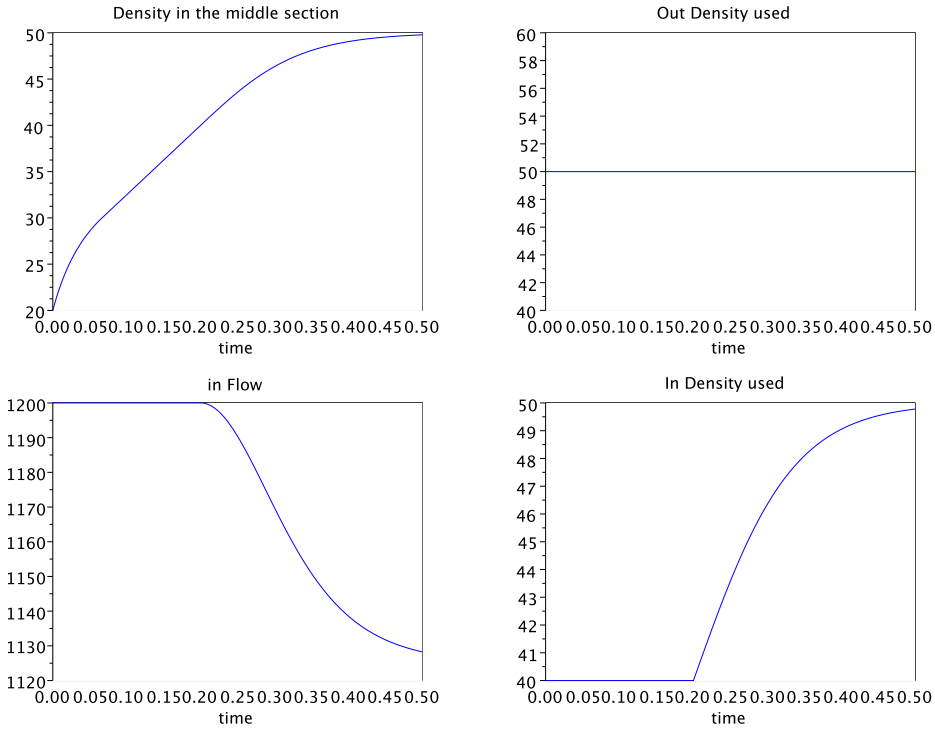

Figure 8.15: Results when $\rho_l = 70$, $\rho_0 = 20$, and $\rho_r = 50$

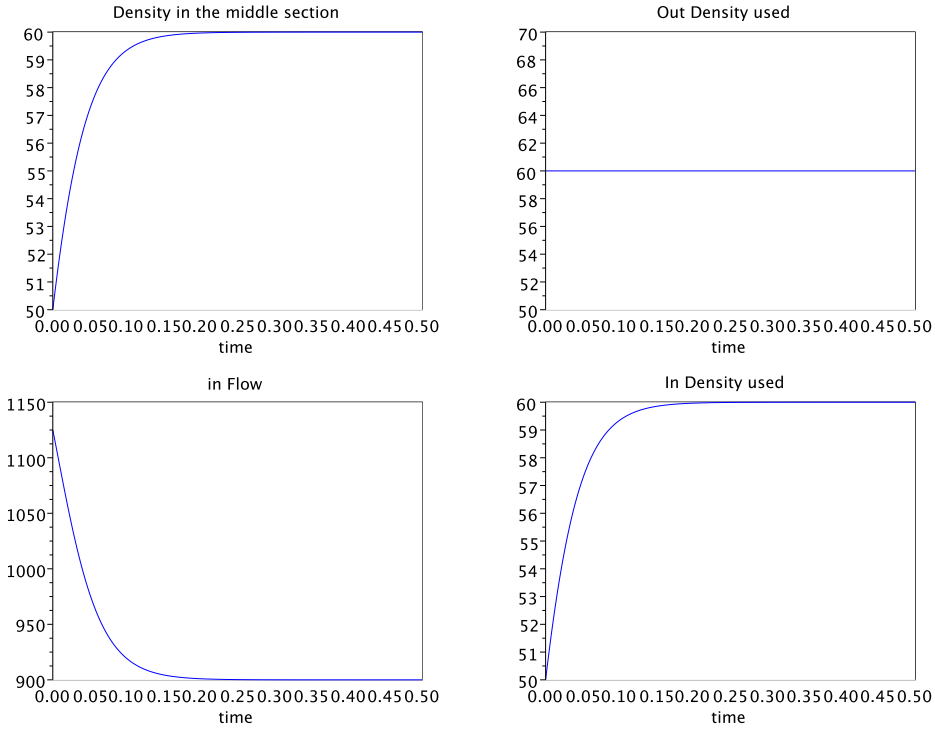

Figure 8.16: Results when $\rho_l = 50$, $\rho_0 = 60$, and $\rho_r = 50$

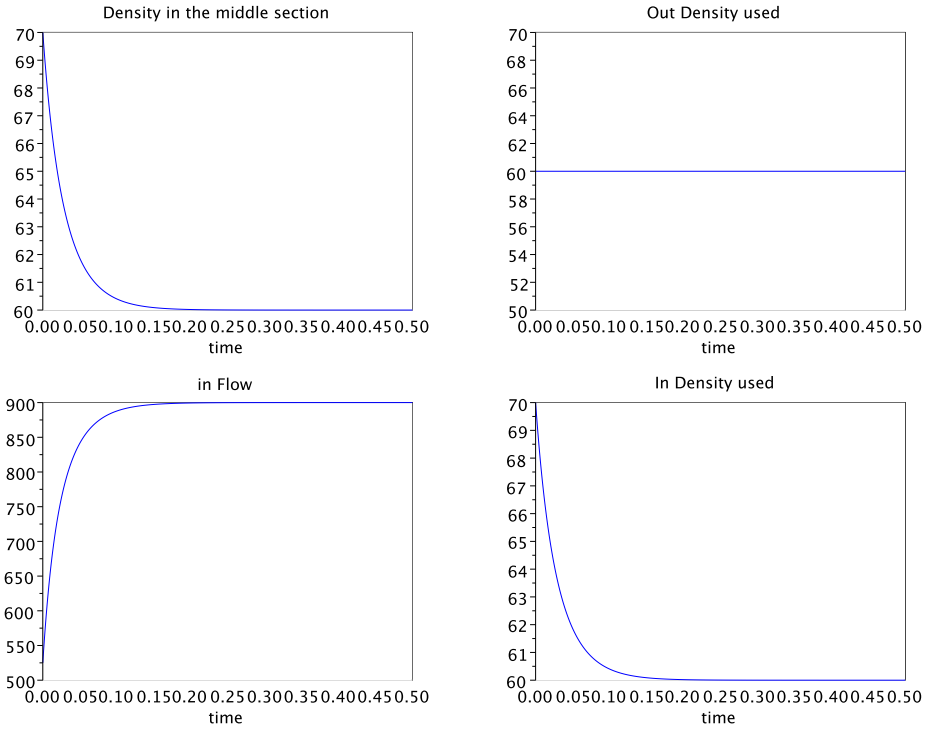

Figure 8.17: Results when $\rho_l = 60$, $\rho_0 = 70$, and $\rho_r = 60$

8.6.3 Simulation Results

After the model was verified, the hybrid control scheme developed in this study is applied to the model. Different scenarios for boundary as well as initial conditions where carefully chosen to cover all possibilities as stated in Table 8.2 which also states the figures associated with each scenario.

Table 8.2: Scenarios Tested

ρ_l	ρ_0	ρ_r	Figure
20	10	20	8.18
20	30	20	8.19
20	50	20	8.20
20	70	20	8.21
50	20	70	8.22
60	50	60	8.23
60	70	60	8.24
70	20	50	8.25

The purpose of the control is to maintain the density of the section of the freeway at the critical density which maximizes the flow. In this particular simulation model, the critical density is given by 40.

When $\rho_l = 20$, $\rho_0 = 10$, and $\rho_r = 20$, the input flow of the control is shown to increase until density in the section of interest equals the critical density or when the control reaches its maximum allowed inflow rate as demonstrated in Figure 8.18. An identical behavior is depicted in the simulations in Figure 8.19. In both scenarios, all densities are less than critical density. Therefore, the first Godunov condition is applied in both cases.

When $\rho_l = 20$, $\rho_0 = 50$, and $\rho_r = 20$, the densities at both side of the middle section are light and less the critical density. Therefore, the density at the middle section decreases based

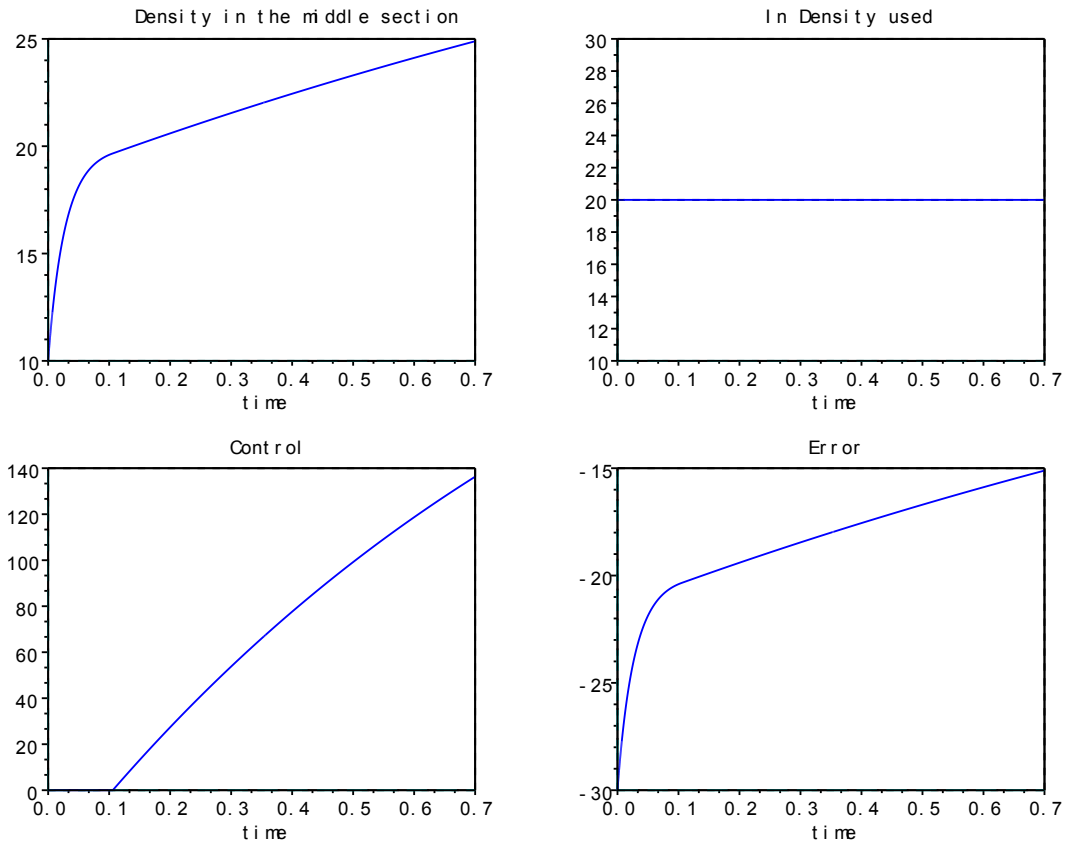

Figure 8.18: Results when $\rho_l = 20$, $\rho_0 = 10$, and $\rho_r = 20$

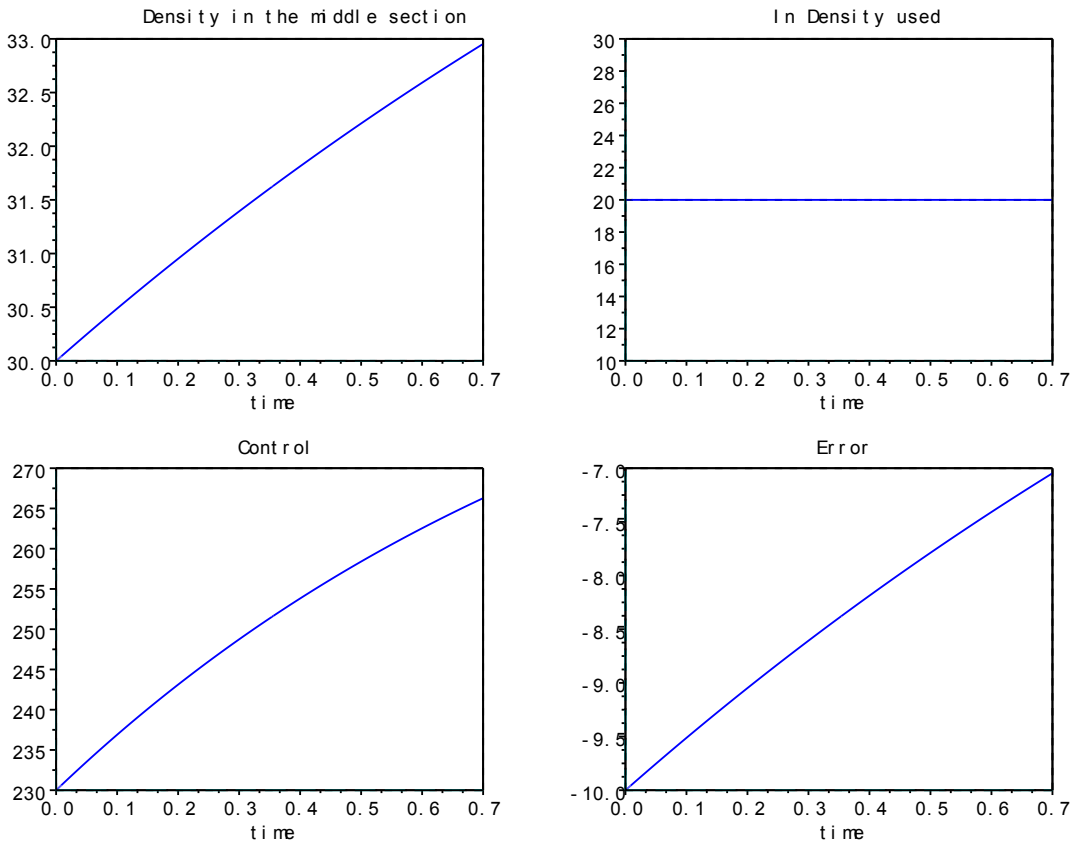

Figure 8.19: Results when$\rho_l = 20$, $\rho_0 = 30$, and $\rho_r = 20$

on the conservation dynamics. The control increases the inflow as the density in the middle section decreases. It is observed in Figure 8.20 that the error goes to zero and the density of the middle section converges to the desired density. Note that at the first boundary, Godunov's third condition is applied with a positive shock speed, where the simulation configuration in Figure 8.21 the shock speed is negative indicating that the density on the right of the boundary must be used in order to determine the inflow. It is shown in the results in Figure 8.21 that even when the shock speed is negative, the control developed leads the center segment to have the maximum flow if it is assumed to be provided.

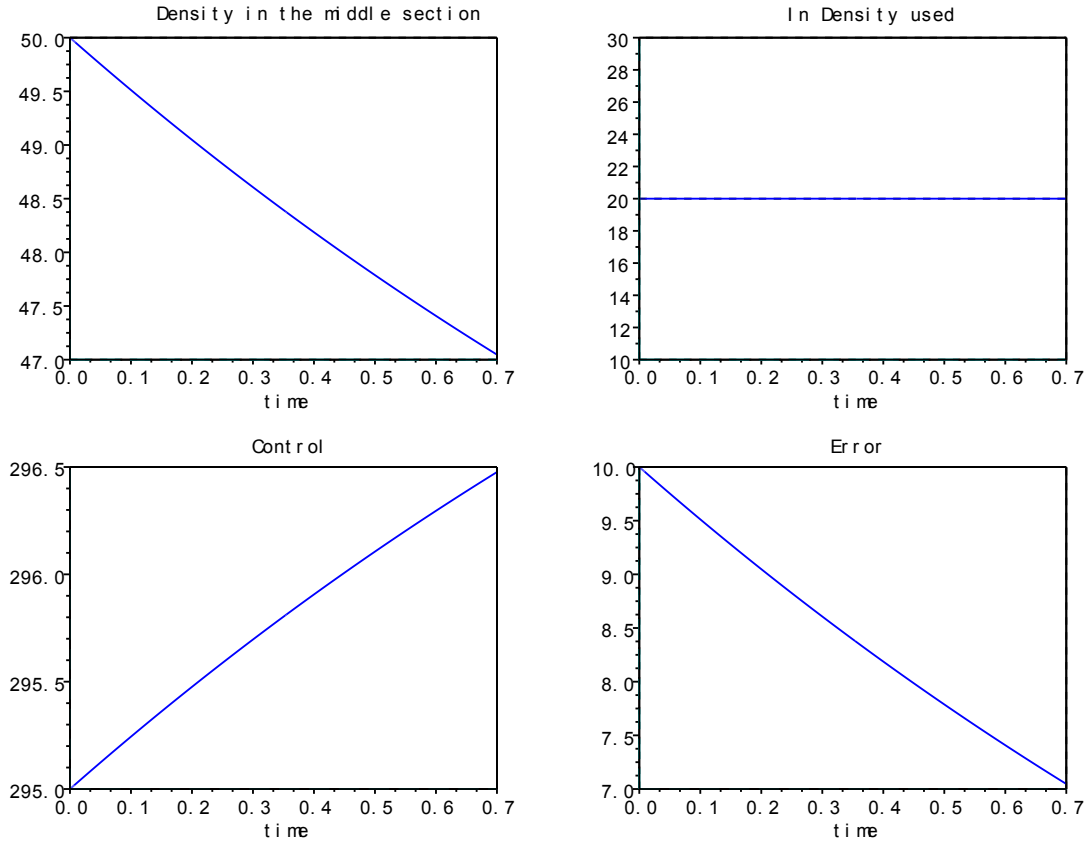

Figure 8.20: Results when $\rho_l = 20$, $\rho_0 = 50$, and $\rho_r = 20$

When $\rho_l = 50$, $\rho_0 = 20$, and $\rho_r = 70$, eventually the middle section becomes congested and takes on the density of $\rho_r = 70$. Since the ramp can only control the inflow, it is not possible

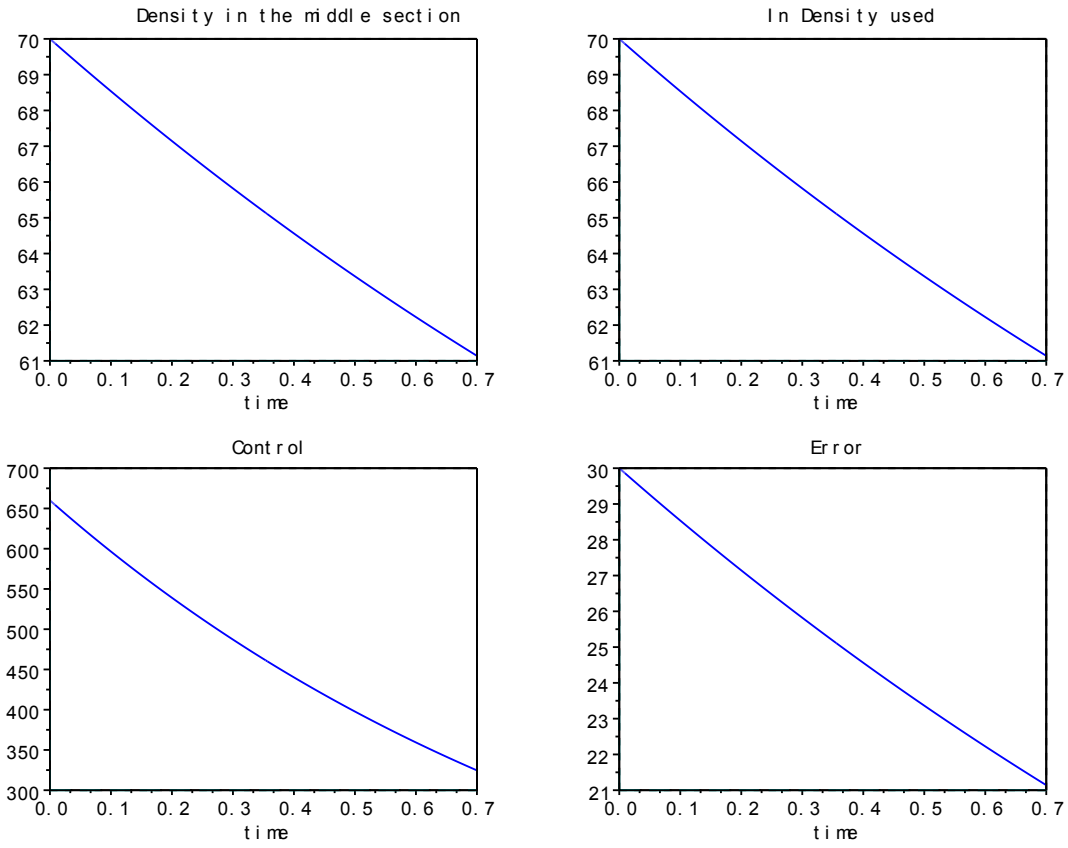

Figure 8.21: Results when $\rho_l = 20$, $\rho_0 = 70$, and $\rho_r = 20$

to take out undesired densities from the middle section. Therefore, as stated earlier, the minimum possible inflow controlled is zero as depicted in Figure 8.22. In this case, the control error will not converge to zero. The same reasoning applies to the simulation results in Figure 8.23.

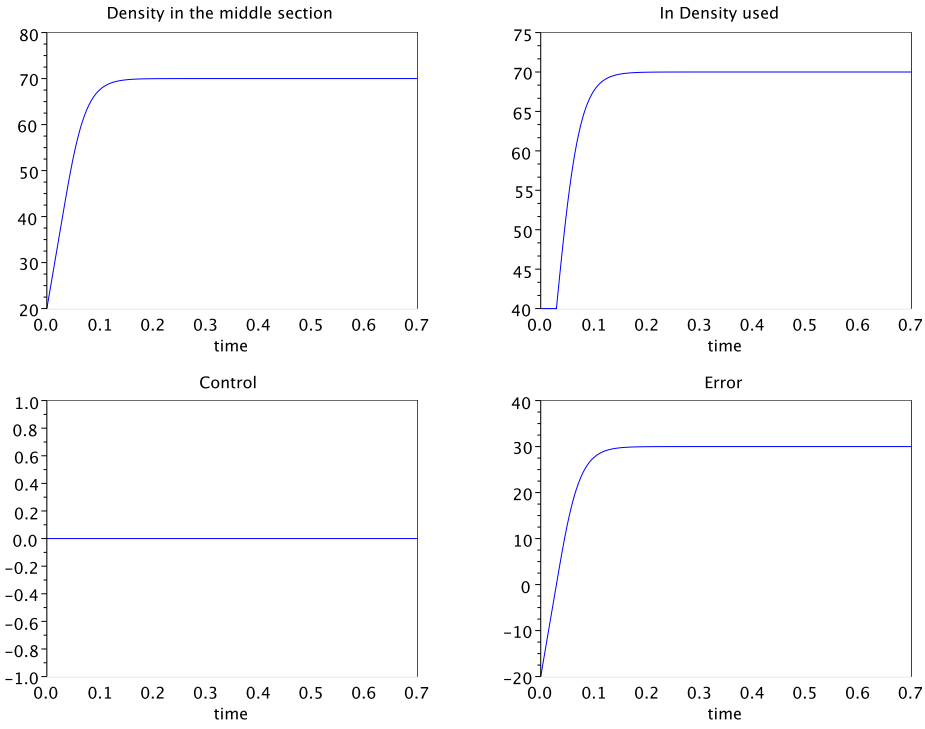

Figure 8.22: Results when $\rho_l = 50$, $\rho_0 = 20$, and $\rho_r = 70$

When $\rho_l = 60$, $\rho_0 = 70$, and $\rho_r = 60$ indicating densities above the critical densities on all sections, the control reduces the inflow until it reaches the minimum inflow possible as demonstrated in the plots in Figure 8.24.

When $\rho_l = 70$, $\rho_0 = 20$, and $\rho_r = 50$, the middle section will eventually reach the density $\rho_r = 50$ based on Godunov's conditions as well as the conservation law dynamics. Therefore, as shown in the simulation results in Figure 8.25, the inflow is zero from the control scheme and the error does not converge to zero for the same reason mentioned earlier stating the

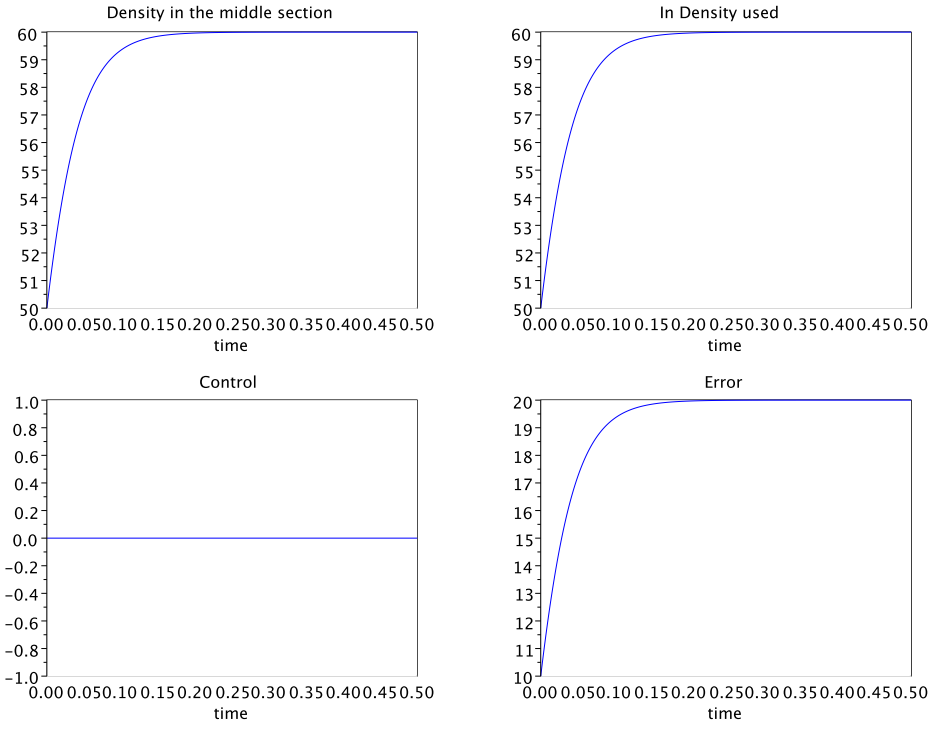

Figure 8.23: Results when $\rho_l = 60$, $\rho_0 = 50$, and $\rho_r = 60$

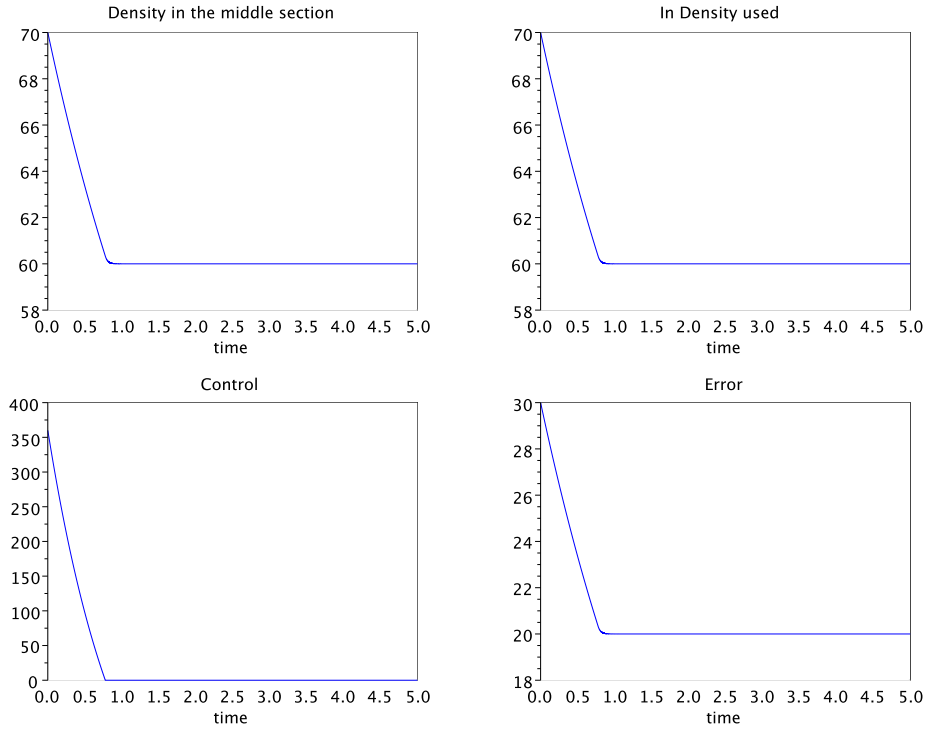

Figure 8.24: Results when $\rho_l = 60$, $\rho_0 = 70$, and $\rho_r = 60$

developed control cannot absorbe access flow it can only provide additional flow.

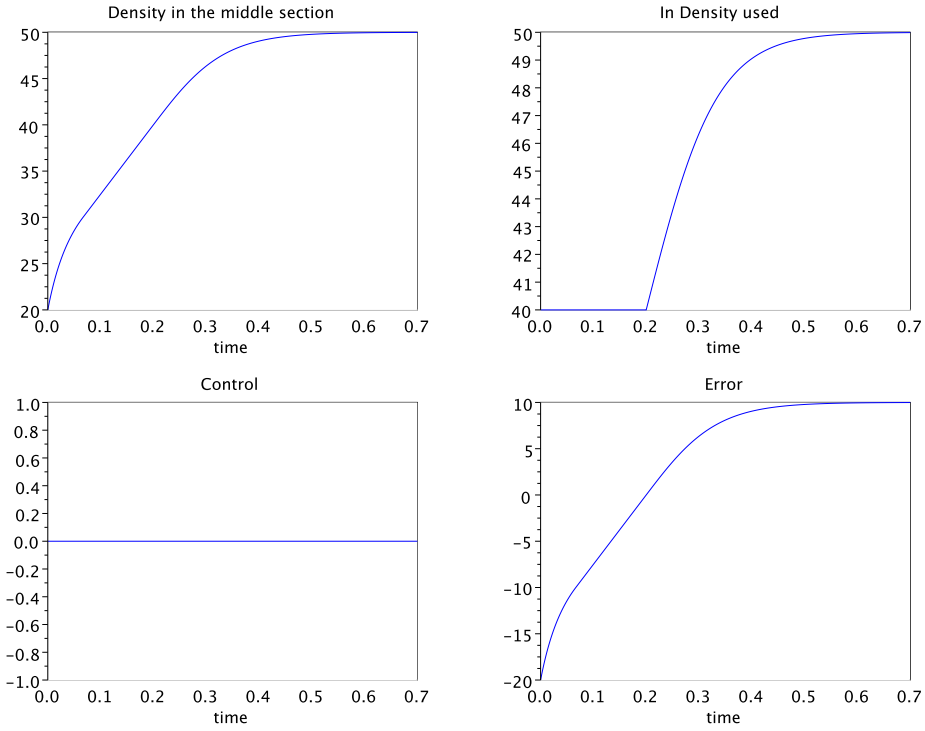

Figure 8.25: Results when $\rho_l = 70$, $\rho_0 = 20$, and $\rho_r = 50$

8.7 Hybrid Control Implementation Case Study

In order to demonstrate the implementation of the proposed hybrid control in real life application, the North-bound Tropicana on-ramp was chosen with the assistance of the Freeway and Arterial System of Transportation (FAST). Data is collected on the chosen ramp, parameters were estimated, and then a model was developed to fit the characteristics of the specific ramp chosen. The existing control law was obtained then implemented in simulations along with the developed model. The proposed hybrid control was then compared to the existing one through simulations as well.

8.7.1 Description of Scenario

The ramp in this case study was chosen with the assistance of FAST personnel. The selection criteria of the ramp are composed of several requirements. It is vital that the chosen ramp has a ramp meter that is controlled by the freeway sensors. Furthermore, for model fitting purposes, it is crucial that the chosen location covers a wide range of traffic conditions in terms of density, flow, and speed.

8.7.1.1 Location

The location that is chosen to conduct this study is the North-bound Tropicana Avenue to Interstate-15 as depicted in Figure 8.26. The main line consists of five lanes where two of which are express lanes; however, all five lanes are treated as regular lanes at this location since vehicles can freely access any lane. The on-ramp has three lanes.

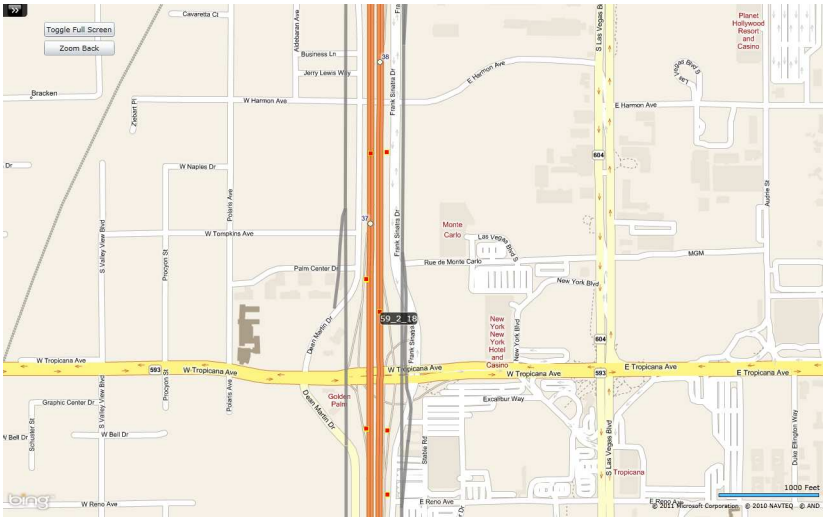

Figure 8.26: The North-bound Tropicana Avenue to Interstate-15 location taken from FAST website http://rtcsnv.com/mpo/fast/dashboard.cfm [1]

8.7.1.2 Data Sources

The data is collected at the desired location by FAST. Most freeway detectors are radar based; however, the detection on the Interstate 15 at the Tropicana location uses loop detectors. The counts are polled every 5 minutes, and then the data is aggregated and reported every 15 minutes. At this location, the freeway detector has a roadway id: 59 and a segment id 2. The data from this sensor is used by the ramp controller in order to control the flow when operated in traffic responsive mode. The counts on the ramp, however, are obtained from video detection. The location of the detector at the North-bound Tropicana on-ramp is shown in Figure 8.27. It is indicated by "Ramp Meter 10".

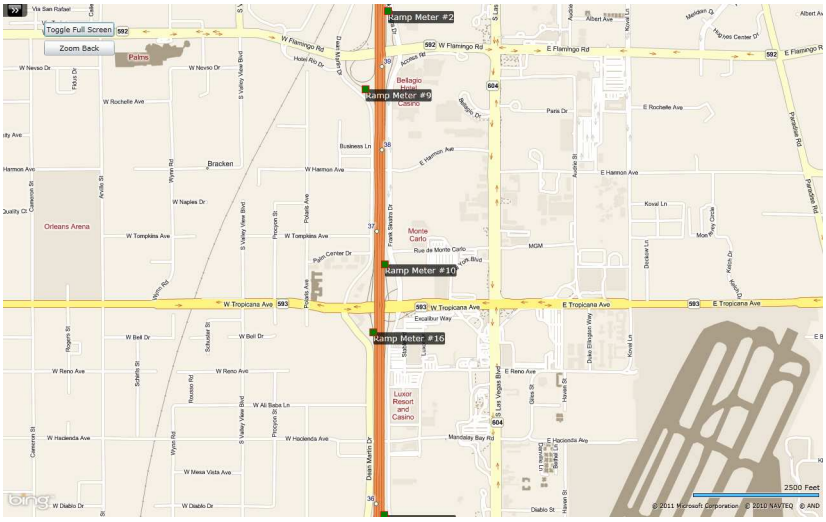

Figure 8.27: The location of the North-bound Tropicana Avenue to Interstate-15 ramp detector taken from FAST's website http://rtcsnv.com /mpo/fast/ dashboard.cfm [1]

8.7.1.3 Data Description

In order to obtain a well balanced data range, the data points must uniformly cover the range such that it is not biased towards a certain traffic condition. Therefore, the data is obtain for a Thursday between 6:00am and 12:00pm since it is observed that various traffic conditions occur throughout this weekday. This provides enough data points to estimate the macroscopic traffic model. Depicted in Figure 8.28 is the volume-speed plot of North-bound Tropicana Avenue to Interstate-15 obtained from FAST's website.

The data can be obtained from FAST's website in the format shown in 8.29[1]. A number of attributes are available as shown in Figure 8.29, such as Speed, Volume, Volume by vehicle size, and Occupancy. The attributes that were used in this study were Speed and Volume.

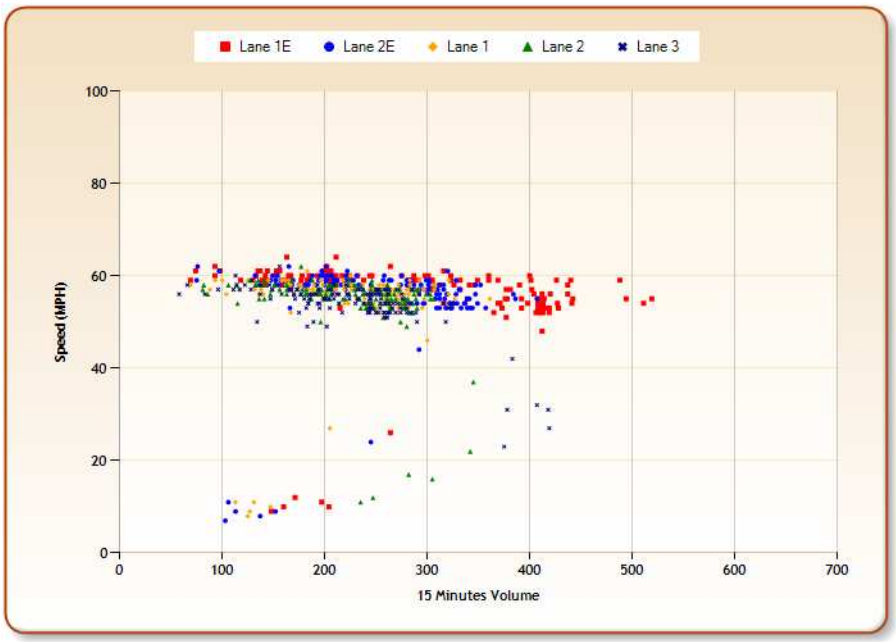

Figure 8.28: The speed-volume plot of North-bound Tropicana Avenue to Interstate-15 taken from FAST's website http://rtcsnv.com/mpo/fast/dashboard.cfm [1]

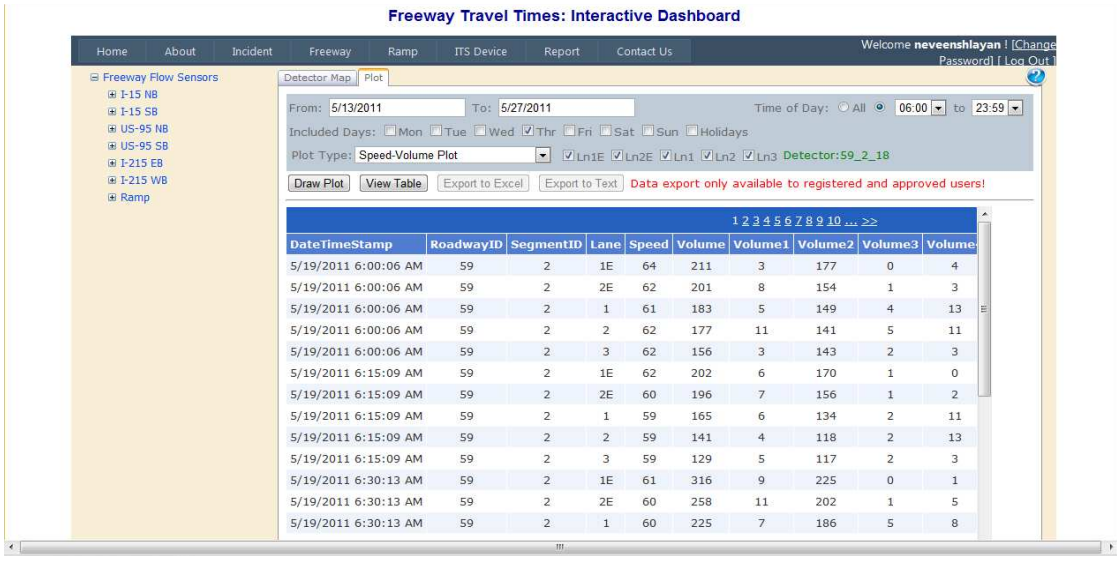

Figure 8.29: Detector data from North-bound Tropicana Avenue to Interstate-15 taken from FAST's website http://rtcsnv.com/mpo/fast/dashboard.cfm [1]

8.7.2 Parameter Estimation

8.7.2.1 What are the Needed Parameters?

As stated earlier, the traffic flow using Greenshields model is given by

$$f(t) = v_f \rho(t)(1 - \frac{\rho(t)}{\rho_m}) \tag{8.14}$$

From Equation 8.14, it is evident that v_f and ρ_m are needed in order to model the chosen ramp. The flow f is provided from the data as well as the speed V. In order to determine the density ρ, the relationship $f = V * \rho$ is used. It is desired to estimate v_f and ρ_m. It becomes clear that Least Square Estimation (LSE) can be used if Equation 8.14 is rewritten as in Equation 8.15.

$$f(t) = v_f \rho(t) - \frac{v_f}{\rho_m} \rho(t)^2 \tag{8.15}$$

Equation 8.15 has the following general form

$$y = w_1 \beta_1 + w_2 \beta_2 \tag{8.16}$$

where,

$y = f(t)$

$w_1 = v_f$

$\beta_1 = \rho$

$w_2 = \frac{v_f}{\rho_m}$

$\beta_2 = \rho^2$

The problem now is transformed into a linear equation where LSE can be used in order to estimate $w_1 = v_f$ and $w_2 = \frac{v_f}{\rho_m}$ where ρ_m can then be calculated.

8.7.3 Projection Theorem

Theorem 8.7.1. *Let H be a Hilber Space and S be a closed subspace of H. Then, $\forall y \in H \exists$ a unique $s_0 \in M$ such that $\|y - s_0\| \leq \|y - s\| \, \forall s \in S$ and $(y - s_0) \perp S$. [110]*

The projection theorem states that given closed subspace of a complete inner product space or Hilbert space and a member of that Hilbert space, one can find a unique member that lies in the subspace which is the closest to the given member of the Hilbert space.

Using the resulting property or sufficient condition that the vector representing the distance between the member of the Hilbert space to be approximated and its closest approximation in the given subspace is perpendicular to the subspace, one can easily obtain the Least Square Estimator (LSE) result.

8.7.4 Least Square Estimation

Equation 8.16 describes the model that is used to describe the freeway segment of interest indicating the parameters that need to be estimated. Rewriting Equation 8.16 in a matrix form, let

$$W = \begin{bmatrix} w_1 & w_2 \end{bmatrix} = \begin{bmatrix} \rho & -\rho^2 \end{bmatrix}$$

and

$$\beta = \begin{bmatrix} \beta_1 \\ \beta_2 \end{bmatrix} = \begin{bmatrix} v_f \\ \frac{v_f}{\rho_m} \end{bmatrix}$$

then the following is obtained,

$$y = W\beta \tag{8.17}$$

where y and W are obtained from the measured data and β is the vector of parameters to be estimated, $\hat{\beta}$.

Applying the Projection Theorem, it is observed that

$$W'(y - W\hat{\beta}) = 0 \tag{8.18}$$

then the best estimate of β is given by

$$\hat{\beta} = [W'W]^{-1}W'y \tag{8.19}$$

8.7.5 Discrete On-Line Parameter Estimation- Recursive Least Square Estimation

The best estimate given in Equation 8.19 can be used on a large set of data. However, in case parameters need to be updated in real time as new sensor measurements are obtained, Recursive Least Square Estimation (RLSE) is used. The RLSE is derived by rewriting $y - \hat{y}$ as follows

$$y - \hat{y} = W\hat{\beta}_{k+1} - W\hat{\beta}_k \tag{8.20}$$

The RLSE is given by

$$\hat{\beta}_{k+1} = \hat{\beta}_k + [W'W]^{-1}W'(y - W\hat{\beta}_k) \tag{8.21}$$

8.7.6 Continuous On-Line Parameter Estimation and Exponential Forgetting

When dynamics are continuous or not discretized, one must implement the on-line parameter estimation in a continuous manner as well.

The derivation of the continuous RLSE results from the basic idea behind LSE which is

minimizing the total prediction error as given by Equation 8.22 [111].

$$J = \int_0^t \left\| y(r) - W(r)\hat{\beta}(t) \right\|^2 dr \tag{8.22}$$

By performing clever manipulations [111] and by defining the gain $P(t)$ as

$$P(t) = [\int_0^t W'(r)W(r)dr]^{-1} \tag{8.23}$$

the following differential continuous RLSE equations are obtained for $\hat{\beta}$ and P

$$\dot{\hat{\beta}} = -P(t)W'(\hat{y} - y) \tag{8.24}$$

$$\dot{P} = -PW'WP \tag{8.25}$$

When performing exponential forgetting, Equation 8.25 is modified as follows

$$\dot{P} = \lambda P - PW'WP \tag{8.26}$$

8.7.6.1 Data Formatting

As shown in Figure 8.29, speed, v, data is provided as miles per hour where volume data or flow f is provided as vehicles per 15 minutes. Flow data is converted to vehicles per hour, then density ρ is obtained by dividing flow by speed. The final formatted data is depicted in Table 8.3.

Table 8.3: Formatted sensor data used for parameter estimation

Speed V	Flow veh/15min	Flow f veh/hr	Density ρ veh/mile	ρ^2

8.8 MATLAB Implementation

LSE and RLSE are implemented using MATLAB as demonstrated in Programs 18 and 19. Both algorithms read data that resides in some file then performs the LSE based on the bulk matrix equation presented in Equation 8.19 where the RLSE uses the formula in Equation 8.21 in order to recursively estimate the parameters.

Program 18 Implementation of Least Square Estimation in MATLAB

```
clear
clc

%Data from file
data = xlsread('EstimationData.xlsx');
n    = size(data,1);%numnber of measurements
w1   = data(1:n,2);
w2   = data(1:n,3);
y    = data(1:n,1);
W  = [w1 w2]
a = W
y
c = inv(W'*W)*W'*y
[b,se_b,mse] = lscov(W,y)
```

Program 19 Implementation of Recursive Least Square Estimation in MATLAB

```
rhom = 85;
vf= 69;
bhat = [vf rhom]';
bhat2 = [vf rhom]';
for j=1:n,
    w1   = data(j,2);
    w2   = data(j,3);
    y    = data(j,1);
    W  = [w1 w2];
    yhat=W*bhat;
    bhat = bhat +  W
(y-yhat);
end
bhat
```

8.8.0.2 Estimated Parameters

When applying the data using the developed MATLAB algorithems, the following parameter estimates are obtained:

$v_f = 69.5815$mile/hr

$v_f/\rho_m = 0.8038 \Rightarrow \rho_m = 86.57$veh/mile

8.8.1 Existing Ramp Control

The ramp meter at the North-bound Tropicana location has two operation modes, fixed rate and traffic responsive. Table 8.4 describes the operation modes. The ramp is turned on during the morning peak 6:00am to 9:00am in traffic responsive mode. The ramp meter is turned on at the maximum fixed rate, 30 vehicles per minute(veh/min), between 1:00pm and and 6:00pm. It is important to mention that the operations of the traffic operations personnel take into account the traffic condition on the ramp as well in determining the flow rate.

Table 8.4: The North-bound Tropicana ramp meter operation modes

Time	**Operation Mode**	**Description**
6:00am-9:00am	Traffic Responsive	$v < 22 \Rightarrow Rate = 20$ veh/min $22 < v < 26 \Rightarrow Rate = 22$ veh/min $26 < v < 34 \Rightarrow Rate = 24$ veh/min $34 < v < 38 \Rightarrow Rate = 26$ veh/min $38 < v < 46 \Rightarrow Rate = 28$ veh/min $46 < v < 56 \Rightarrow Rate = 30$ veh/min
1:00pm-6:00pm	Fixed Rate	30 veh/min
Other	Turned off	Vehicles can flow freely

8.8.2 Comparative Simulations

8.8.2.1 Simulations of Existing Control

Program 20 is the implementation of the existing control of the chosen ramp meter based on the responsive mode. One of the main differences between the existing control and the proposed one is that the existing control is based only on the speed at which the speed of the inflow. However, the proposed control is based on the density of the freeway segment which is determined by using densities on both sides of the segment or boundary conditions. The parameters used are based on the data collected and the least square estimation used previously which resulted in $v_f = 69.5815$ mile/hr and $\rho_m = 86.57$veh/mile.

8.8.2.2 Simulation Results of Proposed and Existing Hybrid Control

Figure 8.30 demonstrates the advantage of implementing the proposed Godunov-based control vs. the existing ramp meter control. It is observed that if there is enough demand at the ramp, then the density on the freeway segment reaches jam density in a very short amount of time. On the other hand, the density of the freeway gradually increases then stabilizes

Program 20 Implementation of the existing ramp meter control in MATLAB

```
function dy = ExistRampControl(t,y)
vf = 70;
rhom = 86;
rhos = 43;
rhol = 20;
rhor = 20;
k=0.5;
fmax = vf*(1-rhos /rhom).*rhos;
umax = 0.75 .* fmax;
umin = 0;
rfout = Godunov(y,rhor);
rfin = Godunov(rhol,y);
v = vf*(1-rfin /rhom);
fin = vf*(1-rfin /rhom).*rfin;
fout = vf*(1-rfout /rhom).*rfout;
case1 = v <= 22 & v >= 0;
case2 = v <= 26 & v > 22;
case3 = v <= 34 & v > 26;
case4 = v <= 38 & v > 34;
case5 = v <= 46 & v > 38;
case6 = v <= 56 & v > 46;
case7 = v > 56;
u = 1200 .* case1 + 1320 .* case2 + 1440 .* case3 + 1560 .* case4
+ 1680 .* case5 + 1800 .* case6 + umax .* case7;
dy = fin - fout + u;
```

about the critical or desired density. It is evident that the proposed hybrid control is a more suitable mechanism of controlling the ramp if the purpose is to maintain the freeway at the maximum flow.

8.8.3 Simulations of Hybrid Self Tuning Regulator

Self-tuning adaptive control can be performed by updating the parameters with each sensor measurement obtained by using Recursive Least Square Estimation (RLSE). In case of simulations, the new data is obtained from the system's dynamics. The RLSE developed in Equation 8.21 is appropriate for discrete systems. However, a continuous version is needed in order to implement the RLSE to update the parameters in the simulations of the adaptive hybrid control. Therefore, Equations 8.24 and 8.25 are used in the implementation of the algorithm in MATLAB. Program 21 is the MATLAB implementation of the function that

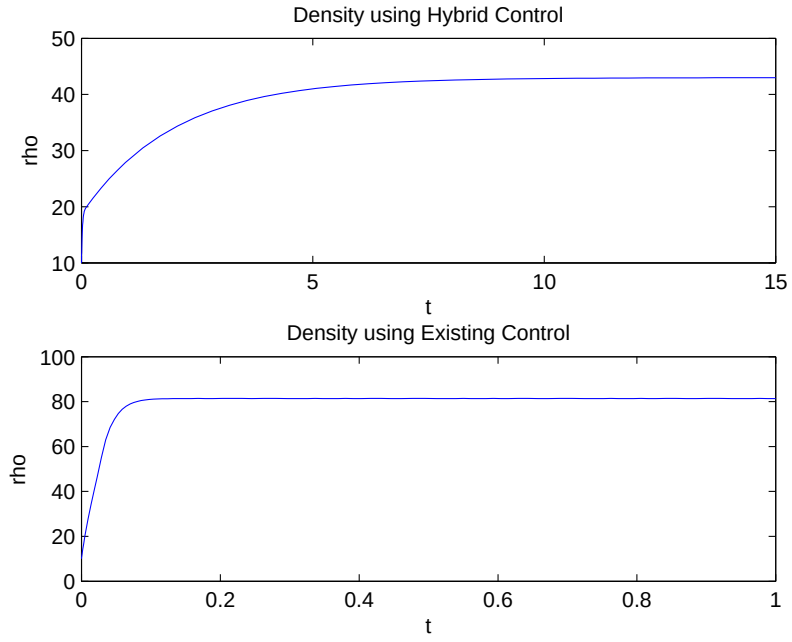

Figure 8.30: The freeway segment density using the proposed Godunov-based control vs. the existing ramp meter control

updates the system's dynamics parameters using recursive least squares.

The plots in Figure 8.31 are the results when running the simulations at a very small gain, initial density $\rho_0 = 10$, and initial estimates of $0.8 * v_f$ and $0.9 * v_f/\rho_m$. The plots in Figure 8.32 are the results when running the simulations at initial density $\rho_0 = 50$. The plots in Figure 8.33 are the results when running the simulations at initial density $\rho_0 = 70$. As demonstrated in the 'Density using hybrid Control' plot, the density converges to the desired critical density that maximizes the flow. Even though, the initial estimates of the parameters v_f and v_f/ρ_m were not accurate, it is demonstrated in the 'Free Flow' and 'vf/rhom' plots that they eventually converge to the actual parameters values.

Program 21 Implementation of the hybrid self tuning regulator in MATLAB

```
function dx = NewRampControl(t, x)
vf = 70;
rhom = 86;
rhos = 43;
rhol = 20;
rhor = 20;
k=0.5;

fmax = vf*(1-rhos /rhom).*rhos;
umax = 0.75 * fmax;
rfout = Godunov(x(1),rhor);
rfin = Godunov(rhol,x(1));
fin = x(2).*rfin - x(3)* rfin^2;
fout = x(2).*rfout - x(3)* rfout^2;
up = fout - fin - k .* (x(1) - rhos);
case1 = up <= umax & up >= 0;
case2 = up > umax;
case3 = up < 0;
u = up * case1 + umax * case2 + 0 * case3;

y = x(1) * vf * (1- x(1)/rhom);
w1 = x(1);
w2 = -x(1)^2;
lambda = 10;
dx(1) = fin - fout + u;

dx(2) = (w1 * x(4)+w2 * x(5)) * (y-(w1 * x(2) + w2 * x(3)));
dx(3) = (w1 * x(6)+w2 * x(7)) * (y-(w1 * x(2) + w2 * x(3)));
dx(4) = -(w1 * x(4)+w2 * x(5)) * (w1 * x(4)+w2 * x(6));
dx(5) = -(w1 * x(4)+w2 * x(5)) * (w1 * x(5)+w2 * x(7));
dx(6) = -(w1 * x(6)+w2 * x(7)) * (w1 * x(4)+w2 * x(6));
dx(7) = -(w1 * x(6)+w2 * x(7)) * (w1 * x(5)+w2 * x(7));
```

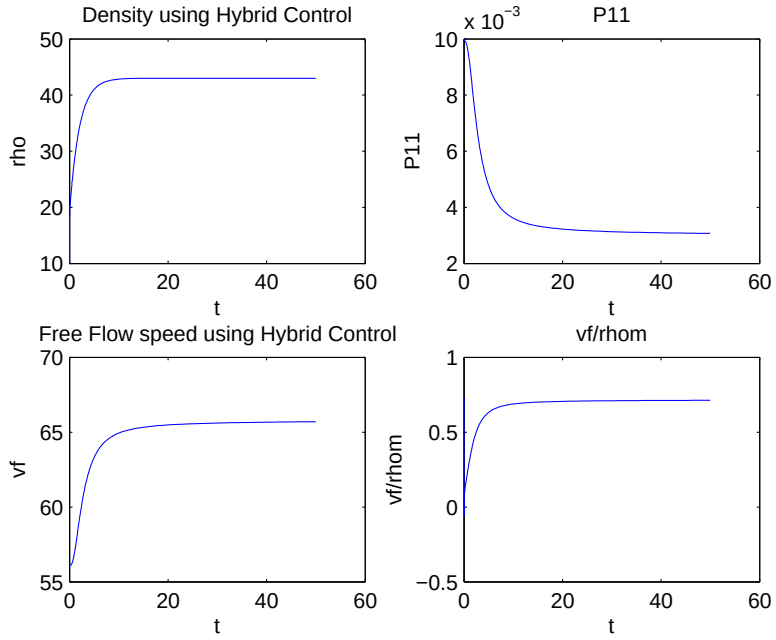

Figure 8.31: The freeway segment density and parameters values based on the self tuning regulator, $\rho_0 = 10$

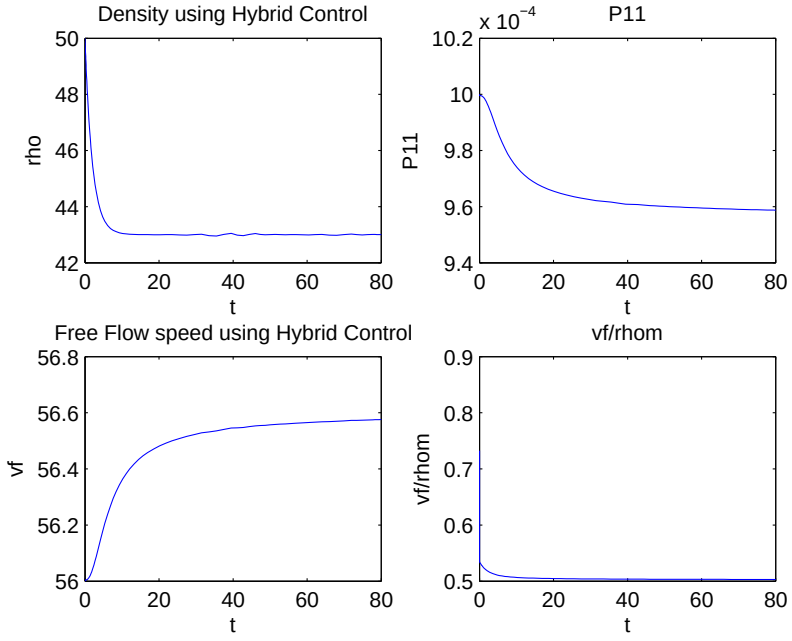

Figure 8.32: The freeway segment density and parameters values based on the self tuning regulator, $\rho_0 = 50$

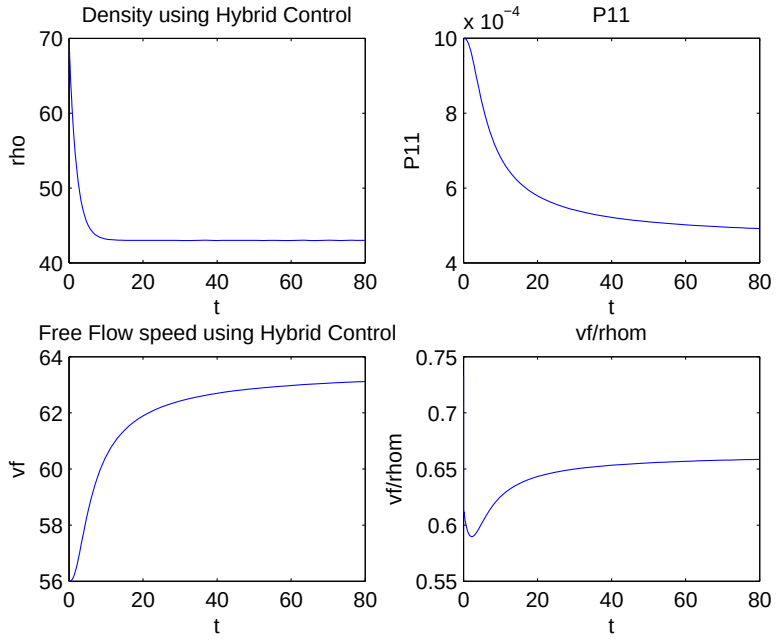

Figure 8.33: The freeway segment density and parameters values based on the self tuning regulator, $\rho_0 = 70$

8.8.4 Simulations of Exponential Forgetting of Parameters

In many scenarios, actual parameters of the modeled system can change over time due to many factors such as environmental, or in other words the system has time varying parameters [111]. In order to overcome this issue, exponential forgetting of parameters can be used in self tuning regulators in order to give more weight to new measurements in parameter estimation. Program 22 is the implementation of the hybrid self tuning regulator with exponential parameter forgetting in MATLAB. This algorithm uses Equation 8.26 in order to implement exponential forgetting.

The plots in Figure 8.34 are the results when running the simulations at a very small gain, initial density of $\rho_0 = 10$ and initial estimates of $0.8 * v_f$ and $0.9 * v_f/\rho_m$. The plots

Program 22 Implementation of the hybrid self tuning regulator with exponential parameter forgetting in MATLAB

```
y = x(1) * vf * (1- x(1)/rhom);
w1 = x(1);
w2 = -x(1)^2;
lambda = 10;
dx(1) = fin - fout + u;
%with exponantial forgetting
dx(2) = (w1 * x(4)+w2 * x(5)) * (y-(w1 * x(2) + w2 * x(3)));
dx(3) = (w1 * x(6)+w2 * x(7)) * (y-(w1 * x(2) + w2 * x(3)));
dx(4) = lambda * x(4)-(w1 * x(4)+w2 * x(5)) * (w1 * x(4)+w2 * x(6));
dx(5) =  lambda * x(5)-(w1 * x(4)+w2 * x(5)) * (w1 * x(5)+w2 * x(7));
dx(6) =  lambda * x(6)-(w1 * x(6)+w2 * x(7)) * (w1 * x(4)+w2 * x(6));
dx(7) =  lambda * x(7)-(w1 * x(6)+w2 * x(7)) * (w1 * x(5)+w2 * x(7));

dx = dx(:);
```

in Figure 8.35 are the results when running the simulations at a very small gain, initial density of $\rho_0 = 50$. The plots in Figure 8.36 are the results when running the simulations at a very small gain, initial density of $\rho_0 = 70$ As demonstrated in the 'Density using hybrid Control' plot, the density converges to the desired critical density that maximizes the flow. Even though, the initial estimates of the parameters v_f and v_f/ρ_m were not accurate, it is demonstrated in the 'Free Flow' and 'vf/rhom' plots that they eventually converge to the actual parameters values.

When the results of self tuning regulator with exponential forgetting, Figures 8.34, 8.35, and 8.36 , are compared with results obtained from self tuning regulator without exponential forgetting, Figures 8.31, 8.32, and 8.33, it is evident that the parameter updating does not result in the same values. In self tuning regulator with exponential forgetting, the parameter values are affected at a higher degree by the most recent measurements. For instance, at $\rho_0 = 70$ the 'vf' plot in Figure 8.33,approximately 64, is closer to the v_f initially calculated which is 70. However, in self tuning with exponential forgetting, the 'vf' plot in Figure 8.36 indicates v_f estimation of less than 56, which is significantly less than the v_f initially calculated which is 70. This result is justified by noting that speed new measurements of

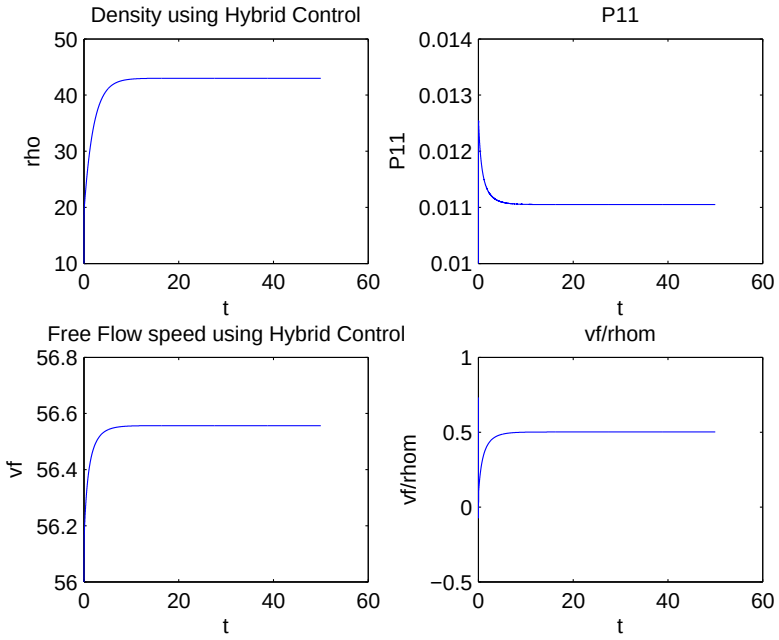

Figure 8.34: The freeway segment density and parameters values based on the self tuning regulator with exponential forgetting- $\rho_0 = 10$

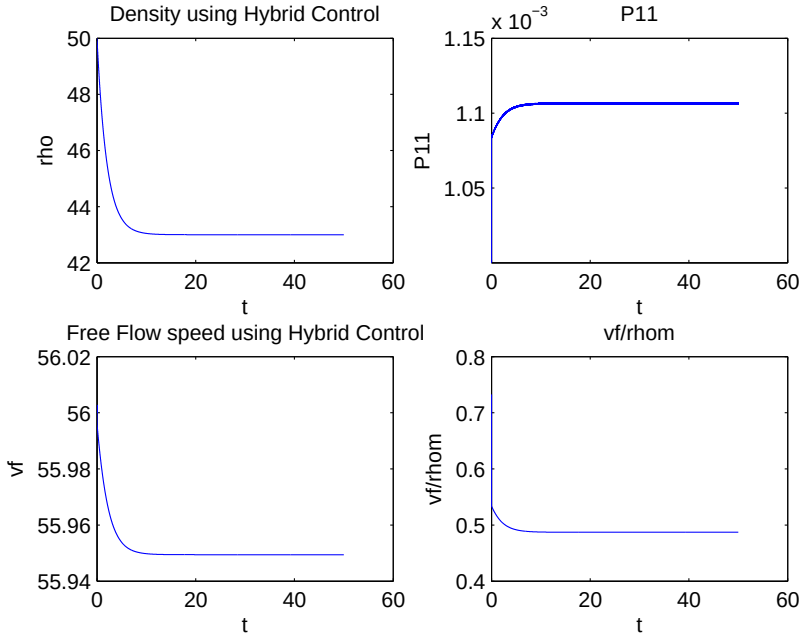

Figure 8.35: The freeway segment density and parameters values based on the self tuning regulator with exponential forgetting- $\rho_0 = 50$

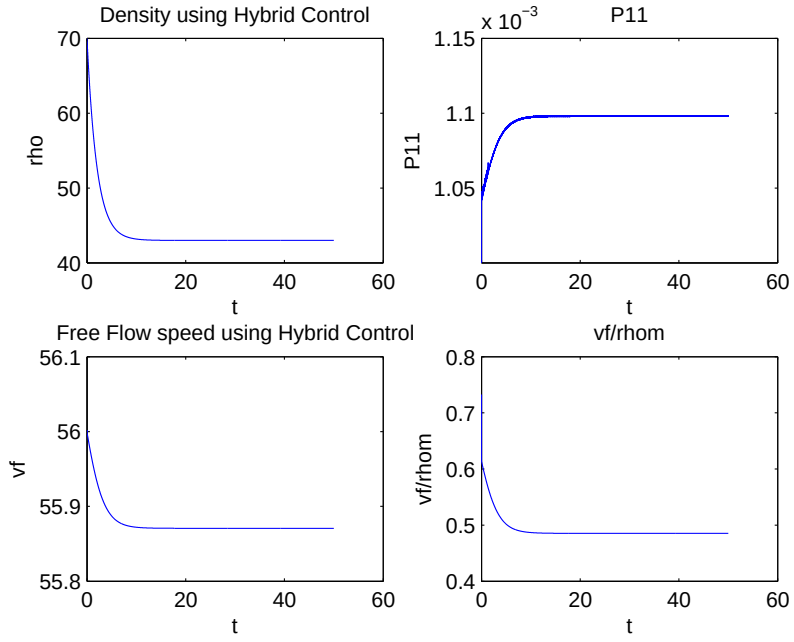

Figure 8.36: The freeway segment density and parameters values based on the self tuning regulator with exponential forgetting- $\rho_0 = 70$

speed are low at initial density of 70 which close to jam density; with exponential forgetting, new measurements weigh much more than old ones.

8.9 Conclusions and Future Work

This chapter presented a novel method for the feedback control design of an isolated ramp based on space discretizing the hyperbolic distributed model for the traffic. The discretization was performed using the Godunov method that has better nominal behavior representation of the dynamics than some other existing models in the literature. The Godunov method renders the dynamics to be autonomously switched hybrid dynamics, which are feedback linearized to obtain a feedback control asymptotically stabilizing ramp meter con-

trol law. The study presented the theoretical derivation of the model and the control design. Simulations were performed using the developed control scheme on the hybrid dynamics. The simulation model was first validated then the control was applied. Various scenarios were tested in order to cover all possible Godunov conditions at the boundary of the section. The simulation results have demonstrated that the developed feedback control has excellent performance under the various real life scenarios. A case study was conducted on the North-bound Tropicana and Interstate 15, a major on-ramp. In this case study, data was collected using FAST's freeway sensors. The ramp-meter's control strategy was obtained as well. Parameters of the specific location were obtained from data using LSE as well as RLSE. Then, simulations were performed comparing the Godunov based hybrid control strategy proposed in this study and the existing control scheme. It was observed that if there is enough demand at the ramp, then the density on the freeway segment reaches jam density in a very short amount of time. On the other hand, the density of the freeway gradually increases then stabilizes about the critical or desired density.

Part VI

Conclusions and Future Work

CHAPTER 9

Conclusions

9.1 Summary

Chapter 2 demonstrated incident management modeling using formal languages and automata theory. Formal languages methodology provides the ability to perform rigorous debugging and analysis through which robustness of the Incident Management system can be achieved upon implementation. This approach allows analysis to be conducted of processes concurrently executed processes that have specifications for liveness and safety properties specifications. The purpose of this approach is to model the traffic management processes in various coordinating agencies and then to find out if undesirable situations, such as "semaphores locking" exist. This method offers flexibility in modeling various Incident Management systems that account for many possible existing scenarios. Formal modeling can lead to the development of customized systems resulting in a more successful Incident Management process. The approach studied in this study can be expanded to include a wider range of resources for every process within the agencies as well as to model additional agencies that might be involved in the Incident Management process. In addition, this model can be enhanced to include real-time information within the states representing traffic conditions or other continuous, random activities. Finally, real-time data and statistics can be incorporated to support predictions and estimations.

Using formal methods, modeling provides practical and accessible techniques that aid evaluating designs for concurrent software. The incident management process is composed of a combination of sequential and concurrent events that are performed by multiple agencies. Therefore, it is inevitable that incident management software must feature high level of concurrency in its design. Formal methods are found to be very suitable and natural for incident management modeling, from which incident management software can be developed. Using formal methods modeling and its associated features, such as concurrency and property checking, can provide flexible and appropriate tools for software design, leading to enhancement in communications, response, and management. From a practical point of view, formal methods modeling as well as associated software are used in order to ensure that the incident management process is well defined. The user - and in this case, the user can be any of the responder agencies, the Department of Transportation, or any party that has an active role in managing incidents - takes an active role in determining the structure of the model and defining the desired safety and liveness properties.

Formal methods based approach is particularly useful for complex systems where high levels of hierarchy and concurrency are required. Complex models can be built based on modular structure. The software allows modular interaction through event sharing. This method is also useful when quantification of qualitative procedures is needed. For instance, the various Incident Management systems across the nation are evaluated based on the Incident Command. However, the Incident Command system stands as a document that is described qualitatively. This introduces challenges in achieving a common means of evaluation as well as a common structure among the different IM systems.

Chapter 3 compares the flow detector volume data to manual counted traffic video volume data. Since, traffic videos can have varying levels of clarity depending on different factors such as the angle, distance, occlusion, and clarity due to environment, a new technique for statistical analysis for comparison was developed. This technique used clarity ratings of the manual counters. Analysis was performed to obtain a model relating the rating numbers to consistency variation, which was then used for paired t-test for final comparison. This technique was used on data collected and the results were presented.

In Chapter 4 the classical reliability approaches were introduced, variability based on normalized standard deviation, analysis of Variance ANOVA, travel time mean estimation, reliability as a measure of non-failures, and information theory based approach. These methos were applied to the I-15 corridor in Las Vegas. Two types of analysis were conducted, day-to-day and within the day reliability, on the DMS data obtained from FAST using the six proposed methods. It was found that that these measures are not always consistent when compared.

In Chapter 5, it was found that information theory provides a direct measure of uncertainty from which the reliability measure can be easily derived. To indicate variability, classical reliability measures mainly use statistical variance as well as its different forms. There is no doubt that these measures somewhat represent certainty; however, the proposed entropy based reliability considers not only variance but also all statistical moments of a probability density function. This follows from the fact that the entropy formulation uses the probabil-

ity density function as a whole in order to extract the certainty associated with the travel time.

Chapter 6 demonstrated measuring the reliability of networked roadway segments. In this study it is found that the algebraic structure of the reliability of a network is consistent with the semi-ring min-plus algebraic structure. This provides us with well established properties that can simplify the algebra over networks' reliability. This study discovers the structure of the algebraic space when reliability is measured for a network.

In Chapter 7, a Bayesian Safety Analyzer (BSA) is constructed based on various data sources including crash data and traffic data. It is demonstrated how posterior probabilities can be computed and how data can be used to train the Bayesian structure composed of a large amount of parameters. Bayesian analysis is proved to be a very efficient probabilistic method for analyzing a large set of data in order to better estimate dependencies and likelihood of occurrence of various events. The developed BSA can be used in the incident management process. It can assist decision makers in estimating the severity of a certain incident based on given attributes in order to better prepare. BSA can also be used in order to assess the transportation system's safety.

Chapter 8 presented a novel method for the feedback control design of an isolated ramp based on space discretizing the hyperbolic distributed model for the traffic. The discretiza-

tion was performed using the Godunov method that has better nominal behavior representation of the dynamics than some other existing models in the literature. The Godunov method renders the dynamics to be autonomously switched hybrid dynamics, which are feedback linearized to obtain a feedback control asymptotically stabilizing ramp meter control law. The study presented the theoretical derivation of the model and the control design. Simulations were performed using the developed control scheme on the hybrid dynamics. The simulation model was first validated then the control was applied. Various scenarios were tested in order to cover all possible Godunov conditions at the boundary of the section. The simulation results have demonstrated that the developed feedback control has excellent performance under the various real life scenarios. A case study was conducted on the North-bound Tropicana and Interstate 15, a major on-ramp. In this case study, data was collected using FAST's freeway sensors. The ramp-meter's control strategy was obtained as well. Parameters of the specific location were obtained from data using LSE as well as RLSE. Then, simulations were performed comparing the Godunov based hybrid control strategy proposed in this study and the existing control scheme. It was observed that if there is enough demand at the ramp, then the density on the freeway segment reaches jam density in a very short amount of time. On the other hand, the density of the freeway gradually increases then stabilizes about the critical or desired density.

9.2 Contributions

The contributions of this dissertation work are listed below.

9.2.1 Modeling

- **Formal Language Modeling of Incident Management:** Formal language and automata theory is used for modeling, analyzing, and implementing traffic incident management process.
- **Hybrid Modeling of a freeway on-ramp:** Godunov based conditions are used in determining boundary conditions of the hyperbolic PDE used in modeling traffic flow on a freeway section.

9.2.2 Sensing

- **Detector Validation:** A weighted t- statistics developed in order to compare a set of uncertain data with another set of uncertain data with various levels of uncertainty.

9.2.3 State Estimation

- **Hybrid Estimation:** Estimation techniques are developed in order to estimate from the data the time of occurrence of various events such as the time of incident and the time of incident clearance.

9.2.4 Performance Analysis

- **Reliability Theory:** Average travel time is a good indicator of the performance of a highway segment or a transportation network in general. However, by itself, it lacks

information about the overall performance of the transportation system. Hence, for proper assessment of the transportation system's performance, this research developes and uses five different reliability measures for freeway and arterials in Las Vegas: variability based on normalized standard deviation, analysis of variance (ANOVA), average time mean estimation, reliability as a measure of non-failures, and information theory.

- **Entropy Based Reliability:** A novel travel time reliability is developed that is based on measuring the uncertainty of travel time from data.

- **Network Reliability:** Max-plus algebra is proposed in order to extend the reliability measure of a component to network reliability.

- **Bayesian Networks:** A Bayesian network is a probabilistic model which represents relationships between uncertain variables and can be used as a framework for various applications. This research develops a Bayesian traffic safety analyzer using crash data and other surrogate information to estimate risks at various locations.

9.2.5 Control

- **Hybrid Ramp Control:**A hybrid control scheme is developed in order to maintain a given freeway segment at certain desired conditions.

9.3 Future Work

There are many areas of this dissertation that can be enhanced by further research. These are listed below. Formal methods modeling of incident management will be extended to hybrid modeling in future work. Future work can also include developing algorithms in order to automate data formatting from multiple sources into one file that integrates all required data and feeds into the developed BSA. In the future, the minimal path problem using a probabilistic approach based on failure analysis will be considered. Dependency of roadway links is a major issue that will also be considered in future studies of reliability.

BIBLIOGRAPHY

[1] Gang Xie. Freeway travel times: Interactive dashboard.

[2] Office of Operation. Traffic Incident Management. *Federal Highway Administration*, (FHWA-OP-04-052), 2004.

[3] Jodi L. Carson. Traffic Incident Management and Quick Clearence Laws. *Texas Transportation Institute*, (FHWA-HOP-09-005), 2008.

[4] U.S.DOT, FHWA, and FTA. Incident Management Successful Practices, 2000.

[5] U.S. Department of Transportation. Best Practices In Traffic Incident Management. *Federal Highway Administration*, 2010.

[6] Jodi L. Carson, Fred L. Mannering, Bill Legg, Jennifer Nee, and Doohee Nam. Are Incident Management Programs Effective? *Transportation Reasearch Record*, (1683):8–13, 1999.

[7] Rui Chen, Raj Sharman, H. Raghav Rao, and Shambhu J. Upadhyaya. Coordination in Emergency Response Management. *Communications of the ACM*, (5):68–73, 2008.

[8] Mingwei HU, Hao Tang, Der horng Lee, and Qixin Shi. Development of the Real Time Evalutation and Decision Support System for Incident Management. *Intelligent Transportation Systems.Proceedings.IEEE*, (1):426–431, 2003.

[9] Henry Sullivan. Assessing the National Incident Management System. *Conference Papers- Midwestern Political Science Association*, pages 1–15, 2007.

[10] Fries R. Hamlin C. Chowdhury M. Ma Y. and Ozbay K. Operational Impacts of Incident Quick Clearance Legislation: a Simulation Analysis. *Journal of Advanced Transportation*, 2010.

[11] Skabardonis A. Petty K. Bertini R. Varaiya P. Noeimi H. and Rydzewski D. I-880 Field Experiment: Analysis of Incident Data. *Transportation Research Record: Journal of the Transportation Research Board*, pages 72–79, 2007.

[12] Karlaftis M. Latoski P. Richards N. and Sinha K. ITS Impacts on Safety and Traffic Management: An Investigation of Secondary Crash Causes. *Journal of Intelligent Transportation Systems*, (4):39–52, 1999.

[13] Pal R. Latoski S. Sinha K. Investigation of Freeway Incident Characteristics and Their Influence in Planning an Incident Management Program. *Transportation Research Record: Journal of the Transportation Research Board*, pages 46–55, 1998.

[14] Sravanthi Konduri, Samuel Labi, and Kumares C. Sinha. Incident Occurrence Models for Freeway Incident Management. *Transportation Research Record*, (1856):125–134, 2003.

[15] Scherer W. and Kripalani A. Accident Management Using Wireless Networks: Estimating Incident Related Congestion on Freeways Based on Incident Severity. *Project Report for the Center for ITS Implementation Research*, 2007.

[16] John J. Wirtz, Joseph L. Schofer, and David F. Schulz. Using Simulation to test Traffic Incident Management Strategies. *Transportation Reasearch Record*, (1923):82–90, 2005.

[17] Mark Hooendoorn, Catholijn . Jonker, Jan Treur, and Marian Verhaegh. Agent Based Analysis and Support for Incident Management. *Safety Science*, (47):1163–1174, 2009.

[18] Ozbay K. Xiao W. Jaiswal G. Bartin B. Kachroo P. and Gursoy M. Evaluation of incident management strategies and technologies using an integrated traffic/incident management simulation. *World Review of Intermodal Transportation Research*, pages 155–186, 2009.

[19] Marco Roccetti, Mario Gerla, Claudio E. Plalazzi, and Giovanni Pau Stefano Ferretti. First Responders' Crystal Ball: How to Scry the Emergency from a Remote Vehicle. *Performance, Computing, and Communications ConferenceIEEE*, (1):556–561, 2007.

[20] Jin Ki Kim, H. Raghav Rao, Raj Sharman, and Shambhu Upadyaya. Framework for Analyzing Critical Incident Management System (CIMS). In *39th Hawaii International Conference on System Sciences*, pages 7695–2507, 2006.

[21] Raktim Pal, Steven P. Latoski, and Kumares C. Sinha. Investigation of Freeway Incident Characteristics and Their Influence in Planning an Incident Management Programs. *Transportation Research Record: Journal of the Transportation Research Board*, (1603):46–55, 2007.

[22] Richard A. Raub and Joseph L. Schofer. Managing Incidents on Urban Arterial Roadways. *Transportation Reasearch Record*, (1603):12–19, 1997.

[23] U.S.DOT, FHWA, and FTA. Simplified Guide to the Incident Command System for Transportation Professionals. *Federal Highway Administration*, (FHW-HOP-06-004), 2006.

[24] Rita Brohman. Technical Memorandum, Existing Conditions, Mission Goals and Objectives. *Traffic Incident Management Coalition*, (1):40, 2008.

[25] Gyorgy E. Revesz. *Introduction to Formal Languages*. Dover Publications, 1991.

[26] J. Glenn Brookshear. *Theory of Computation, Formal Languages, Automata, and Complexity*. The Benjamin/Cummings Publishing, 1989.

[27] Jeff Magee and Jeff Kramer. *Concurrency, State Models and Java Programming*. John Wiley, 2006.

[28] Zohar Manna and Amir Pnueli. *The Temporal Logic of Reactive and Concurrent Systems*. Springer-Verlag, 1991.

[29] M. H. Kang, B. W. Choi, K C. Koh, J. H. Lee, and G. T. Park. Experimental study of a vehicle detector with an amr sensor. *Sensors and Actuators A*, 118:278–284, 2005.

[30] A. Chen, S. Ryu., and P. Chootinan. l_∞-norm path flow estimator for handling traffic count inconsistencies: Formulation and solution algorithm. *Journal of Transportation Engineering*, 136:565?575, 2010.

[31] M. Fathy and M. Y. Siyal. Measuring traffic movements at junctions using image processing techniques. *Pattern Recognition Letters*, 18:493–500, 1997.

[32] P. Zhuang, Y Shang, and B. Hua. Statistical methods to estimate vehicle count using traffic cameras. *Multidim System Sign Process*, 20(7):121–133, 2009.

[33] D. W. Zimmerman. Conditional probabilities of rejecting h0 by pooled and separate-variances t tests given heterogeneity of sample variances. *Communications in Statistics*, 33:69–81, 2004.

[34] Erwin Kreyszig. *Introductory Mathematical Statistics: Principle and Methods*. John Wiley & Sons Inc., 1970.

[35] Enide A.I. Bogers, Hans WC Van Lint, and HENK J Van Zuylen. Travel time reliability: Effective measures from a behavioral point of view. *Transportation Research Record: Journal of the Transportation Research Board*, page 114, 2008.

[36] Chao Chen, Alexander Skabardonis, and Pravin Varaiya. Travel-time reliability as a measure of service. *Transportation Research Record: Journal of the Transportation Research Board*, (1855):7479, 2003.

[37] T. Lomax, D. Schrank, S. Turner, and R. Margiotta. Selecting travel reliability measures. *Texas Transportation Institute and Cambridge Systematics*, 2003.

[38] Jun-Seok Oh and Younshik Chung. Calculation of Travel Time Variability from Loop Detector Data. *Transportation Research Record: Journal of the Transportation Research Board*, (1945):1223, 2006.

[39] J. Lint, H. Zuylen, and H. Tu. Travel time unreliability on freeways: Why measures based on variance tell you only half the story. *Transportation Research Part A*, (42):258–277, 2008.

[40] Yu Nie and Yueyue Fan. Arriving-on-Time Problem, Discrete Algorithm that Ensures Convergence. *Transportation Research Record: Journal of the Transportation Research Board*, (1964):193–200, 2006.

[41] Lam S.H., M. Jing, and A.A. Memon. Effects of Real-Time Information on Route Choice Behavior: New Modeling Framework and Simulation Study in Behavioral Responses to ITS. *Eindhoven*, 2003.

[42] I.G. Black and J.G. Towriss. Demand Effects of Travel Time Reliability. *Final report prepared for London assessment division. UK Department of transport*, 1993.

[43] J.W.C. Van Lint and H.J. Van Zuylen. Monitoring and Predicting Freeway Travel Time Reliability. *Transportation Research Record*, (1917):54–62, 2005.

[44] Cambridge Systematics Inc. Traffic Congestion and Reliability Trends and Advanced Strategies for Congestion Mitigation. *Prepared for Federal Highway Administration*, page 140, 2005.

[45] Ronald E. Walpole. *Introduction to Statistics*. Macmillan Publications, 1968.

[46] Richard A. Johnson. *Miller and Freund's Probability and Statistics for Engineers*. Prentice Hall, 1994.

[47] Gordon Raisbeck. *Information Theory*. The MIT Press, 1964.

[48] A.I. Khincihn. *Mathematical Foundations of Information Theory*. Dover Publications, Inc, 1957.

[49] Fazlollah M. Reza. *An Introduction to Information Theory*. Dover Publications, Inc, 1994.

[50] Kimley-Hom and Associates. FreewayManagement System Software Manual. *Prepared for Nevada Department of Transportation*, 2004.

[51] Kimley-Hom and Associates. FreewayManagement System Operator Manual. *Prepared for Nevada Department of Transportation*, 2009.

[52] Network layers.

[53] UW Information Technology. The osi model.

[54] Sheldon Ross. *Introduction to Probability Models.* Academic Press, 1993.

[55] Bernd Heidergott, Geert Jan Olsder, and Jacob van der Woude. *Max Plus at Work Modeling and Analysis od Synchronized Systems: A course on Max-Plus Algebra and Its Application.* Princeton Series in Applied Mathematics, 2006.

[56] Kasie G. Farlow. Max-Plus Algebra. *Master's Thesis*, (Virginia Polytechnic Institute and State University), 2009.

[57] Jean Cochet-Terrasson and Stephane Gaubert. Policy iteration algorithm for shortest path problems. 2000.

[58] Donald E. Kirk. *Optimal Control Theory.* Dover, 2004.

[59] Kevin Murphy. How to use the bayes net toolbox, 2007.

[60] David Malakoff. Statistics: Bayes offers a 'new' way to make sense of numbers. *Science*, 286(5444):1460–1464, 1999.

[61] Peter D. Hoff. *A First Course in Bayesian Statistical Methods.* Springer Texts in Statistics, 2009.

[62] Peter M. Lee. *Bayesian Statistics: An Introduction.* Wiley, 2003.

[63] Kaan ozbay and Nebahat Noyan. Application of bayesian networks to analyze in analyzing incidents and decision-makin. *Transportation Research Board*, 38(3):542–555, 2005.

[64] Kaan ozbay and Nebahat Noyan. Estimation of incident clearance times using bayesian networks approach. *Accident Analysis and Prevention*, 38(3):542–555, 2006.

[65] JUNG-BEOM LEE. Calibration of traffic simulation models using simultaneous perturbation stochastic approximation (spsa) method extended through bayesian sampling methodology. *Rutgers, The State University of New Jersey*, Dissertation, 2008.

[66] Jos Holguin-Veras2 Ozlem Yanmaz-Tuzel, Kaan Ozbay. Value of travel time estimation using hierarchical bayesian mixed logit approach. *Transportation Research Record: Journal of the Transportation Research Board*, pages 85–96, 2010.

[67] Liang Xiaolin Zhang Rongmei. An its for traffic accident processing based on cbr and br. *Computer Science and Information Technology (ICCSIT), 2010 3rd IEEE International Conference*, 4:126 – 130, 2010.

[68] Changshui Zhang Shiliang Sun and Guoqiang Yu. A bayesian network approach to traf?c flow forecasting. *Intelligent Transportation Systems, IEEE Transactions*, 7:124 – 132, 2006.

[69] Maolei Zhang Rui Tian, Zhaosheng Yang. Method of road traffic accidents causes analysis based on data mining. *Computational Intelligence and Software Engineering (CiSE), 2010 International Conference*, pages 1 – 4, 2010.

[70] Xin-ping Yan Ming Ma, Chao-zhong Wu. An analysis method for uncovering the nature of road traffic accident based on gray relation. *IEEE International Conference on Grey Systems and Intelligent Services*, pages 105 – 110, 2007.

[71] Sun Yue-kun He Song-bai, Wang Ya-jun and Gao Wen wei Chen Qiang An Ya-qin. The research of multidimensional association rule in traffic accidents. *Wireless Communications, Networking and Mobile Computing, 2008. WiCOM '08. 4th International Conference*, pages 1 – 4, 2010.

[72] Young-Seol Lee ju Won Hwang and Sung-Bae Cho. Hierarchical probabilistic network-based system for traffic accident detection at intersections. *Symposia and Workshops on Ubiquitous, Autonomic and Trusted Computing*, pages 211 – 216, 2010.

[73] Wu Lurong. Fuzzy distribution fitting for law of traffic accidents based on matlab. *Sixth International Conference on Fuzzy Systems and Knowledge Discovery*, 6:227 – 231, 2009.

[74] Christian P. Robert. *The Bayesian Choice: From Decision-Theoretic Foundations to Computational Implementation*. Springer Texts in Statistics, 2007.

[75] Jose M. Bernardo and Adrian F. M. Smith. *Bayesian Theory*. Wiley Series in Probability and Statistics, 2000.

[76] Hal S. Stern Andrew Gelman, John Carlin and Donald B. Rubin. *Bayesian Data Analysis*. Chapman and Hall/CRC, 2004.

[77] J. A. Wattleworth. System demand capacity analysis on the inbound gulf freeway. *Texas Transportation Institute*, 24-8, 1964.

[78] D. R. Drew. Gap acceptance caharacteristics for ramp freeway surveillance and control. *Texas Transportation Institute*, 24-12, 1965.

[79] C. Pinnell, D. R. Drew, W. R. McCasland, and J. A. Wattleworth. Inbound gulf freeway ramp control study i. *Texas Transportation Institute*, 24-10, 1965.

[80] C. Pinnell, D. R. Drew, W. R. McCasland, and J. A. Wattleworth. Inbound gulf freeway ramp control study ii. *Texas Transportation Institute*, 24-10, 1965.

[81] ITE. Traffic control systems handbook. *Institute of Transportation Engineers*, 4.14-4.40, 1996.

[82] L. S. Yuan and J. B. Kreer. Adjustment of freeway ramp metering rates to balance entrance ramp queues. *Transportation Research*, 5:127–133, 1971.

[83] J. A. Wattleworth and D. S. Berry. Peak period control of a freeway system - some theoretical investigations. *Highway Research Record*, 89:1–25, 1964.

[84] A. D. May. Optimization techniques applied to improving freeway operations. *Transportation Research Record*, 495:75–91, 1965.

[85] B. Hellinga and M. Van Aerde. Examining the potential of using ramp metering as a component of an atms. *Transportation Research Record*, 1494:75–83, 1995.

[86] H. Zhang, S. Ritchie, and W. Recker. On the optimal ramp control problem: When does ramp metering work? *Transportation Research Board Annual Conference*, 1995.

[87] M. Papageorgiou, H. S. Habib, and J. M. Blosseville. Alinea: A local feedback control law for on-ramp metering. *Transportation Research Record*, 1320:58–64, 1991.

[88] Leon L. Chen, Adolph D. May, and David M. Auslander. Freeway ramp control using fuzzy set theory for inexact reasoning. *Transportation Research A*, 24(1):15–25, 1990.

[89] N. B. Goldstein and K. S. P. Kumar. A decentralized control strategy for freeway regulation. *Transportation Research B*, 16B(4):279–290, 1982.

[90] H. Zhang, S. Ritchie, and Z. Lo. A local neural network controller for freeway ramp metering. *IFAC Transportation Systems, PRC*, pages 655–658, 1994.

[91] D. P. Masher, D. W. Ross, P. J. Wong, P. L. Tuan, H. M. Zeidler, and S. Petracek. Guidelines for design and operation of ramp control systems. *Stanford Research Institute*, 1975.

[92] H. Hadj-Salem, M. M. Davee, J. M. Blosseville, and M. Papageorgiou. Alinea: Unoutil de regulation d?acces isole sur autoroute. *Rapport INRETS 80*, 1988.

[93] R. La Pera and R. Nenzi. Tana - an operating surveillance system for highway traffic control. *Proc., Institute of Electrical and Electronics Engineers*, 61:542–556, 1973.

[94] N. Helleland, W. Joeppen, and P. Reichelt. Die rampendosierung an der a5 bonn/siegburg der bab 3 in richtung koln. *Strassenverkehrstechnik*, 22:44–51, 1978.

[95] NN. Ramp metering in auckland. *Traffic Engineering and Control*, 24:552–553, 1983.

[96] D. Owens and M. J. Schofield. Access contr on the m6 motorway: Evaluation of britain?s first ramp metering scheme. *Traffic Engineering and Control*, 29:616–623, 1988.

[97] H. Buijn and F. Middelham. Ramp metering control in the netherlands. *Proc., 3rd IEE International Conf. on Road Traffic Control*, pages 199–203, 1990.

[98] Pushkin Kachroo and Kaan Ozbay. *Feedback Ramp Metering for Intelligent Transportations Systems*. Kluwer, 2003.

[99] Pushkin Kachroo, Kaan Ozbay, Sungkwon Kang, and John A. Burns. System dynamics and feedback control formulations for real time dynamic traffic routing. *Mathl. Comput. Modelling*, 27(9-11):27–49, 1998.

[100] Pushkin Kachroo and Kumar Krishen. System dynamics and feedback control design formulations for real time ramp metering. *Transactions of the SDPS, Journal of Integrated Design and Process Science*, 4(1):37–54, 2000.

[101] M. J. Lighthill and G. B. Whitham. On kinematic waves. i:flow movement in long rivers. ii:a theory of traffic on long crowded roods. In *Proc. Royal Soc.*, number A229, pages 281–345, 1955.

[102] P. I. Richards. Shockwaves on the highway. *Operationa Research*, 4:42–51, 1956.

[103] B. D. Greenshields. A study in highway capacity. *Highway Research Board*, 14:458, 1935.

[104] G. B. Whitham. *Linear and Nonlinear Waves*. John Wiley, N.Y., 1974.

[105] Richard Haberman. *Mathematical Models: Mechanical Vibrations, Population Dynamics, and Traffic Flow*. SIAM, 1987.

[106] Pushkin Kachroo. *Pedestrian Dynamics: Mathematical Theory and Evacuation*. CRC, 2009.

[107] Randall J. Leveque. *Numerical Methods for Conservation Laws*. Birkhauser, 2005.

[108] Peter D. Lax. *Hyperbolic Systems of Conservation Laws and the Mathematical Theory of Shock Waves*. SIAM, 1987.

[109] Arjan J. van der Schaft and Hans Schumacher. *An Introduction to Hybrid Dynamical Systems*. Springer, 1999.

[110] David G. Luenberger. *Optimization by Vector Space Methods*. Wiley, 1969.

[111] Jean-Jacques E. Slotine and Weiping Li. *Applied Nonlinear Control*. Prentice Hall, 1991.

VITA

EDUCATION

University of Nevada, Las Vegas, Las Vegas, NV
Ph.D., Electrical Engineering, expected 2011;
Advisor: Professor Pushkin Kachroo
Topic: Hybrid Dynamical Systems, Networks, and Control

University of Nevada, Las Vegas, Las Vegas, NV
M.S., Mathematics, expected 2011;
Advisor: Professor David Costa and Professor Zhonghai Ding
Topic: Hybrid Estimation

University of Nevada, Las Vegas, Las Vegas, NV
M.S., Electrical Engineering, 2008;
Advisor: Professor Rama Venkat
Topic: Novel RGBW Pixel for LED Displays
Minor: Computer Engineering

University of Nevada, Las Vegas, Las Vegas, NV
B.S., Electrical Engineering, 2006;
Advisor: Rama Venkat
Topic: Wireless, Solar Powered Sensor Networks
Minor: Mathematics

Fundamentals of Engineering (F.E.)

Engineer Intern, State of Nevada, Electrical Engineering

AWARDS

- Research Grant, Medical Imaging, NSTech, 2011
- Travel Grant, Graduate and Professional Student Association, 2011
- Travel Grant, UNLV Foundation, 2011
- Outstanding Student of the Year, Transportation Research Center, USDOT 2011
- 2010 Eisenhower Graduate Fellowship Award, Federal Highway, 2010
- International Test and Evaluation Association (ITEA) Scholarship Award, 2010
- Outstanding Student of the Year, Transportation Research Center, USDOT 2010
- Graduate Access Scholarship, 2008
- Dean's List Award, 2006, 2008
- Outstanding EE senior student, 2006
- Cum Laude, 2006
- Grand Prize for Best Engineering Project Award, 2006

RESEARCH AREAS

- Computed Neutron Tomography
- Theoretical and Applied Feedback Control
- Nonlinear and Hybrid Control Systems
- Intelligent Transportation Systems
- Traffic and Vehicle Control
- Applied Mathematics
- Statistics and Random Processes
- Complex Systems and Networks: Transportation, Communication, Sensor, and Power Networks
- Electronics and Photonics: LED Displays, Embedded Systems, Networks on Chip

Selected Graduate Mathematics and Engineering Courses

- Non-Linear Controls

- Probability and Stochastic Processes
- Determination and Estimation of Signals
- Optimization
- Real Analysis
- Functional Analysis
- Partial Deferential Equations
- Topology
- Verification and Testing
- Wireless Communications
- Analysis of Telecommunications Networks
- Advanced Digital logic
- Modern Processor Architecture

WORK EXPERIENCE

2009-present Researcher, Transportation Research Center, UNLV
Worked on medical imaging, hybrid dynamical systems and controls, complex networks, performance measures and sustainability, Bayesian safety analyzer, Dijkstra algorithm vs. rolling horizon, freeway and arterial reliability analysis using new mathematical theories and approaches, secondary congestion/ incidents study, congestion pricing, website development using HTML and Java, Database management and analysis using R, PhpMyAdmin, MySQL, VBA, and simulations using macroscopic and mesoscopic software. Managed several projects and participated in proposal writing.

2008-2009 Instructor, ITT Technical Institute, Henderson, Nevada
Taught several courses in programming, electronics, and controls.

2007-2008 Research Assistantship, Department of Electrical and Computer Engineering, UNLV
Worked on research and development of photonics and LED displays, video and digital signal processing, constructing algorithms in AHDL and Basic, improving power consumption, clarity, and life time of LED displays, programming FPGAs, CPLDs, and Microcontrollers, ASIC, various hardware interface, circuit debugging, troubleshooting, oscilloscope, digital logic analyzer, and PCB layout.

2007-2008 Teaching Assistantship, Department of Electrical and Computer Engineering, UNLV
Taught several laboratories in analog circuit design and solid states.

2005-2006 Student Researcher, Department of Electrical and Computer Engineering, UNLV
Conducted an independent study on ICs architecture, Hardware Description Languages (HDL), and display systems, embedded systems FPGAs, CPLDs, microcontrollers and programming in AHDL and Basic, and hardware testing.

2003-2004 Student Tutor, College of Southern Nevada, Las Vegas
Tutored all math levels, Science, and English.

BOOKS

1. Neveen Shlayan and Rama Venkat, *LED Displays: Energy Efficient RGBW Pixel Configuration for LED Displays*, 2009.
2. Neveen Shlayan and Pushkin Kachroo, *Transportronics, Introduction to Transportation Electronics*, IEEE and John Wiley and Sons , 2011. (Under contract)
3. Pushkin Kachroo, Neveen Shlayan, and Asad Khattak, *Secondary Incidents*. (Under preparation)

JOURNAL PUBLICATIONS

1. Neveen Shlayan, Pushkin Kachroo, "The Min-Plus Algebra of Transportation Networks Reliability based on Information Theory", the IEEE Transactions on Reliability, 2011. (Submitted)
2. Neveen Shlayan, Pushkin Kachroo, "Feedback Ramp Metering using Godunov Method based Hybrid Model", the Journal of Dynamic Systems, Measurement and Control, 2011. (Submitted)
3. Neveen Shlayan, Pushkin Kachroo, "Formal Language Modeling and Simulations of Incident Management", IEEE Intelligent Transportation Systems Transactions, 2011. (Submitted)
4. Alexander Paz, Pushkin Kachroo, and Neveen Shlayan, "Non-intrusive Traffic Sensor Assessment Using Imperfect Information and Weighted t-Test", Mathematical and Computer Modeling, 2011. (Submitted)

5. Neveen Shlayan, Rama Venkat, Paolo Ginobbi, and Ashok Singh, "Energy Efficient RGBW Pixel Configuration for LED Displays", IEEE Transactions, Journal of Display Technology, 2008.

6. Neveen Shlayan, Rama Venkat, Paolo Ginobbi, and Glenn Mercier, "A Novel RGBW Pixel for LED Displays", Systems Science - The International Journal by Wroclaw University of Technology, 2008.

FULL PAPER REFEREED CONFERENCE PUBLICATIONS

1. Neveen Shlayan, Pushkin Kachroo, Sabiha Wadoo, "The Min-Plus Algebra of Transportation Networks Reliability based on Information Theory",IEEE ITSC 2011.

2. Neveen Shlayan, Pushkin Kachroo, Sabiha Wadoo, "Bayesian Safety Analyzer Using Multiple Data Sources of Accidents",IEEE ITSC 2011.

3. Pushkin Kachroo, Neveen Shlayan, Sabiha Wadoo, "Feedback Ramp Metering using Godunov Method based Hybrid Model",IEEE ITSC 2011.

4. Pushkin Kachroo, Kaan Ozbay, Neveen Shlayan, and Sabiha Wadoo, "Feedback Based Dynamic Congestion Pricing", Transportation Research Board, 2010.

5. Neveen Shlayan, Rama Venkat, Paolo Ginobbi, and Glenn Mercier, "A Novel RGBW Pixel for LED Displays", icseng,pp.407-411, 2008 19th International Conference on Systems Engineering, 2008.

6. Dawid Zydek, Neveen Shlayan, Emma Regentova, and Henry Selvaraj. "Review of Packet Switching Technologies for Future NoC", icseng,pp.306-311, 2008 19th International Conference on Systems Engineering, 2008.

COURSES TAUGHT

UNLV Courses

1. Introduction to Engineering, 2010

2. Circuits II Laboratory, 2008

3. Electronics II Laboratory, 2008

ITT Tech Courses

1. Electronic Circuit design II, 2010
2. Embedded Systems (in C), 2009
3. Process Control, 2009
4. C Programming in Linux, 2008
5. Advanced Circuit Design, 2008

PROFESSIONAL AFFILIATIONS

- IEEE Member
- Tau Beta Pi, Engineering Honor Society
- Phi Theta Kappa Society-Alpha Xi Beta, international scholastic order

SERVICE

- Subcommittee member for the Traffic Flow Theory and Characteristics Committee, Transportation Research Board, 2011
- Papers reviewer, Transportation Research Board Annual Conference, 2009, 2010
- Papers reviewer, IEEE Transactions on Systems, Man, and Cybernetics, Part A: Systems and Humans, 2010, 2011